SEISMIC MICROZONATION STUDIES OF MEERUT CITY

(FSP Code: M4SHMZ/NC/NR//2017/12047)

(Field Season: 2016-17 and 2017-18)

By

Rajesh Chaturvedi, Sr. Geologist; Nazia Khan, Geologist; Poulami Chaki, Geologist
Arjun Rai, Asstt. Geophysicist; Ranveer Singh Negi, Asstt. Geophysicist;
A. K. Mishra, Asstt. Geophysicist

GEOLOGICAL SURVEY OF INDIA

I. INTRODUCTION

Seismic vulnerability in India is well evidenced by numerous past earthquake-related calamities. A damaging earthquake intrinsically unleashes devastation instantaneously in large area without leaving much scope for prevention of loss after its occurrence. In India earthquakes have taken a toll of more than 100,000 lives in the last 100 years. During the period from 1991 to 2006, more than 23,000 lives were lost due to 6 major earthquakes in India (Uttarkashi, 1991; Latur, 1993; Jabalpur, 1997; Chamoli, 1999; Bhuj, 2001; Kashmir, 2005), which also caused enormous damage to property and public infrastructure. According to the Vulnerability Atlas of India prepared by Building Materials and Technology Promotion Council (BMTPC, 2006), more than 59 percent of the total land cover in the country is susceptible to seismic hazard.

It has been found that after an earthquake the casualties are caused primarily due to the collapse of buildings. In India, such casualties after a damaging earthquake are many times more than those caused by a similar intensity earthquake in countries like USA, Japan, etc. The main reason for this is that the civil structures in these countries are built with structural mitigation measures to reduce the seismic risk. This emphasises the need for strict compliance of town planning by-laws and earthquake-resistant building codes in India as the unplanned urbanization is expanding rapidly across the country to accommodate the rapidly increasing population. Over the period of last 4-5 decades certain measures have been taken for preparation of guidelines by different government agencies with an aim of reducing the seismic risk in India. However, the damage pattern after an earthquake at different places is not uniform as it is strongly influenced by the local site conditions. Therefore, assessment of the seismic hazard in an area mainly involves classifying the sites in different seismic micro-zones on the basis of potential seismic vulnerability of the site as well as the structures over it.

Seismic microzonation has generally been recognized as the most accepted tool in seismic hazard assessment and risk evaluation. It is defined as the zonation with respect to ground motion characteristics taking into account source and site conditions [TC4-ISSMGE, 1999]. The microzonation of a region generates detailed maps that depict the hazard at much larger scales. Seismic microzonation is the generic name for subdividing a region into individual areas having similar potentials of hazardous earthquake effects, defining their specific seismic behaviour for engineering design and land-use planning.

Seismic microzonation studies provide the expected characteristics and level of ground shaking in a region and also the potentially associated seismic phenomena such as liquefaction, lateral spreading, landslides, tsunamis, etc. The site characterization or assessment of site response during earthquakes is one of the crucial phases of seismic microzonation**.** The detailed geology, seismo-tectonics and geotechnical characteristics of the area are the basic inputs to be considered in the microzonation process. The geotechnical soil properties and the depth of the bedrock are very important in the site response studies, as these strongly influence the amplification and attenuation of strong motion amplitudes. So, detailed geological, geophysical and geotechnical data are required for seismic site characterization of the region. Generally, the damage to the buildings founded on soft sandy or clayey soil will be higher than that in similar type of buildings having their foundation on hard bedrock.

Based on tectonic features and records of past earthquakes, a Seismic Zoning Map of India (Figure 1.1) has been prepared by a committee of experts under the auspices of Bureau of Indian Standard (BIS Code: IS: 1893: Part I, 2002). Meerut lies in Zone IV in this map. The civil constructions in Meerut City are under high to medium vulnerability class for earthquakes, as per the Vulnerability Atlas of India (BMPTC-2006). However, northern boundary of Uttar Pradesh with that of Uttarakhand is in close proximity to Zone V. The Zone IV is broadly associated with a seismic intensity VIII on MSK scale. As per the policy of National Disaster Management Authority (NDMA) the cities falling in Zone-V and IV of the Seismic Zoning Map of India having a population of more than 0.5 million are to be taken up first in priority for seismic microzonation investigations.

The Geological Survey of India, Northern Region has already completed seismic microzonation studies of few cities, such as, Dehradun (Field Season:2002-03 to2004-2005), Chandigarh (Field Season: 2005-06 and 2006-07), Jammu (Field Season: 2007-08 and 2008-09), Jalandhar (Field Season: 2009-10, 2010-11 and 2011-12), Panchkula (Field Season: 2013-14), Amritsar (Field Season: 2014-15 and 2015-16) and Srinagar (Field Season: 2014-

15, 2015-16 and 2016-17). As per the Draft Master Plan of Meerut City 2012-2021 (2nd Phase), an area of about 450 sq km is to be developed and included in Meerut. Out of this, 300 sq km area under Municipal Corporation, Meerut and adjacent village settlements were taken up under the Field Season Programme of Geological Survey of India, Northern Region **(FSP No.M4SHMZ/NC/NR/2017/12047)** for seismic microzonation studies during two field seasons (2016-17 and 2017-18) as an integrated study by Earthquake Geology Division, Geophysics Division, Drilling Division and Geotechnical Lab, Northern Region. The details of NQT are given in Table 1.1.

1.1 Methodology

This study follows the broad methodology laid down as per Standard Operating Procedure (SOP) of GSI for Level 'B' seismic microzonation. The broad methodology is described as follow-

1. Preparation of various thematic maps like geological, geomorphological, land use and land cover map and seismo-tectonic map based on previous reports and available data of the area along with addition of field data, if any.
2. Drilling of 28 boreholes with SPT (standard penetration test) in the area including 26 bore holes of 30 m depth and 2 bore holes of 60 m depth, followed by core logging for lithological variations and core sampling for analysis of geotechnical properties, viz. grain size analysis and others.
3. Preparation of ground water depth map based on ground water depth data obtained during drilling of 28 boreholes along with interpreted groundwater depth map by geophysical survey.
4. Carrying out Standard Penetration Test (SPT) in the drill holes at 1.5 m intervals to determine N values of the subsurface soil layers eventually to determine the geotechnical properties including shear wave velocity of the subsurface profile at the drill sites.
5. Determination of average Shear Wave Velocity (Vs) using geotechnical SPT (N) values and properties of shallow (i.e. up to 30 m depth) subsurface soil layers followed by preparation of Shear Wave Velocity Map and calculation of Average Horizontal Spectral Amplification for weak ground motions and strong ground motions and also the Predominant Frequency.
6. The geophysical survey including noise/micro tremor observations for determination of

predominant frequency and peak amplification, VES (Vertical Electrical Sounding) for determination of lithological variation and groundwater condition and, Multichannel Analysis of Surface Waves (MASW) to calculate the instrumental shear wave velocity at surface.

7. Estimation of liquefaction susceptibility based on grain size analysis and its derivative curves and safety factor at different depths of study area.
8. Finally integration of all the thematic maps' (viz. Geological, geomorphic, land use, average shear velocity, peak amplification, liquefaction susceptibility and predominant frequency maps) data for preparation of seismic microzonation map of study area on Arc GIS platform along with its statistical validation.

Table 1.1: Nature and quantum of work and time schedule (FS 2016-17 and 2017-18)

Sl. No	Nature of work	Total work load envisaged	Work completed
Geological studies (1: 25,000)			
1.	Preparation of geological map by compilation and collation of available data and selective field checks.	300 sq km	300 sq km
2.	Preparation of geomorphological map by compilation and collation of available data and selective field checks.	300 sq km	300 sq km
3	Preparation of Borehole Plan for drilling and reconnaissance survey to finalise the locations.	300 sq km	300 sq km
4	Preparation of land use map (on the basis of IRS imagery)	300 sq km	300 sq km
5	Preparation of Ground water map.	300 sq km	300 sq km
6	Preparation of shear wave velocity map (Vs30) using SPT data with the help of empirical relation between N value and shear wave velocity.	300 sq km	300 sq km
7	Preparation of site response map. (Based on drilling and geophysical investigation data)	300 sq km	300 sq km
8	Grain size analysis	100 No. core samples	110 No. core samples
9	Drilling with SPT at 1.5m interval (in a grid interval of 12 sq km approx.)	a) 26 bore holes each of 30m length-780m + 2 B.H. of 60m length-120m Total length=900m. b) SPT-20 no. per B.H. in all 26 B.H.-572 nos. +6 nos. between 30m and 60m in 2 deeper bore holes Total SPT= 584 nos. c) core logging=900 m	a) 900m b) SPT=584nos. c) core logging = 900 m
14	Noise survey utilizing digital MEQ recorders.	300 sq km	300 sq km
15	Electric resistivity soundings surveys.	100 Nos.	100 Nos.
16	Determination of shear wave velocity using 24 channel seismograh and MASW.	50 Nos.	56 Nos.

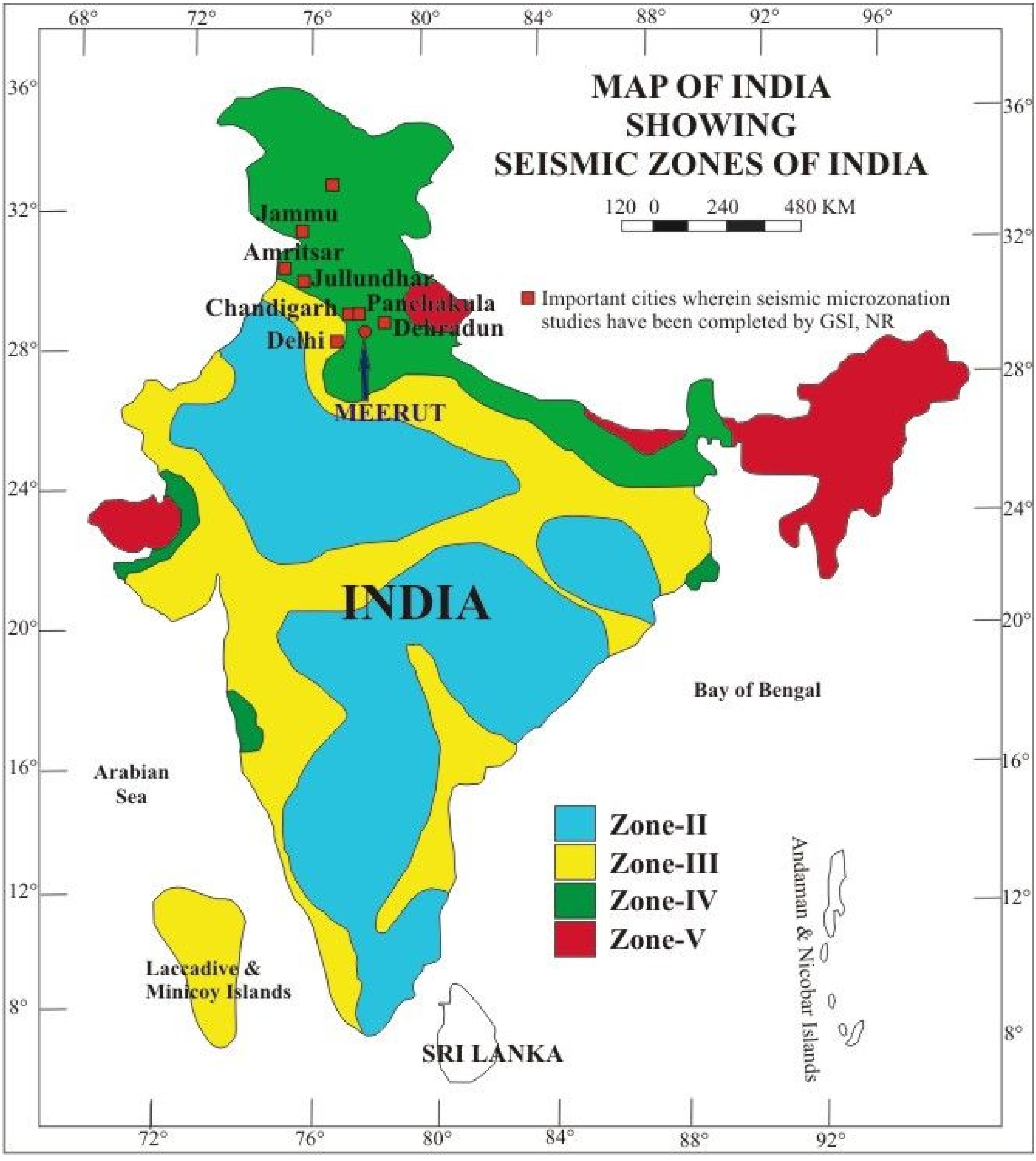

Fig. 1.1: Seismic Zoning Map of India (BIS, 1893-2002), showing location of Meerut

1.2 Location and Accessibility

The study area covers part of Survey of India Toposheet No. 53 G / 12, 13 and 53 H / 9, 13 between Latitudes N 28^0 54' 42" and N 29^0 07' 39" and Longitudes E 77^0 37' 30" and 77^0 47' 30" of Meerut district, Uttar Pradesh. Meerut is located in the north-western part of the State (Figure 1.2) and is well connected with Delhi, Ghaziabad and Dehradun by National Highway No. 58. Interior parts of the area are connected by a number of metalled and unmetalled link roads. There are two bus terminals in Meerut City namely Bhainsali Bus Terminal and Sohrab Gate Bus Terminal from where Uttar Pradesh Road Transport Corporation (UPSRTC) buses ply to other cities. Meerut is connected with Delhi-Saharanpur railway section and direct trains are available from here for important cities of the country. A small airport named as Dr. Bhim Rao Ambedakar Airport is situated at Partapur, Meerut.

1.3 Physiography and Drainage

Meerut City falls in interfluve region between Ganga River (to the east) and Yamuna River (to the west) of the Gangetic Plain. Meerut is settled on a level plain area having elevation variation from about 210 m to about 223 m. Kali River is the solitary drainage in the eastern part of Meerut flowing north to south. The general slope is towards southerly direction. The soil/sediments in Meerut City are composed of the Pleistocene to sub-Recent age alluvial sediments of fluvial systems originated in the Himalayas. These alluvial deposits consist of mainly clay, silt and sand. The aeolian sediments forming small mounds are present at a few places in the eastern and southern parts. Many natural and manmade small ponds are present in the Meerut City. Overall physiography of the Meerut City is upland surface of the Older Alluvium of the Gangetic Plain.

1.4 Vegetation

Meerut City is mainly an urban agglomeration along with some peripheral sub-urban area showing agricultural practices. The principal kharif crops are paddy, cotton, maize and sugarcane along with subsidiary crops of kharif vegetables. The principal rabi crops are wheat, gram, barley and barseem. Some species of trees also grow luxuriantly such as Mango, Neem, Shisham, Kikar, Jamun and Pipal constituting the natural vegetation in the area. The Babul trees are spread over the area where reh deposits (alkaline soil) are present. Meerut caters the need of surrounding areas as a major commercial centre and agriculture product distribution centre.

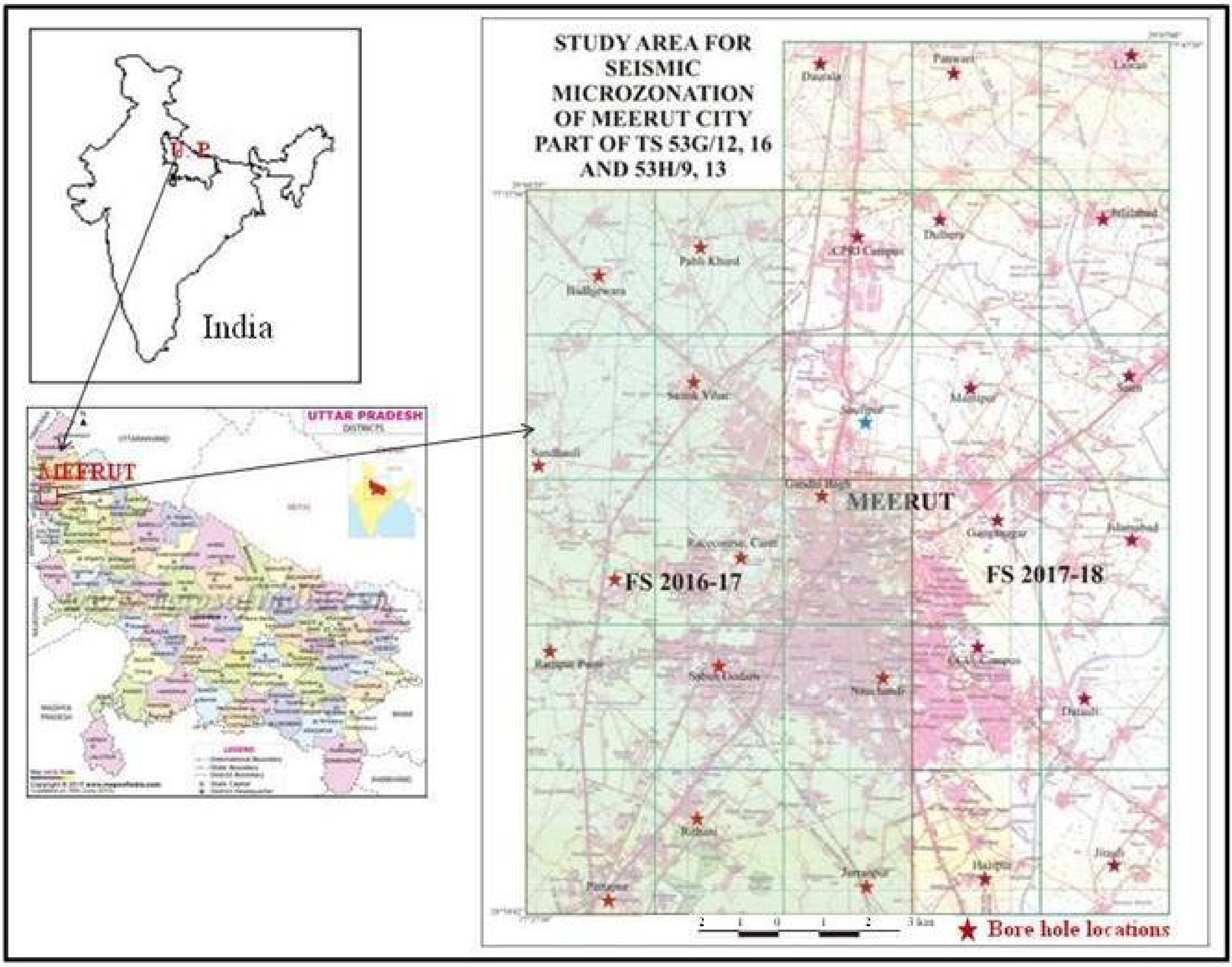

Fig. 1.2: Location map of the study area

1.5 Climate

The climate is characterized by generally dry weather except during the brief south-west monsoon season (June to September); a hot summer and a bracing winter. The area experiences winter season (November to March) when temperatures range from 16°C (61 °F) to about 4°C (39 °F), the summer season (April to June) when temperatures can reach up to 49 °C (120 °F). Meerut receives on an average of 845 mm annual rainfall. About 75% of the rainfall in the district is received during the period from June to September and about 18% occurs during the period from December to February. Relative humidity in Meerut varies between 25% to 80%. The lowest recorded temperature since 1970 is -0.4 °C (32.2 °F) recorded on 6 Jan 2013. The dominant wind direction in Meerut and the surrounding areas is from North-West to South-East.

1.6 History and Demography

The city may have derived its name from the Sanskrit word *'Mayarashtra'*, the capital of the kingdom of Mayasura, Mandodari's father and Ravana's father-in-law. The name *Mayarashtra* in the course of time got shortened to Meerut. Relics and remains dating proves that this region was the capital of the Kauravas and Pandavas. Since Meerut is between Indraprastha (present day Delhi) and Hastinapur, there are a number of sites dating back to the ages of Ramayana, as well.

Meerut also encompasses one Harappan settlement known as Alamgirpur. It was also the eastern-most settlement of the Indus valley civilisation. Meerut had been a centre of Buddhism in the period of Mauryan Emperor Ashoka (273 BC to 232 BC), and remains of Buddhist structures were found near the Jama Masjid in the present day city. The Ashoka Pillar, at Delhi ridge, next to the 'Bara Hindu Rao Hospital', near Delhi University, was carried to Delhi from Meerut, by Firoz Shah Tughluq (1351 AD to 1388 AD).

Later, parts of the Meerut district came under the rule of Walter Reinhardt, the English ruler who ruled Sardhana during those times. The Britishers by then had established their hold in India, and had established the Cantonment in Meerut in 1803.

Meerut is popularly associated with the First War of Indian Independence. The Sepoy Mutiny as it is popularly called saw its beginnings here at Meerut Cantonment. After a series of diabolical laws, oppressive rules, the Indians were waiting for an opportunity to revolt against the British. The Indian soldiers or the Sepoy were called Kali Paltan by the British. During this time, the British had introduced the new kind of rifle called the Enfield Rifles of 1853. Before loading the rifles the soldiers had to bite the cartridges open to release the powder. The paper cartridges were tightly bound and pre-greased using either tallow that was derived out of beef or with lard that was derived out of pork. This hurt the religious sentiments of both the Hindu and Muslim soldiers. They opposed to follow the orders of Britishers. Under the leadership of Kotwal Dhan Singh Gurjar, the leader of Meerut Kranti movement opened the gates of the jail and set nearly 900 prisoners free, and also killed 50 of the British officers and their families. This marked the nationwide stir and the famous "Dilli Chalo" movement was started with the soldiers in large numbers marching towards Delhi. Meerut was also the venue of the controversial Meerut Conspiracy Case in March 1929, in which several trade unionists, including three Englishmen, were arrested for organising Indian-rail strike. The last session of the Indian National Congress before Indian

independence was held at Victoria Park in Meerut on 26 November 1946. It was in this session that the Constitution-making committee was constituted.

Meerut is the sub-divisional administrative headquarters. It serves as a major hub of education and health centre to its surrounding region. This city is, also, an industrial centre of Uttar Pradesh mainly for sports goods and sugar. Meerut is the second largest city in the National Capital Region, and as of 2011 census the 33rd most populous urban agglomeration and the 26th most populous city in India. It ranked 292 in 2006 and is projected to rank 242 in 2020 in the list of largest cities and urban areas in the world.

The growth of the population is manifold in Meerut (table 1.2and Figure-1.3). The data show that since 1981 to 2011 the population of Meerut has almost increased by 2.5 times.

Table 1.2: The year wise population and its growth during 1901-2011

S. No.	Year	Population (in lacs)
1.	1901	1.21
2.	1911	1.19
3.	1921	1.26
4.	1931	1.41
5.	1941	1.79
6.	1951	2.39
7.	1961	2.95
8.	1971	3.72
9.	1981	5.37
10.	1991	8.50
11.	2001	11.61
12.	2011	13.5

The population density in Meerut City as per 2001 census was of the order of 7400 persons/sq km. The density of Meerut Cantt area then stood at 2600 persons/sq km. In the Older central Meerut City the density is as high as 20000 persons per square kilometre (census, 2001). Such a high population density, in along with the fact that the area falls under Seismic Zone IV made Meerut a fitting case for taking up seismic microzonation studies.

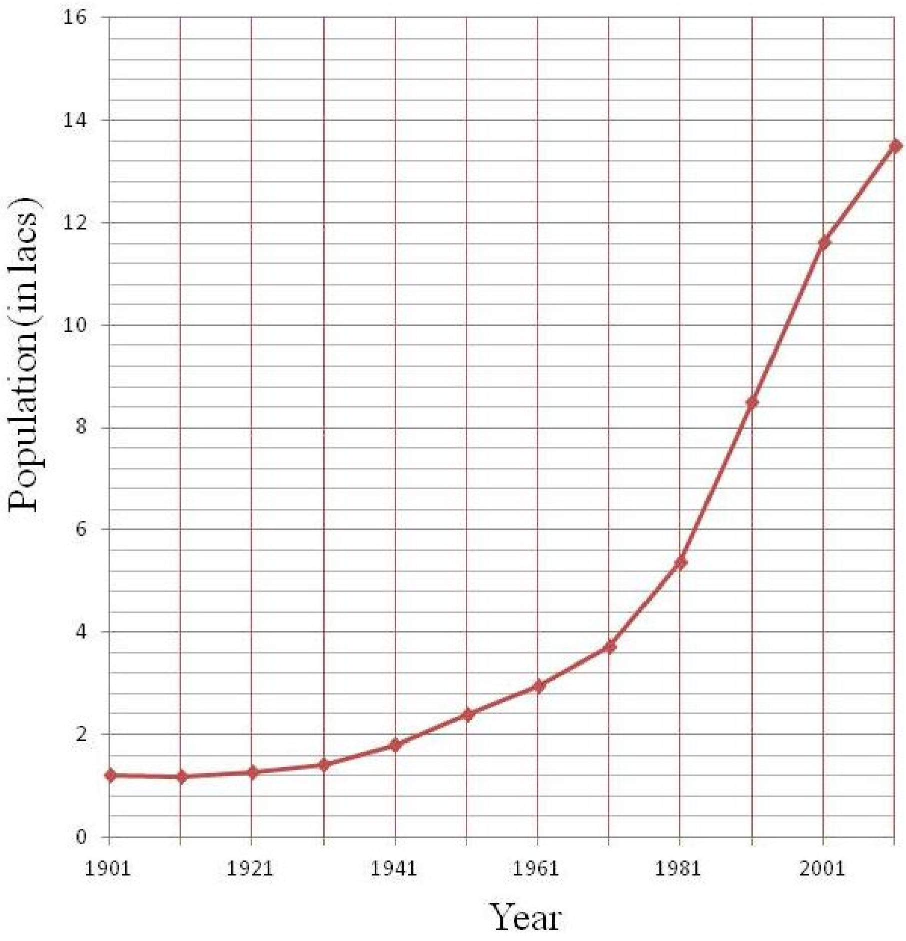

Fig. 1.3: The decadal growth of population of Meerut City from 1901-2011.

1.7 Previous work

The Quaternary geological and geomorphological mapping by Geological Survey of India (GSI) in Meerut and surrounding areas was carried out by many workers. Anand et al., 1990 studied the geology and geomorphology of parts of Ganga Basin, Meerut, Muzaffarnagar and Saharanpur districts, Uttar Pradesh and Gadhole and Khullar, 1991 carried out Quaternary geology and geomorphology of parts of Muzaffarnagar, Bijnor and Meerut districts, Uttar Pradesh. They postulated that the Quaternary sediments are represented by the Older Alluvium and Newer Alluvium. The Older Alluvium designated as Varanasi Older Alluvium is extensively developed and composed of a polycyclic sequence of oxidised yellow to brown coloured silt-clay and micaceous sand. Disseminations of *kankar* as nodular concretions and bands occur in these sediments. The Newer Alluvium is represented by the reworked sediments of the Older Alluvium sediments and Himalaya along the active flood plains. Thussu et al., 1991 studied the Quaternary geology and geomorphology of parts of Ganga Basin in Meerut, Ghaziabad and Bulandashahar districts of Uttar Pradesh including the preliminary appraisal of environmental hazards, landform and land use interrelationship,

mineral resources, sedimentation history and neotectonism in above mentioned areas. He stated that the vast stretch of the Older Alluvium is laid by older fluvial agencies and deposited in gradually sinking foredeep as both channel fill and bank deposits. Phases of deposition are indicated by the presence of thick bedded kankar nodules within the fluvial sequence. Semi-arid conditions are evident by the presence of sand dunes overlying the Varanasi Older Alluvium. The reworked sediments of the Older Alluvium have been deposited along the channel of Kali Nadi as point bar, channel bar and depositional terraces. Direct evidence of neotectonism in the area are lacking, however, entrenchment of Kali Nadi is indicative of neotectonic activity in near past.

1.8 Acknowledgement

The authors humbly acknowledge the help rendered by S/Sh Som Nath Chandel, Additional Director General and Head of Department and earlier Shri S. P. Nim, the then Additional Director General and Head of Department, Northern Region, GSI, Lucknow by way of providing logistics and other infrastructural support. The authors wish to acknowledge Smt. Varsha A. Aglawe, Dy. Director General and Regional Mission Head, Mission-IV in for the valuable suggestions given during the course of study. The authors are indebted to Dr. Ram Jivan Singh, Director, Earthquake Geology Division, GSI, NR, Lucknow for his guidance and valuable suggestions provided throughout the course of this investigation, which to a large extent has contributed in the successful execution and accomplishment of the objectives assigned. The authors express their gratitude to Shri K. C. Joshi, Director (Retd.) for his expert guidance during formulation and initial execution of the project. The authors are thankful to the officers of Geotechnical Laboratory, NR, GSI, Lucknow for timely providing results of analysis of the large number of samples during the course of study. The authors wish to put on record their thankfulness to District Magistrate, Meerut and A. D. M. (F/R), Meerut for providing logistic support in accomplishment of the assignment.The authors express their gratitude towards Station Commander, Meerut Cantt., CEO, Meerut Cantt, Asstt. Director, CPRI, Meerut for providing space for drilling sites in the campuses under their control and extending support during the course of drilling. Lastly but not the least, the authors are thankful to the colleagues, seniors officers, Superintending Geologists and Directors posted at GSI, Lucknow for their valuable suggestions and help given during study.

The authors from Geophysics Division thank Dr. Narendra Singh, Director (GP) and Dr. Sagina Ram, the erstwhile Director (GP) for overall supervision, technical guidance, analysis/interpretation of the data and critical scrutiny of the report during the course of investigations in F.S. 2016-2017 and 2017-18. They also wish to thank Dr. Ram Jivan Singh, Director (Geology), Earthquake Geology Division for his fruitful suggestions and technical discussion during the course of investigation and preparation of the report.

II. GEOLOGY, GEOMORPHOLOGY, LANDUSE AND HYDROLOGY

2.1 Regional Geological Set-up

Meerut City lies in the Indo-Gangetic Plain. Regionally, the Indo Gangetic Plain is bounded by the Himalayan tectonic belt in the north and the Proterozoic rocks of Delhi fold belt and Bundelkhand Gneissic Complex in the south. In the interfluves of Ganga River in the east and Yamuna River in the west, Meerut City is settled on alluvial fill deposits of the Indo Gangetic foredeep and devoid of any hard rock exposures. The study area is mostly represented by the Older Alluvium surface along with little Newer Alluvium. The Older Alluvium consists of oxidised clay, silty clay and micaceous sand layers. The Newer Alluvium comprises non-oxidised sand, silt and clay deposits. The northernmost entity, the Extra-Peninsular Belt (Himalayan Belt) is mainly occupied by "cover sequence of the frontal belt (i.e. Siwalik)" which show clear imprints of the terminal phase of the Himalayan Orogeny.

The Quaternary sediments both of fluvial and aeolian nature are exposed in Meerut area. The fluvial sediments are classified into the Older Alluvium (i. e. Varanasi Older Alluvium) and Newer Alluvium, depending on their lithological association and geomorphic setup. The Newer Alluvium is represented by reworked Older Alluvial sediments and active flood plain deposits. The major part of Meerut City is occupied by the Older Alluvium sediments, represented by Varanasi Alluvium of the Middle to Late Pleistocene age. It comprises polycyclic sequence of oxidised, khaki to brown silt-clay with kankar and fine to medium grained micaceous sand. This sequence has been classified into clayey and sandy facies. The widely developed clayey facies occupies major part of the area whereas sandy facies is developed in patches as flats and mounds. The calcretes are persistent in the Older Alluvium sections. Few sections observed near Jurranpur have persistent 0.75 m to 1m thick kankar beds with iron nodules.

The Newer Alluvium of the Holocene age shows very limited development and is designated as the Channel Alluvium. It is confined to present day course of Hindan River, Kali *Nadi*(West) and Kali *Nadi* (East). It comprises grey, fine to medium grained, micaceous sand and silt. The aeolian deposits of the Holocene age comprise yellowish fine to medium grained sand with minor silt and siliceous *kankar*. Subsurface data at Saharanpur by ONGC,

which is 120 km north of Meerut, indicates that the underlying sediments at a depth 2245 m below the ground surface lie on the basement rocks of the Vindhyan Supergroup.

Regionally, the area is bounded by the Foot Hill Fault/ Himalayan Frontal Thrust (HFT) demarcating the Siwalik foot hills in the north from the Indo-Gangetic Plain in the south. The recent small magnitude earthquake occurrences along HFT are the evidences of neotectonics in the area. On the basis of field observations, the lithostratigraphy and geomorphic features of Meerut and surrounding areas (Figure 2.3) are given in Table 2.1.

Table 2.1: The lithostratigraphy of the study area (Thussu *et al.,* 1991)

Age	**Formation**	**Morpho stratigraphic Unit**	**Geological lithological unit**	**Characteristic Geomorphic/Landform elements**	**Generalised Lithology**
Holocene to Recent	Newer Alluvium	Kali Recent Flood Plain	Kali Recent Alluvium (1-5m thick)	Erosional terraces, channel Deposits, point bars.	Light yellowish to greyish fine to medium sand occurring as isolated mound over the aeolian sediments or as linear patches along the Kali *Nadi*
		Bhur Surface	Sandy facies (1-12m thick) (Aeolian unit)	Aeolian dunes stabilised/Semistabilised dunes, Aeolian flats.	Brownish coloured oxidized, medium to fine micaceous sand with somesilt.
Middle-Upper Pleistocene	Older Alluvium	Varanasi Older Alluvial Plain	Varanasi Older Alluvium (400-600m)	Upland surface with palaeo channels, buried channels, palaeo-taals/ponds	Polycyclic sequence of grey brown sand yellowish sandsilt and clay nodular and bedded kankar & green micaceous sand.

2.2 Geology

The study area mainly comprises sediments ranging in age from the Middle Pleistocene to Upper Pleistocene of the Older Alluvium and consist of polycyclic sequence of coarse to fine yellowish brown sand, silt and clay with kankar (Fig 2.1 a, b and 2.3). The sand is micaceous, brownish grey, fine to coarse grained with sub-angular to sub-rounded grains. It is mainly composed of quartz, biotite, muscovite with accessory minerals like magnetite and feldspar. The silt invariably contains some fraction of clay and fine sand. The upper horizon consists of clay with *kankars* and small iron nodules. The size of *kankar* varies from 0.5 cm to 2 cm. The sand silt and clay layers define horizontal beddings. The small mounds of Aeolian sand and Aeolian flats are exposed near Jurranpur and Datauli. In south western part, near village Rithani, the *Reh* soil occurs (Figure 2.2 and 2.3). Here the salts of

sodium, calcium and magnesium are deposited on the upper layer of the soil by capillary action in semi arid condition. The Reh soils developed in areas having a little more rainfall than the areas of desert soils accompanied by lack of proper drainage. These soils are not fit for agricultural activities. Plenty of babool trees occur in this part of study area.

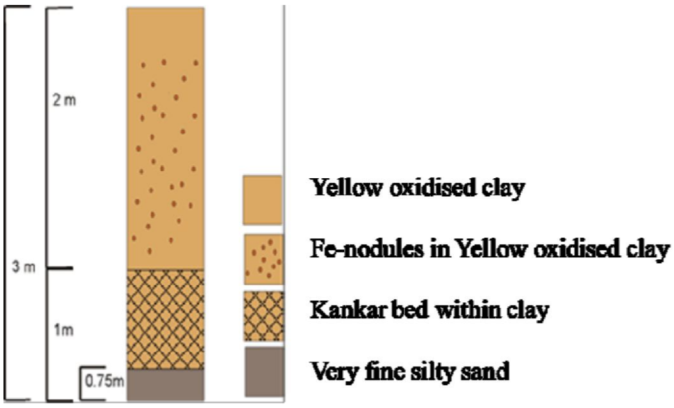

Fig. 2.1(a): Older Alluvium section, Lisari village

Fig. 2.1(b) Older Alluvium section exposed near Jithauli Power Station, Meerut

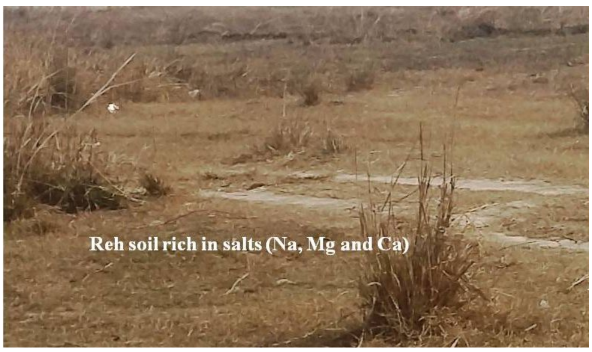

Fig. 2.2: The Reh soil near Rithani village, Meerut.

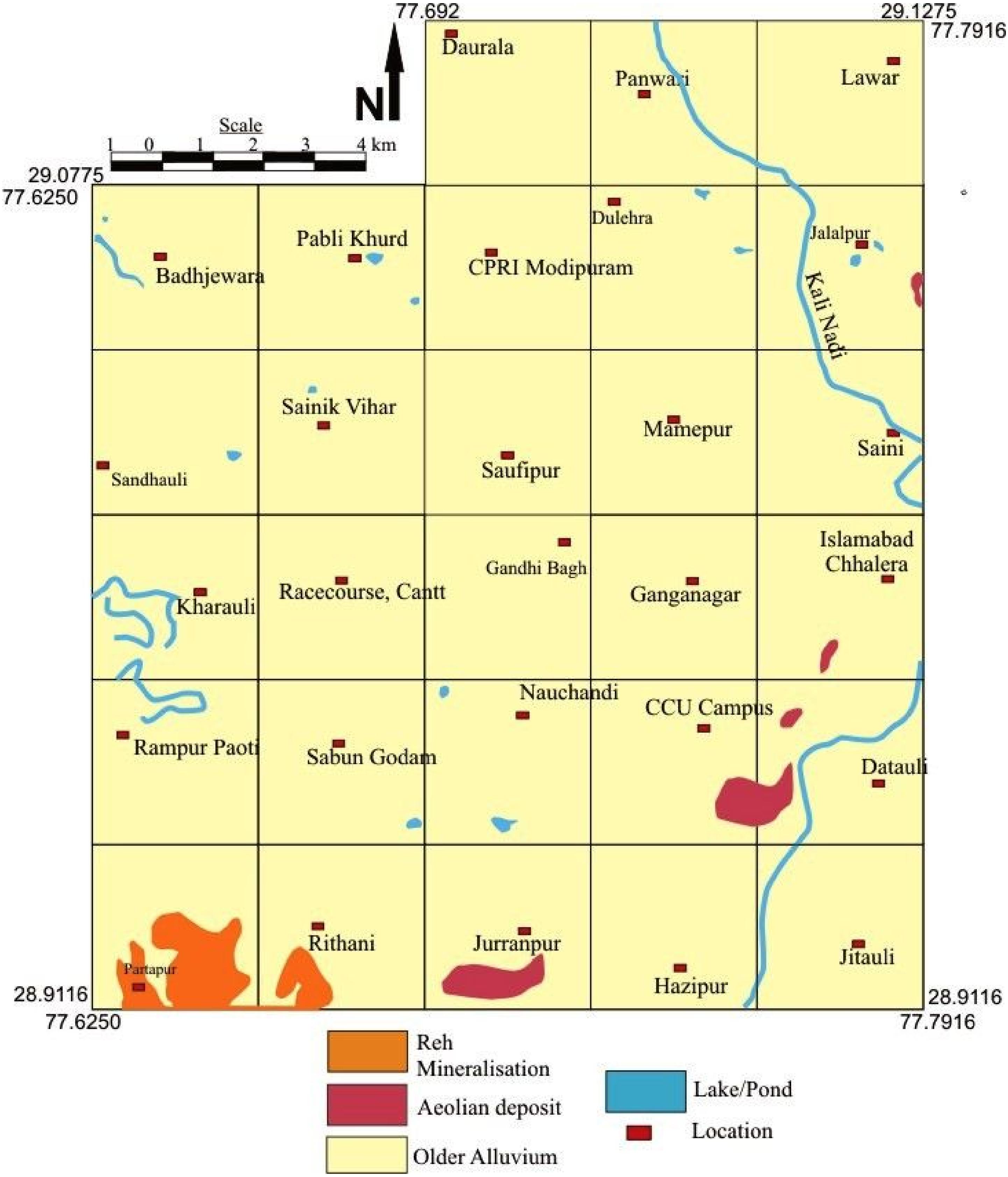

Figure 2.3: The geological map of the area (based on 1:50000 geological map of GSI)

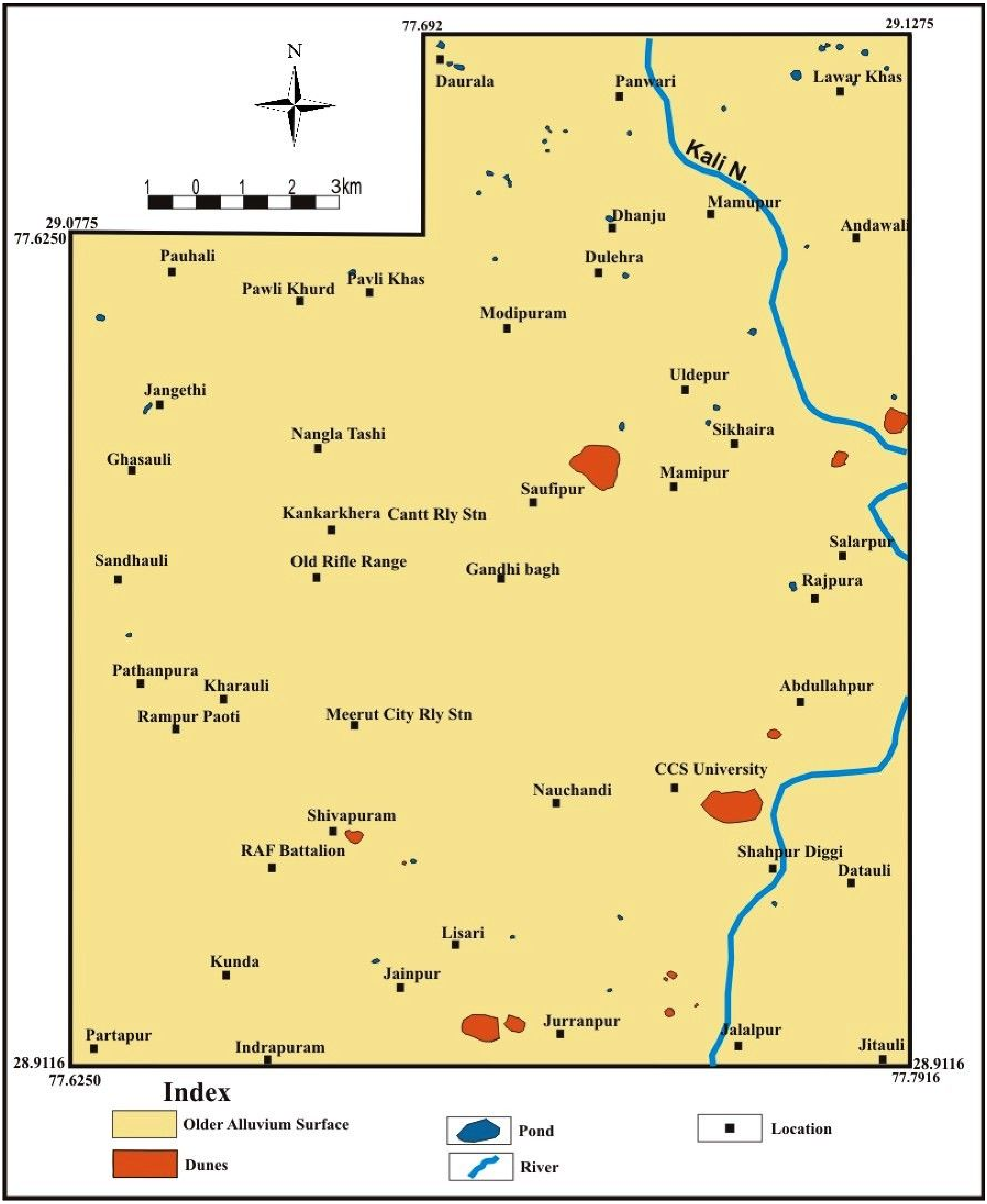

Figure 2.4: The geomorphological map of the area (Meerut City)

2.3 Geomorphology

Majority of geomorphological features in Meerut area owe their origin to the fluvial processes and form the part of Upper Ganga Plain. These are represented by (i) Upland-Varanasi Plain and (ii) Lowland-Newer Alluvium Plain defining flood plain of rivers. The widely developed clayey facies of the Older Alluvium occupies major part of the area whereas sandy facies is developed as mounds and ridges. This Older alluvium upland surface covers major part of the mound area and is the highest flood free surface. It is dotted with palaeochannels, sand mounds and *taals/* ponds (Fig 2.4). The lowland is divisible into Older Flood Plain and Active Flood Plain. The Older Flood Plain, represented by erosional terrace (Te) is developed along Kali *Nadi*(Figure 2.5). The Active Flood Plain is confined to the present day course of Kali *Nadi.* The aeolian surface is represented by isolated aeolian flats, semi stabilised and stabilised dunes around Abdullapur, Jalalpur and Jurranpur villages. There is monotonous flat land topography of the Older Alluvium surface along with few ponds, aeolian mounds and degradational Kali *Nadi* channel.

Fig. 2.5: Erosional Terrace (Te) of Kali Nadi near Jithauli village, Meerut

2.4 Geohydrology

The study area is a part of Kali sub basin which itself is a part of much larger Ganga Yamuna basin, a distinct regional physiographic unit in India. The area is underlain by the Quaternary age alluvial deposits of Himalayan Rivers in the Gangetic foredeep setting. These deposits, which are exposed mostly in road cut/ trench sections comprise fine to coarse grained sand, silt, clay with *kankar*. The area exhibits a gentle southward slope. The studies carried out by CGWB including 3-D multi-log and fence diagram depict the aquifer disposition and lithological variation in Meerut district (Figure 2.6 A and B). The map illustrates the good quality of aquifers in sand layers mostly in north-eastern and south-eastern parts of Meerut. The depth of boreholes ranges from 450 m to 471 m. The geophysical logs of the boreholes by CGWB indicate the presence of fresh water aquifer throughout the depth drilled.

During the course of this investigation, in an area of 300 sq km encompassing Meerut city and surrounding localities, 26 boreholes were drilled down to a depth of 30 m below ground level and 2 bore holes of 60 m depth. The water table depth varies from 8.5 m to 29 m and their spatial distribution in Meerut is shown in Figure 2.6 C, D and E.

The groundwater depth (Table- 2.2) and derivative contour map (Figure 2.7) show shallower ground water depth toward SW and NW portions of the area. In Meerut City, the shallow water depth (up to 10 m) occurs in 14% of total area in SW and NW part. In these areas the probability of occurrence of liquefaction is relatively high. The moderate water table depth (10 m to 15 m) is found in 36% area of Meerut City, where that very strong ground shaking needed for liquefaction. In remaining part of Meerut where water table depth is more than 15 m, the possibility of liquefaction during seismic shaking is negligible. It is deeper in the main city around Nauchandi, Race Course, Gandhi Bag and in the south-eastern part around Jithauli-Datauli areas (Fig. 2.7).

Table 2.2: Ground water depth at different bore hole sites in Meerut City (based on drilling data)

Bore Hole Number	Latitude in degrees N	Longitude in degrees E	Location	Depth of water table below ground level (m)
MER-1	28.92883	77.66072	D.N . Polytechnic,Rithani	15
MER-2	28.91961	77.71378	Jurranpur	12
MER-3	28.98244	77.64958	Kharauli	16.5
MER-4	29.00458	77.62286	Sandhauli	12
MER-5	28.91764	77.64764	Partapur	8.5
MER-6	28.97514	77.63475	Rampur Paoti	13
MER-7	29.0509	77.64553	Badjewra	10.5
MER-8	29.06517	77.66969	Pabli khurd	13.05
MER-9	28.96811	77.67131	Jaswant mill Sabungodam	17.55
MER-10	28.99189	77.68042	Race course,Cantt	19
MER-11	29.00006	77.70392	Gandhi bagh	19.5
MER-12	28.96536	77.70072	Nauchandi	29
MER-13	29.03506	77.65266	Sainik vihar,water tank	10.5
MER-14	28.95489	77.77044	Datauli	21
MER-15	28.91833	77.74347	Hajipur	21
MER-16	28.92181	77.77617	Jithauli near Power house	21.8
MER-17	28.99383	77.78586	Eslamabad chillaura	21
MER-18	29.02983	77.74178	Mamepur	19.5
MER-19	29.03208	77.783	Saini village	18
MER-20	29.07147	77.77644	Jalalpur	15
MER-21	29.0725	77.72947	Dulehra	14.55
MER-22	29.11542	77.69975	Daurala	10.5
MER-23	29.10175	77.73547	Water tank campus,Panwari	14.5
MER-24	29.10383	77.78681	Lawar khaas,cold storage	15
MER-25	28.97214	77.74356	Chaudhary Charan Singh University	22.5
MER-26	29.007	77.75453	Water tank campus,Ganganagar	19.5
MER-27	29.06728	77.70778	CPRI Modipuram	13.5
MER-28	29.02364	77.71139	Saufipur	16.5

A

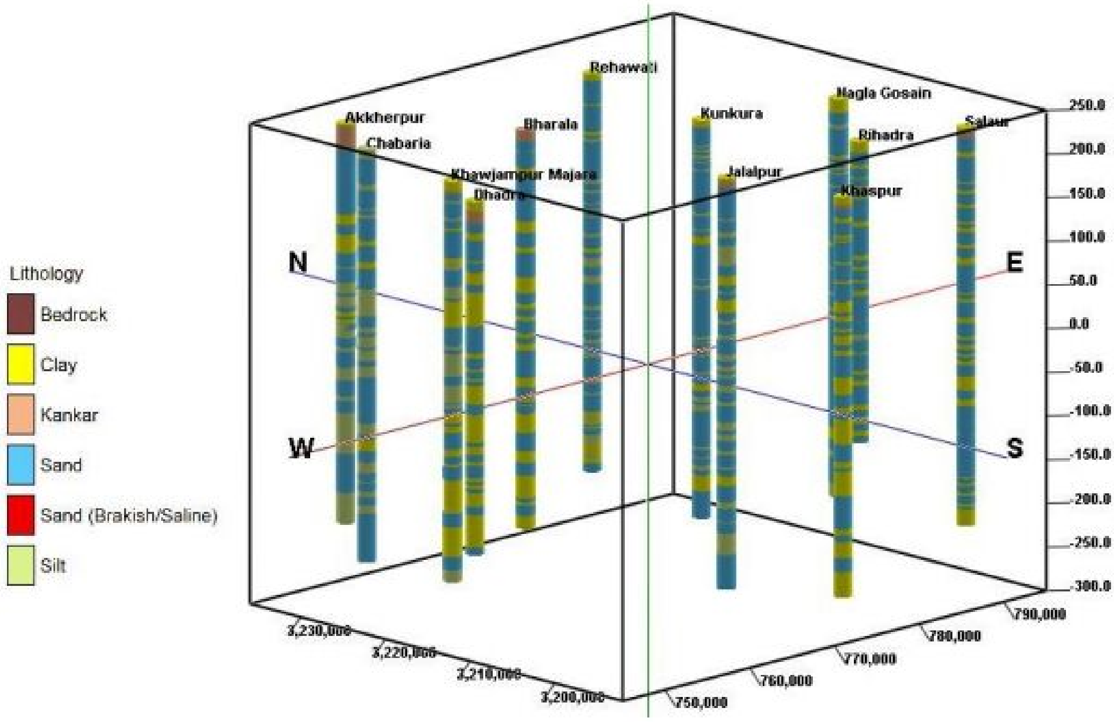
Lithology
Bedrock
Clay
Kankar
Sand
Sand (Brakish/Saline)
Silt
Akkherpur
Chabaria
Khawjampur Majara
Dhadra
Bharala
Rehawati
Kunkura
Jalalpur
Nagla Gosain
Rihadra
Khaspur
Salaur
N
E
W
S
250.0
200.0
150.0
100.0
50.0
0.0
-50.0
-100.0
-150.0
-200.0
-250.0
-300.0
3,230,000
3,220,000
3,210,000
3,200,000
750,000
760,000
770,000
780,000
790,000

B

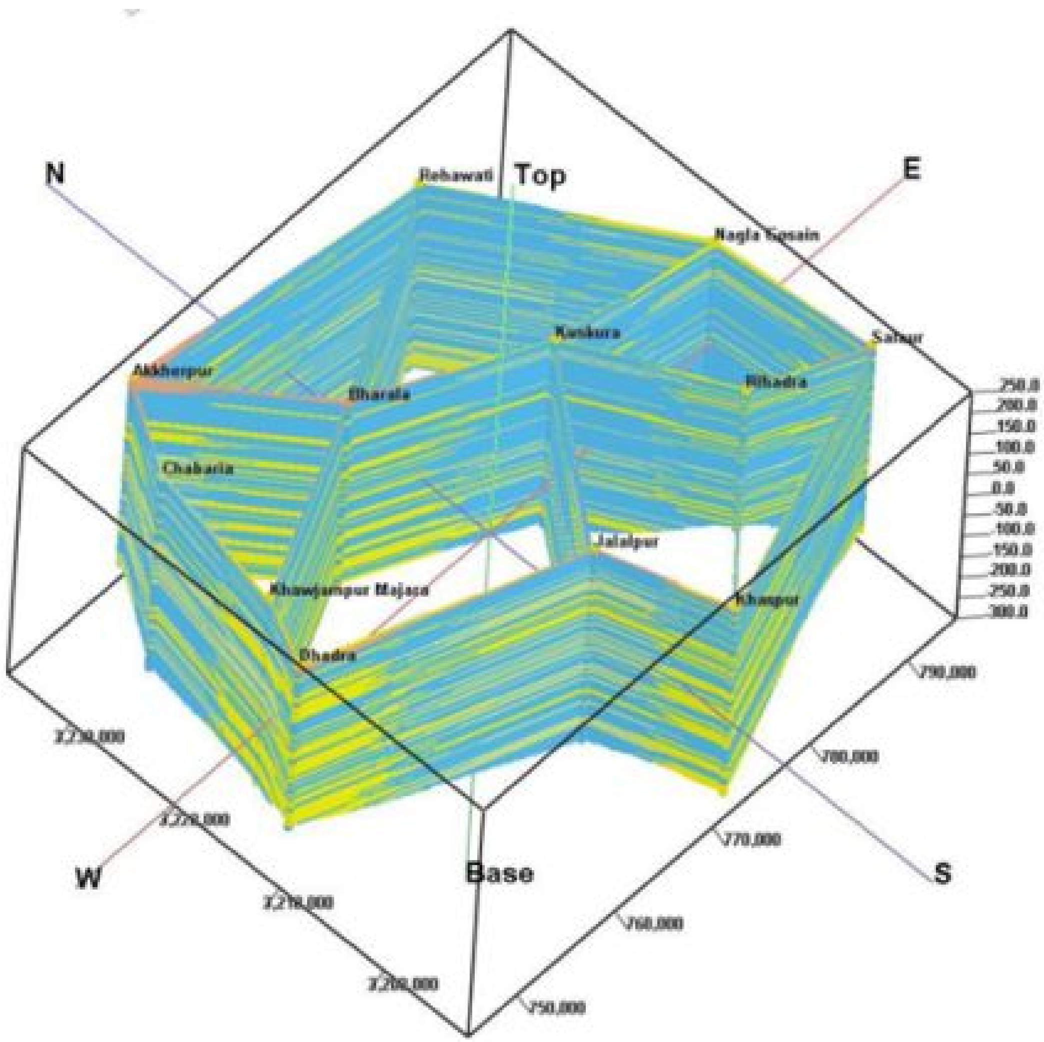
N
E
W
S
Top
Base
Rehawati
Nagla Gosain
Kunkura
Salaur
Akkherpur
Bharala
Rihadra
Chabaria
Jalalpur
Khawjampur Majara
Khaspur
Dhadra
790,000
780,000
770,000
760,000
750,000

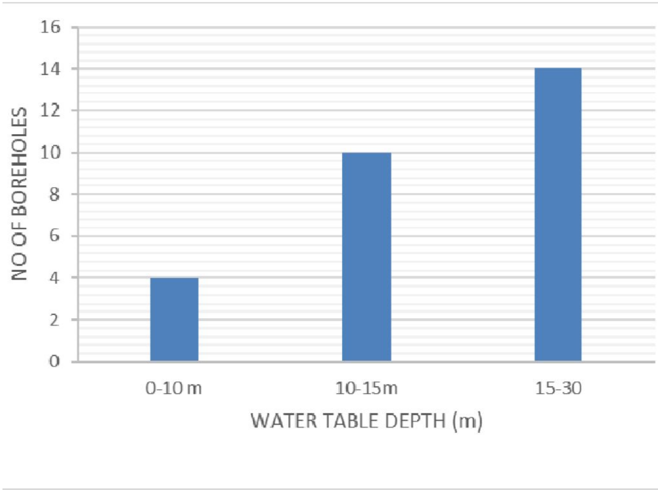

C

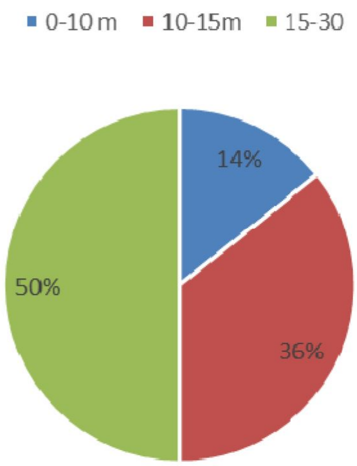

D

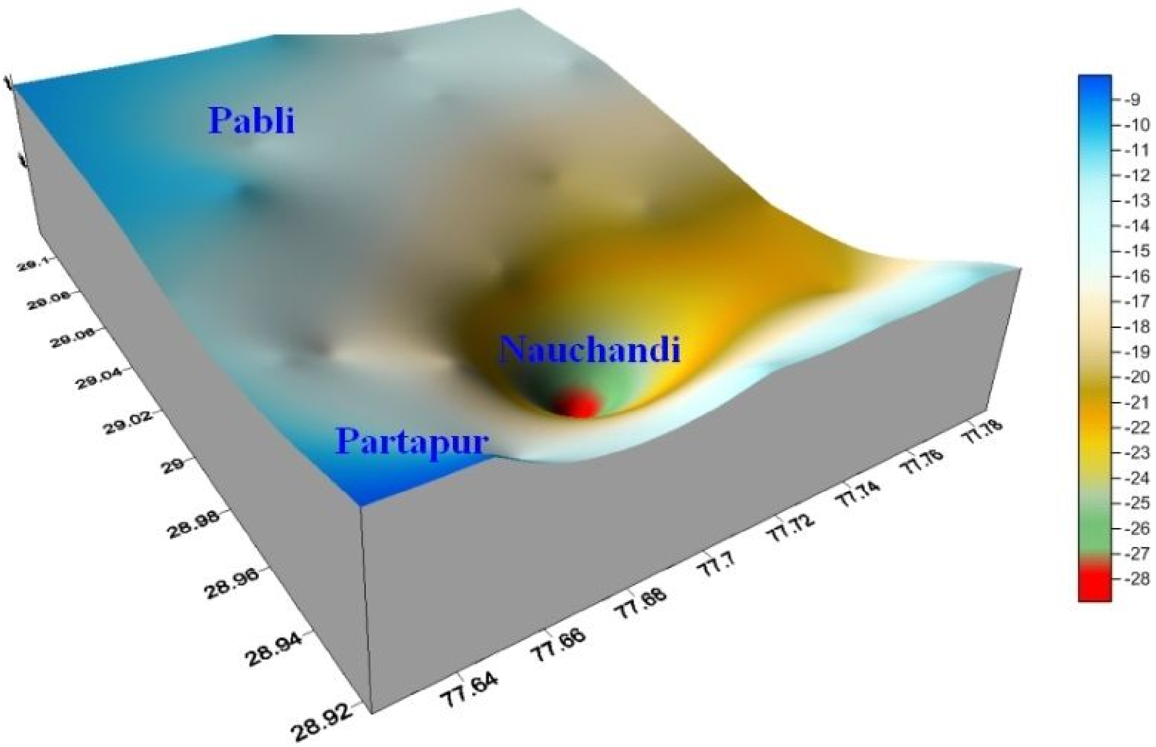

E

Fig. 2.6: A)- 3-D Multi-log; and B)- fence diagram of aquifer disposition and lithological variation of Meerut (CGWB); C) and D)- histogram and pie diagramme showing the distribution of different water table in Meerut; and E)- 3-D depiction of ground water depth at 28 different location in Meerut City

2.5 Mineral Resources

The economic resources of the area are masonary sand and silt-clay. The river sand is suitable for masonary purposes whereas the silt-clay of Varanasi Older Alluvium is being used for making bricks. The subsurface sandy zones form excellent aquifers that sustain

agriculture in the area. Top soil cover, mostly of clay and silty clay layers, are very fertile for agricultural practices. The alkaline soil covers, found in pockets (Figure 2.1) contain Reh deposits, which are rich in sodium bicarbonate.

2.6 Land Use and land Cover

Major part (i.e. 70%) of the total study area is under human settlement. It spreads largely on the Upland Plain which due to their even surface, loamy soil texture and availability of water is suitable for habitation. About 71% area of the part of Meerut City taken for present investigation is under habitation, 25% is under agricultural use, 3% is barren land and 1% under forest covers.

Land Use of the study area (Meerut City) is demarcated with the help of Bhuvan Imagery. Multi-date satellite imageries of IRS-P6 LISS III generated from Green, Red and NIR bands used for land use mapping were visually interpreted to delineate various land use and land cover categories. Field survey was carried out to check the validity of various land use classes and sub classes. Land use land cover classes were digitized using Arc-Info GIS package. The area is divided into the Settlement (including residential, industrial, commercial, public, road network, etc), Agriculture land and Forest Cover (Figure 2.8). Built-upland includes urban as well as rural settlement. The urban settlement is about 60% covering central and northern parts of the study area. Most of the development and human inhabitation are restricted to National highways along Modipuram in the north, Ganganagar colony in the east and along Delhi-Ghaziabad highway in the south. Agriculture land is mainly restricted to peripheral outskirts of the city.

Based on the study of Quickbird imagery of 2008 and IKONOS data of 2013, the urban built-up area of the city was found to be expanded from 3752.3 hectare to 8331 hectare indicating an expansion of more than double during 5 years. The city has grown mainly towards north direction and marginally towards south-west and south-east directions wherein most of the prime agricultural land and vegetated areas were being transformed into built up land. Land use map of Meerut City has been prepared on the basis of the Master Plan 2012-21 (www.mda.nic.in) including different sub classes (Figure 2.9). The map shows probable expansion of Meerut City during 2012-21. The population density of different clusters is shown in the map (Figure 2.9).

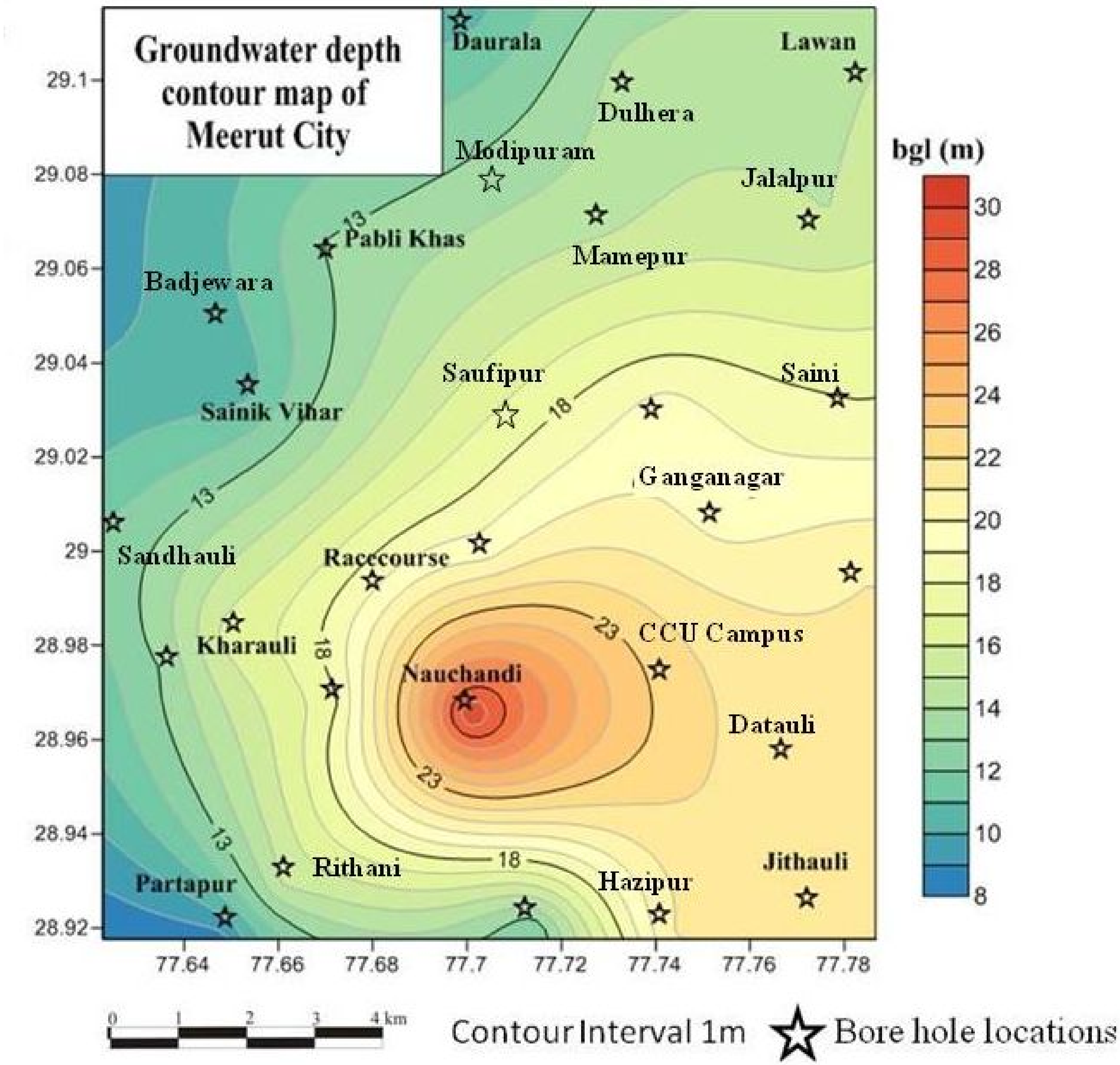

Figure 2.7: Groundwater depth contour map of Meerut area (based on present drilling investigation).

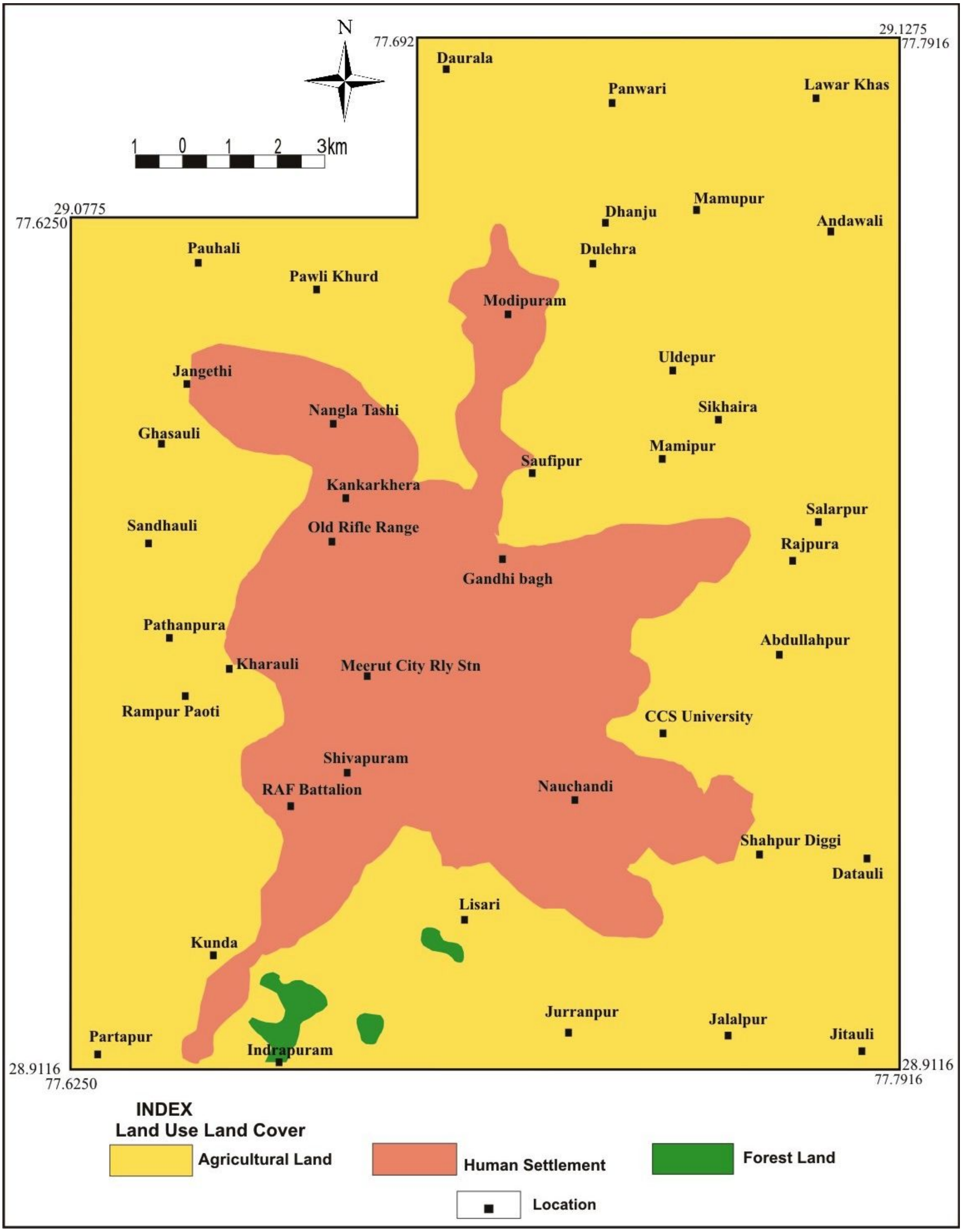

Figure 2.8: Land use map of the study area based on satellite imageries

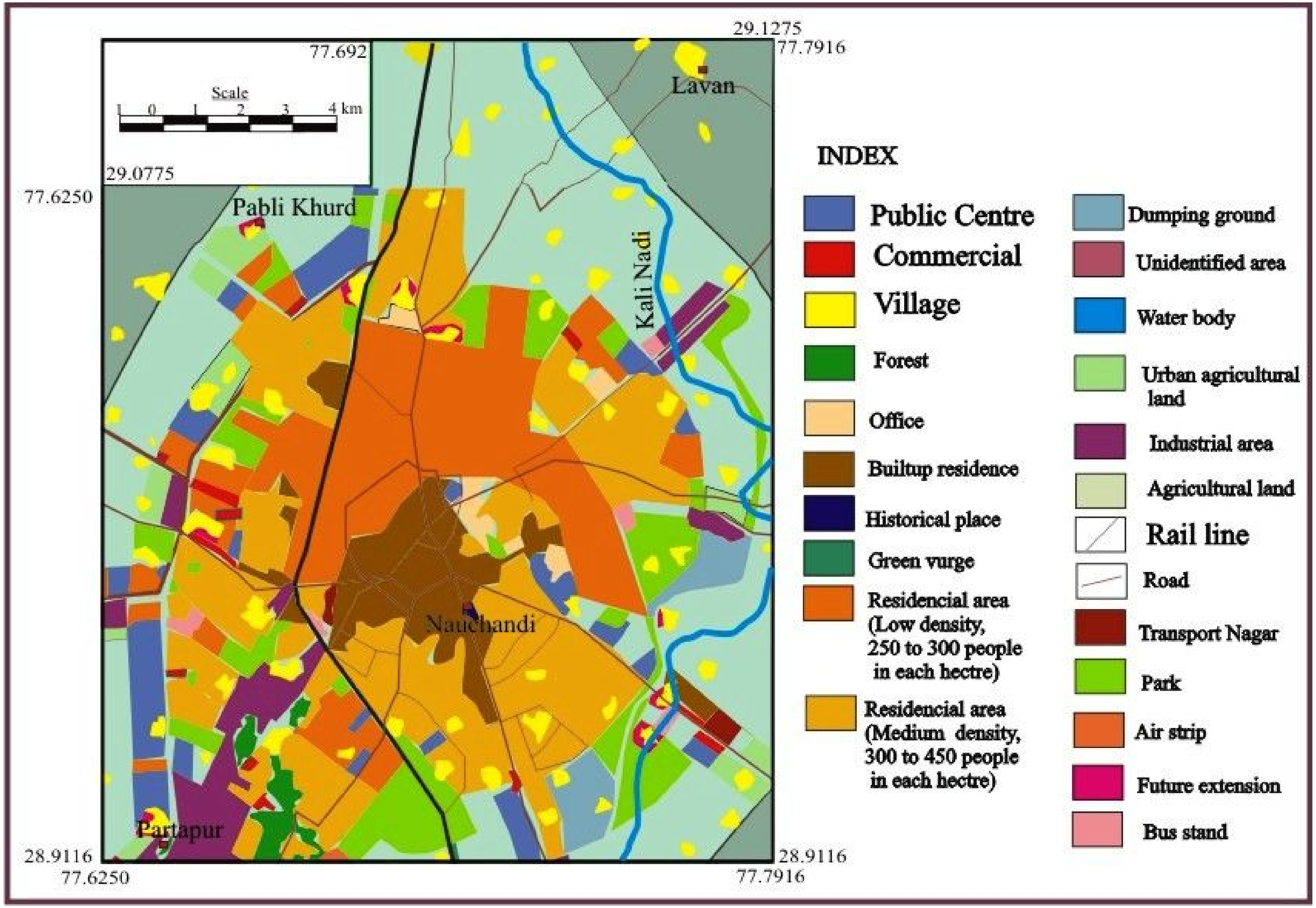

Figure 2.9: Land use map of study area based on Master Plan of Meerut City (2012-21, 2nd phase, www.mda.nic.in)

III. SEISMOTECTONIC SETUP AND THEIR CHARACTERISATION

Estimation of intensity of ground motion at site considering the distance of seismic source and its earthquake generating capability is the prime requisite for seismic microzonation. This needs the categorization and characterisation of all possible sources of seismicity and the seismotectonic elements present in and around the area within 300 km radius (Iyengar and Ghosh, 2004; Gupta, 2005). In present study, the possible seismic sources along with past earthquake records in a radius of 300 km from the site have been considered for preparation of seismotectonic map (Figure 3.1).

3.1 Seismicity

Seismically, Meerut and its neighbourhood areas are liable for slight to moderate damage due to earthquakes. In order to have an idea about the seismicity affecting the Meerut, an area extending up to a radial distance of 300 km around Meerut City was considered and epicentres of past earthquake occurrences since 1900 AD were plotted (Figure 3.1). The Figure 3.1 shows plot of epicentres with different magnitude to get an idea of seismicity in various sections of Himalaya and the foredeep. The plot of earthquake epicentres indicates that the major seismic activity affecting Meerut is confined both in the Foredeep and Himalayan region. The seismicity is represented by the presence of almost regularly spaced earthquake epicentres mainly in Indo-Gangetic Plain and Uttarakhand Himalaya along with few in Himachal Himalaya and somewhat sporadic presence on Delhi Ridge. The seismic sources likely to affect Meerut City are classified in to three clusters of epicentres as detailed below:

i. *Mathura Seismotectonic block at a distance of 160 km SSE;*
ii. *Kangra Seismotectonic block at 300+ km towards NNW and*
iii. *Delhi Regionat a distance of 70 km SSW.*

Historically, the known earliest earthquake affecting the area occurred at Mathura in 1803, M 7.5 along with maximum the intensity experienced at Meerut as IX on MSK scale (GSI Sp. Pub. 59, 2000).The seismic event had affected the region as far as those in Pakistan in the WNW and Kolkata in the ESE. The other significant earthquakes affecting this area include the M 7.8 Kangra Earthquake of 1905, which induced an intensity of VI in the region around Meerut; the M 6.2 Bulandshahar Earthquake of 1956, with ground shaking equivalent to seismic intensity VI on MSK scale. Other than these, the M 6.0 Delhi Earthquake of 1960 has also affected this area.

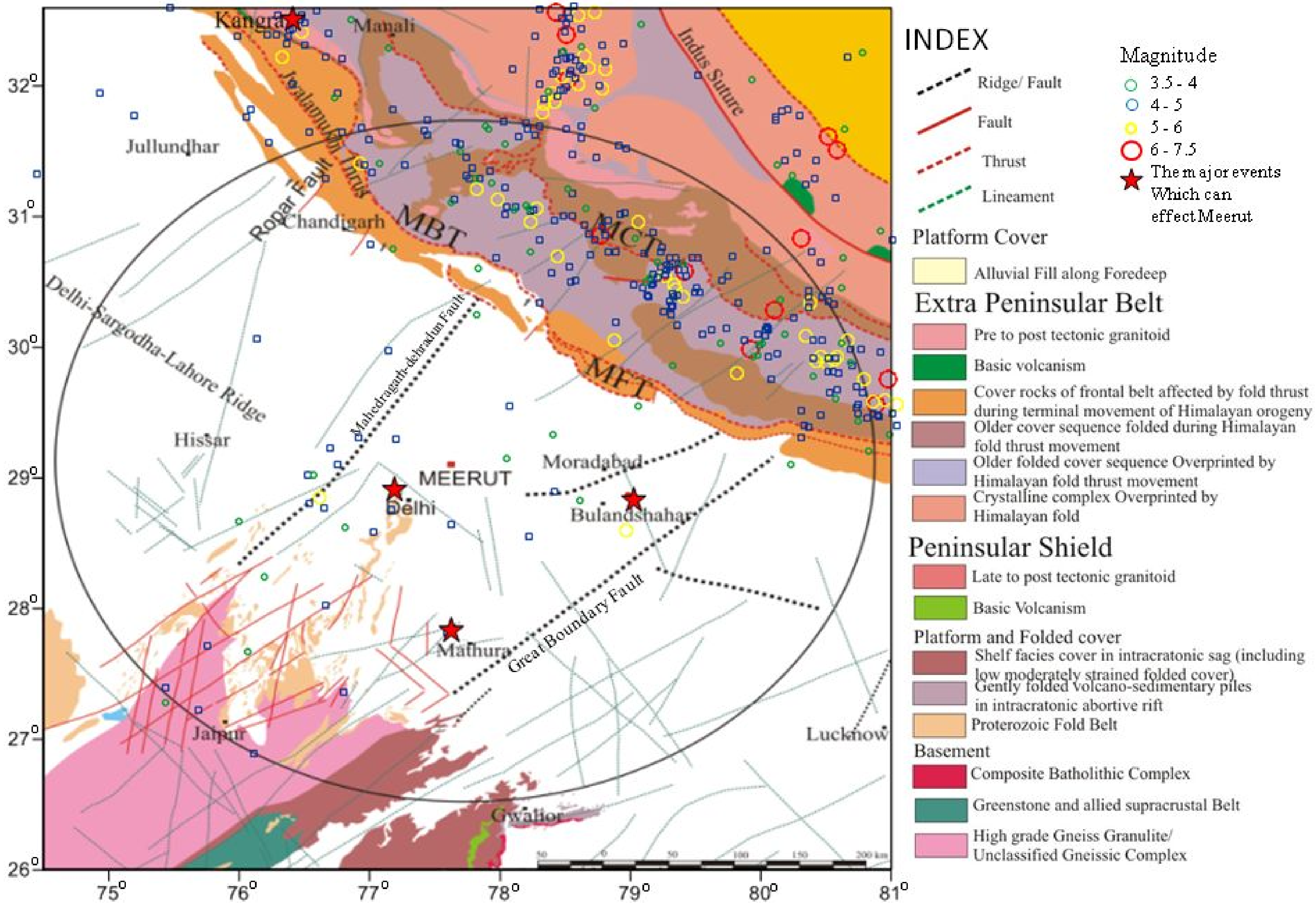

Fig. 3.1: Seismotectonic map showing magnitude wise distribution of epicentres of earthquakes, lineaments/ faults and geology (Based on Seismotectonic Atlas of India and its Environs, GSI, 2000)

3.2 Lineaments/ Faults and Seismogenic Zones

Meerut lies in a down warp of the Himalayan foreland setting known as gangetic foredeep of variable depth of sediments deposited by long-vigorous fluvial sedimentation of the Himalayan rivers. The southernmost and youngest terrain defining thrust system of Himalaya known as the Himalayan Frontal Thrust (HFT) located at about 150 km distance in the north eastern side of Meerut.

Based on regional geological setup, seismic records and geophysical characteristics of the seismogenic sources along with the prevailing tectonic regime in about 300 km radius of Meerut City, the area is divided into mainly following five seismogenic zones (Figure 3.1 and 3.2) as follow-

Seismogenic Zone I: Himalayan Zone

Seismogenic Zone II: Delhi- Hardwar Ridge Zone

Seismogenic Zone III: Moradabad Fault Zone

Seismogenic Zone IV: Rajasthan Great Boundary Fault Zone

Seismogenic Zone V: Mathura Fault Zone

Seismogenic Zone VI : Sohna Fault Zone

The Himalayan seismogenic zone falling in the north of the Meerut region is the most seismically active zone. The largest earthquake in this zone is Kangra Earthquake of 1905 which had a magnitude of 7.8 Mw. A 280 km rupture zone (Molnar, 1987) along Jwalamukhi Thrust (Joshi et al., 2005) is responsible for this earthquake. Nearly 20000 people were killed and huge devastation took place in epicentral and neighbouring areas. The other major earthquake having magnitude 6.6 M_L is in 1991 near Uttarkashi. About 768 persons dead, 5066 injured and 0.1 million houses were damaged during this earthquake (Narula et al., 1996).

The Delhi-Hardwar Ridge lies towards the west of Ganga basin and is considered to be a prolongation of the NNE-SSW directed Peninsular rocks (Aravalli) as a horst delimited by faults. Since 1720 (the first interpreted earthquake near Sohna by Oldham, 1883), the region has experienced about 231 earthquakes all of which below magnitude 5.

The sub-surface Moradabad Fault zone within Gangetic Plain is having a general trend along NE-SW direction. The earthquake of 1956 near Bulandashahar is the biggest instrumentally recorded earthquake near this fault. A magnitude of 6.5 (GSI, 2010) was assigned to the event on the basis of instrumental records of IMD and was felt in a very large area. It was responsible for damage to buildings in which 23 persons were killed in

Bulandshahar and some were injured in Delhi. Since 1720, the region has experienced about 11 earthquakes out of which 7 are below magnitude 5. There are 3 earthquakes in the region for $5 \leq M < 6$ and one earthquake for $M = 6.0$ respectively in this region.

The Great Boundary Fault (GBF) represents a 10-20 km wide zone and demarcates the interface between the Vindhyan Supergroup of rocks on the eastern side and the older rocks including Aravalli Supergroup on the western side. GBF zone is a well-defined fault which runs for about 400 km in the NNE- SSW to NE-SW direction as a major dislocation zone in Rajasthan. The earthquake of 31st Aug., 1803 near Mathura is associated with this zone also in addition to its association with Mathura fault zone. This earthquake was felt as far as Kolkata and caused extensive fissures in fields near Mathura through which water gushed out. Based on macroseismic data, the magnitude of this earthquake has been estimated as 7.5 assigned by India Meteorological Department (IMD) while the same was estimated to be of magnitude 7.0 by Oldham. The epicentral location of this earthquake indicates that the earthquake could be due to movement along postulated Mathura Fault. Since 1720, the region has experienced about 22 earthquakes.

The Mathura Fault zone postulated by Srivastava and Somayajulu (1966) runs in NNW-SSE direction from Mathura in south to Panipat in North. This zone probably controlled the course of Yamuna River parallel to the fault zone. The most disastrous earthquake in this zone was of 1803 near Mathura and as recorded by Oldham and estimated to be of magnitude 7.5. In the Asiatic Annual Register of 1804 (published from London in 1806), there is reference to the earthquake of 1803 at Mathura under the heading “Dreadful Earthquake”. It states that in the night between the 31st August and 1st September, at half an hour after midnight, a severe shock of an earthquake was felt at this place, which lasted for many minutes, and was violent beyond the memory of man. Many of the Pucka buildings were cast down, and Zenanes, hitherto un assailed by violence, were deserted, and their fair inhabitants took refuge in the streets and in the fields, in dishabilles which had no effect to conceal, and in an affright which elevated their charms, seeking protection with men, whose visages it would otherwise have disgraced them to behold. Iyengar (2000) mentioned about damage to the Qutub Minar during the 1803 earthquake in Delhi.

A sub-surface, Sohna Fault zone runs in N-S direction from Sohna to the west of Delhi and has been mapped by Geological Survey of India. Along this fault, a hot spring is reported to occur at Sohna. The earthquake of 15th July 1720 has been described by Oldham (1883) as a dreadful earthquake in which walls of the fortress and many houses in Delhi were destroyed.

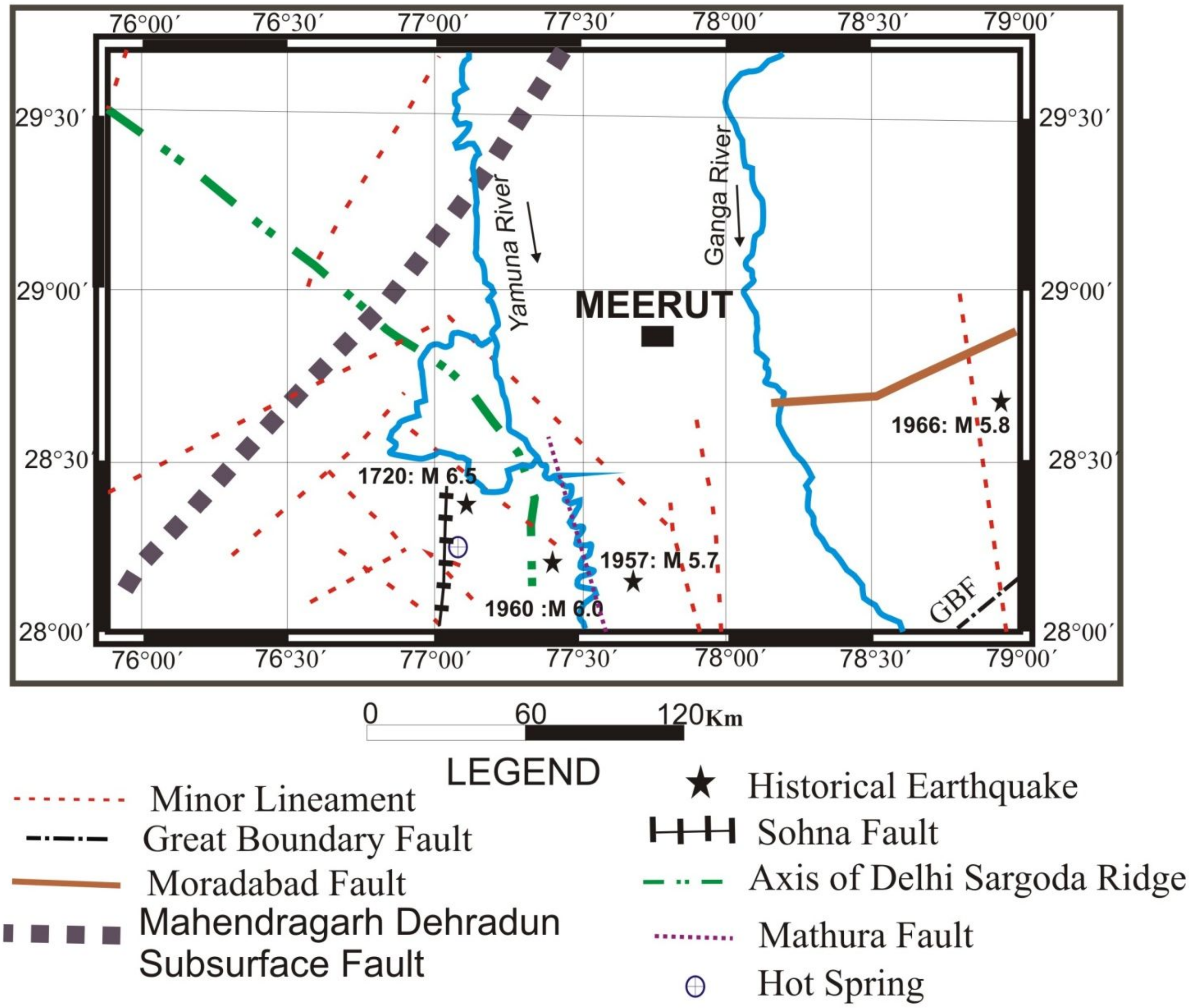

Fig. 3.2 Seismotectonics map around Meerut area (modified after Das Gupta et al., 2000)

It was followed by 4 to 5 aftershocks per day for 40 days and occasional shocks for 4 to 5 months. The likely magnitude for this earthquake, based on macroseismic data has been assigned by IMD as 6.5. The 1960 Delhi earthquake having magnitude 6.0 and depth 5 to 6 km (Muktinath et al., 1968) occurred in this fault zone. The earthquake was felt at Kanpur and Jaipur. Death of 2 persons, damages to property and injuries to about 100 persons were reported from Delhi (GSI Sp. Pub., 2010). Since 1720, the region has experienced about 12 earthquakes.

The Meerut experienced intensity V during far distance Himalayan earthquake namely Uttarkashi (19th Oct., 1991, 6.4 M_B) and Chamoli earthquake (28th March, 1999, 6.8 M_B) (GSI Sp. Pub., 2010).

3.3 Estimation of M_{max}

The maximum magnitude (M_{max}) is an important variable which will affect the site as it reflects the maximum potential of energy which an earthquake can release. It is defined as the magnitude of the largest possible earthquake. Since the largest event within 300 km radius of the study area is 1803 Mathura earthquake of magnitude 7.5, a M_{max} of 8.0 (7.5 = 0.5) is taken as the scenario earthquake. The M_{max} 8.0 is taken as per the thumb rule given by Nuttli et al., 1979 that "*in the standard rule-of-thumb practice, the maximum historical earthquake is increased by half a magnitude unit or, is evaluated through a recurrence relationship, which when extended yield the maximum magnitude*".

3.4 Deterministic estimation of likely ground motion

The intensity in the study area is computed for likely seismic sources based on the Shebalin (1958) and Karnik (1969) relationships:

$I_0 = 1.5\, M - 3.5 \log h + 3$ (by Shebalin)

Where, I_0 = *Max. Intensity, M= EQ Mag., h=focal depth*

$In = I_0 - \gamma \log Dn/h$ (by Karnik)

Where, γ=*Constant (=3.0), In= Intensity of chosen isoseismal,* $Dn=\sqrt{(r^2+h^2)}$,

r=distance of chosen isoseismal from the epicentre

Computing with the help of above equation, following intensity has been calculated for different significant past earthquakes:

Sl. no.	Intensity	Location of seismic event
1	>VIII	Mathura; M 8.0; r-160km; h-15km
2	>VII	Delhi; M 6.5; r-70km; h-15km
3	>VII	Kangra; M 8.3; r-355km; h-15km

However, during Mathura earthquake an intensity of IX is experienced in Meerut (GSI Sp. Pub. 59, 2000).

3.5 Peak ground acceleration

The peak ground acceleration is one of the most important parameters defining the potential for seismic hazard at a particular place. In order to get an estimation of the incoming ground motion at Meerut due to a strong earthquake, a number of approaches have been tried.

The intensity estimated in the last paragraph, though does provide an idea of the ground motions in terms of the intensity, its correlation with PGA is actually very poor. Therefore, as another attempt, PGA has been calculated by using the attenuation relationship for peak vertical ground accelerations for the Himalayan region developed by Sharma (1998):

$$\log(A) = -2.87 + 0.634 M - 1.16 \log (X + e^{0.62 M})$$

where *A is the peak ground vertical acceleration in terms of g, M is the magnitude and X is the hypocentral distance from the source in km.*

Using the above relationship the PGA values were calculated at Meerut from Mathura and Kangra earthquakes. The vertical PGA is .17g by using M (as MCE) as 8.0 and X as 160.7 km from Mathura earthquake and .12g by using M (as MCE) as 8.3 and X as 355.31 km from kangra earthquake. However, Meerut lies in Zone-IV of Seismic Zoning Map of India and have a zone factor of 0.24 (NDMA; 2011).

3.6 Analysis of Seismic Data

The total seismic data around Meerut within 300 km radius as per the USGS catalogue (United States Geological Survey Catalogue) is analysed as per the procedures described by Steppe (1972). The threshold value of reliable data in IMD catalogue is M 4, therefore, the seismic data below M 4 has been discarded. The number of seismic data per decade were grouped in three magnitude ranges, $4.1 < M < 5$; $5.1 < M < 6$ and $M > 6$ (Table 3.1).The table describes the rate of occurrence as a function of time interval of different magnitude classes. The rate is given as N/T, where N is the cumulative number of earthquakes in the time period T.

Earthquake data have been plotted compiled from national data base of USGS. Information on earthquakes in India and neighbourhood, available in various national and International publications and journals, has also been used. The systematic recording of earthquakes was started from 1960 onwards therefore; using major past earthquake events the analysis was done. It is evident from table 3.1 the occurrence rate of lower magnitudes earthquakes are less due to non-availability of smaller magnitude data. The seismic events higher than M 5 are given in table 3.2.

Table 3.1: Rate of occurrence for various magnitude ranges

TIME	TIME	4.1<M<5		5.1<M<6		M>6	
Period	INT.	N	N/T	N	N/T	N	N/T
2008-2017	10	37	0.37	10	0.1	0	0
1998-2017	20	99	4.95	15	0.75	1	0.05
1988-2017	30	149	4.96	17	0.56	2	0.66
1978-2017	40	172	4.3	26	0.65	2	0.05
1968-2017	50	172	3.44	27	0.54	2	0.04
1958-2017	60	172	2.86	28	0.46	3	0.05
1948-2017	70	172	2.45	28	0.4	4	0.057
1938-2017	80	172	2.15	28	0.35	4	0.05

Table 3.2: Significant earthquake occurrences around studied area (source:*www.earthquakes.usgs.gov/earthquakes; GSI Sp. Pub., 2010 and other sources*)

TIME	EPICENTRAL LOCATION	LATITUDE	LONGITUDE	DEPTH	MAG	MAGTYPE
1803	Mathura	27.5	77.68	15	7.5	Ms
1905	Kangra	33	76	15	7.8	Mw
1945	Western Xizang-India border	30.218	80.082	15	6.4	Mw
1956	Bulandshahar, Uttar Pradesh	28.2	77.7	20	6.5	Mb
1958	Uttaranchal, India	29.926	79.9	15	6.1	Mw
1964	Nepal-India border region	29.829	80.474	25	5.9	Mw
1960	Delhi haryana Region	28.2	77.4	5	6	Mb
1966	Uttar Pradesh, India	28.565	78.961	27	5.6	Mw
1976	Western Xizang-India border	31.771	78.348	29	5	Mb
1976	Punjab-Himachal Pradesh border region, India	31.32	76.953	37	5	Mb
1977	Western Xizang-India border	31.786	78.417	40	5.4	Mb
1979	Western Xizang-India border	30.029	80.31	33	5.9	Ms
1979	Uttaranchal, India	30.628	78.445	33	5	Mb
1981	Western Xizang-India border	31.704	78.335	33	5	Mb
1984	Uttaranchal-Uttar Pradesh border region, India	29.99	78.871	33	5.1	Mb
1984	Nepal-India border region	29.867	80.546	21.4	5	Mb
1986	Himachal Pradesh, India	31.049	77.997	33	5.5	Mw
1990	Uttaranchal, India	29.741	79.791	33	5.1	Mb

1991	Uttarkashi, Uttaranchal, India	30.78	78.774	10.3	6.8	Mw
1997	Nepal-India border region	29.845	80.532	33	5.6	Mw
1999	Chamoli, Uttaranchal, India	30.512	79.403	15	6.8	Mb
1999	Uttaranchal, India	30.315	79.387	10	5.4	Mb
1999	Uttaranchal, India	30.376	79.335	10	5.3	Mb
1999	Uttaranchal, India	30.414	79.321	10	5.1	Mb
2005	Uttaranchal, India	30.476	79.255	44	5.1	Mw
2007	Uttaranchal, India	30.881	78.239	19	5.1	Mb
2008	Western Xizang-India border	30.279	80.349	10	5	Mw
2009	Uttaranchal, India	30.879	79.057	52.3	5	Mb
2010	Nepal-India border region	29.872	80.428	16.3	5.2	Mb
2010	Nepal-India border region	29.841	80.397	32.8	5	Mw
2010	Himachal Pradesh, India	31.135	77.839	18.8	5	Mb
2012	Haryana - Delhi region, India	28.809	76.649	10	5.1	Mb
2012	Uttaranchal, India	30.986	78.282	6.2	5.1	Mb
2016	17km NNE of Dharchula, India	29.979	80.6321	31.96	5.2	Mb
2017	35km NW of Pipalkoti, India	30.6339	79.1601	10	5.1	Mb
2017	36km NW of Pipalkoti, India	30.6544	79.1645	16.05	5.1	Mw

IV. SITE RESPONSE STUDIES

4.1 Principles of seismic microzonation

The field based macroseismic study of earthquakes right from 1811-1812 New Madrid earthquakes to the present has quite often revealed areas of isolated high intensity zone within an otherwise low intensity zone/ isoseismal area. Earlier, the thoughts of the scientists / workers always veered around a scientific explanation for the occurrence of isolated seismic high intensity within overall low intensity zone. The study of 1985 Mexico earthquake along with extensive recording on different ground surfaces (*viz.* rock as well as lake sediments) proved to be watershed for understanding the phenomenon of amplification of ground motions. The analysis of these recordings in time as well as frequency domains shed a new light on the hitherto-considered-as-ambiguity for selective destruction of the cultural features, actually due to amplification caused by passage of the seismic waves through the soft rocks or soil. Since then, a lot of real time data has been recorded and new researches have been undertaken to open new vistas in this field of selective destruction with a view to achieving capability of mitigating the earthquake damage or hazard posed by such a phenomenon. Thus, using the knowledge in this field, systematic studies on small or regional scale are undertaken to demarcate the regions having different seismic hazard levels. This exercise, when carried out on a regional scale provides a broad idea about the hazard levels and known as the **seismic zoning.** It is usually undertaken for a whole country. However, a detailed exercise undertaken to further delineate areas of different seismic hazard levels within a city comes in the realm of **seismic microzonation**.

4.1.1 Concept and theory

The seismic microzonation of a particular site may be described in the following sentences (Joshi *et al.* 2007):

- Seismic microzonation, which is essentially an exercise on large scale, classifies inhabited areas, especially important cities, into zones of different seismic hazard levels.
- Such maps are prepared by contouring a grid of closely spaced sites for equal seismic hazard levels.
- These seismic hazard levels are determined / decided by integrating the chances of

occurrence of an earthquake of certain severity with the ***seismic response of different sites*** within a city.

- This kind of microzonation is one of the most important inputs for formulation of suitable urban development strategy/ code, building seismically safe structures and for hazard preparedness and mitigation.

Out of the above mentioned points the seismic response of different sites is the most important issue, which eventually is responsible for different zones of maximum expected level of ground motions. It is, therefore, imperative to know about the different site amplification effects or response, which are described as under –

1. Amplification effects related with low density unlithified sedimentary sites.
2. Amplification effects related with strong lateral discontinuities.
3. Amplification effects related with surface topography.

The above three aspects broadly encompass the effects related directly with the wave propagation and do not include large irreversible effects on the ground surface. Nevertheless, the induced effects at different sites comprising liquefaction and earthquake-triggered landslides have very significant bearing on engineering structures.

4.1.2 Site amplification effects

For a better understanding of the actual exercise on microzonation, first the theoretical basis of the amplification of the seismic waves or ground motions due to the above mentioned conditions are being discussed. The property which has the maximum effect on the ground motion is the impedance of the medium. The impedance, which basically is the resistance to the ground particle motion for horizontally polarised shear waves, can be defined as the product of the density (ρ), the shear wave velocity (β) and the cosine of the angle of incidence (Aki and Richards, 1980). As the velocity of propagation of seismic waves tends to increase with depth, these waves, usually impinge upon the upper parts of the earth crust vertically, implying that the angle of incidence (i) can be assumed to be almost equal to zero, and Cos (i) equal to one. Ground particle velocity or its amplitude is inversely proportional to the square root of the impedance. When a seismic wave passes through a region of increasing impedance, the resistance to the particle motion also increases. As a result to conserve the energy the particle velocity and therefore, the amplitude of the ground

motion decreases. Hence, it can be assumed that, other conditions being constant, ground motions at same distances from the source will be higher on low density soil having low shear wave velocity than on the high density medium having high velocity.

There is another phenomenon called ‘absorption’, also known as ‘damping’ or ‘inelastic attenuation’, which has a palliative effect on the waves. The damping, which normally is higher on soft soils, works against the effects of impedance. While the lower impedance on soft soils increases the amplitude; the higher absorption tends to mitigate the increment. The effect of absorption is more on higher frequencies because of the greater loss of energy in greater interaction of the seismic energy with the soft soil. It therefore, follows that in small earthquakes, which have predominantly higher frequencies, the rock sites with high density, high velocity will show stronger peaks than the soft soil with low density, low velocity. However, in bigger earthquakes, generating a predominantly low frequency spectrum, the effects on soft soils will be much higher than that on hard rocks.

In addition to the above, contrast in the properties of different layers also affects the amplitude of the ground motion. For the sake of simplicity, a case of two layered medium e.g. soft rock overlying a hard one, can be considered. In the event of an upcoming wave entering a relatively very low impedance medium from a high impedance medium, the amplitude gets amplified in proportion to the ratio of impedance or impedance contrast between the two media. For a one layer (horizontally layered) 1D structure impinged vertically by plane SH waves the amplification is given by

$A_0 = 1/1/C + 0.5\pi, \zeta$

Where C (impedance contrast) = $\rho 2\ \beta 2\ / \rho 1\ \beta 1$, ρ & β are density and shear wave velocity for sediment (=1) and underlying rock (=2) and ζ = damping constant. In this, connection this may be stated that Su *et al.,* 1992, while studying relation between amplification and surficial geology, have observed that the high frequency wave obey ray - theoretical law more than the low frequency waves for a given homogeneity. The site amplification may therefore be more proportional to the inverse of the square root of the impedance following the ray theory. The low frequency, on the other hand, may be influenced more by resonance for which peak amplification scales with the inverse of the impedance linearly. Thus, we can expect the range of site amplification at lower frequencies be about twice that of higher frequencies.

However, at the sharp boundary between such contrasting media a part of wave energy is lost as some of it is reflected back, and some energy is used up in conversion to

other wave types, such as from P to S waves. Therefore, the resultant amplitude is less than what is expected because of a simple impedance contrast. Besides this some of the seismic waves transmitted into the upper soft medium, themselves get trapped there and start reverberating. When such reverberating waves are in phase, resonance occurs.

From the above discussion, it follows that in the simplest model, the impedance contrast between the underlying and overlying layers and absorption effects, both working in time domain and the effects of resonance in the frequency domain, ultimately combine to produce the ground motion. Since in nature such simple configuration rarely exists, two and three dimensional models are required to reach closer to the actual behavior of seismic waves.

Besides the amplification of vertically propagating shear waves, there is another remarkable amplification effect caused by resonance of surface waves in a valley filled with soft sediments. Bard and Bouchon (1985) have given an excellent theoretical explanation of such effects. According to them, surface waves are generated at the edge of the valley and they propagate laterally back and forth across the valley. During this, lateral resonance occurs together with the vertical resonance. This leads to a two dimensional resonance pattern. In such a case the whole valley vibrates with a single frequency though the amplitude varying at different locations. In such a case, the frequency at the middle of the valley, where the sediments are supposed to be the thickest, is less than what otherwise would be expected in a one dimensional (parallel layers) scenario. The amplitude, however, is much higher.

In addition to above described effects, geometrical effects caused by surface topography and lateral discontinuities are the ones, which at places may cause considerable enhancement of the ground motions. It has been experienced many times that after an earthquake the damage on the top of a ridge is exceptionally high. During Uttarkashi earthquake of 20th October 1991 a correlation between coseismic slides and the geometry of the ridges was found (Joshi *et al.* 1996). During the course of macroseismic surveys, it has been observed that strong lateral discontinuities had caused significant increase in the seismic intensity. Zones, located along strong lateral discontinuities (e.g. softer materials like debris, weathered rocks, etc. lying beside the harder material) have shown significantly higher damage.

There are various approaches for carrying out seismic microzonation, depending on the available information, budget, time, and above all, the risk level of the area under study.

4.2 Methodology

To begin with, for carrying out seismic microzonation study one has to choose the methodology depending on the available information, budget, time, and above all, the risk level of the area under study (Bard, 2000). The ultimate aim of microzonation, however, should be to define the seismic coefficients after measurement/computation of site response of the ground or the area with respect to the expected ground motions. The seismic coefficients thus determined could be used for designing seismically resistant structures in the area.

The seismic recording or response at a recording site is actually a sum total effect of -
i) source parameters of the event and its distance from the recording site;
ii) the attenuation characterstics of the media through which the wave travels; and
iii) the geotechnical characteristics of the site which modifies the wave parameters.

However, for the purpose of the microzonation studies, which are generally carried out for a city, the above mentioned first two factors are responsible for shaping the wave characteristics for the whole city, used as input ground motions. Therefore once the input ground motions are estimated the whole exercise for the seismic microzonation studies boils down to determination of seismic response at different sites within the study area.

The approaches include direct measurement of site response with the help of different tools, such as, macroseismic surveys, micro tremors, weak motions, etc. Careful macroseismic surveys provide a broad idea of the response of different sites. Microtremors, which include ambient vibrations caused by natural or artificial disturbances, e.g. wind, sea waves, traffic, machinery, etc. are best suited for the measurement of the predominant period of the ground, though some workers have also used it to measure the amplification of seismic waves. Weak motions, which refer to weak ground motions originating from micro earthquakes, aftershocks of big events, mine or quarry blasts, nuclear tests, etc., are useful in assessing the predominant period and the amplification characteristics of different sites.

For estimation of site response from earthquake data the important exercise is to remove the source and path effects. Borcherdt (1970) introduced a simple procedure to divide the spectrum observed at the site in question by the same observed in reference site, preferably competent bedrock. The resulting spectral ratio constitutes an estimate of site response, if reference site has a negligible site response. Lermo and Chavez-Garcia (1993) based on certain studies suggested that source and path effects could be accounted for if the horizontal component of shear wave spectra at each site is divided by vertical component.

Nakamura (1989) proposed a technique to determine site response based on micro-tremor recordings. According to him, the spectral ratio between the horizontal and the vertical motion at a single site is much less sensitive to the actual origin of microtremors.

In addition to the direct measurement of the site response, geotechnical and geophysical methods are also there, the results of which may help in calculations of the predominant period as well as the amplification characteristics of different sites. Standard Penetration Test (SPT) is a very useful tool for this purpose. There are several empirical relationships between 'N' values (number of blows for penetration of 30 cm) and shear wave velocity, which in turn, are related to the amplification of the amplitude of the seismic waves passing through the medium. The shear wave velocities thus determined in conjunction with the thickness of the soft layer gives the predominant period/frequency, at which the resonance occurs and results in enhancement of the ground motion. The Average Shear wave velocity down to 30m depth has also been determined by Multichannel Analysis of Surface Waves (MASW). In this the direct measurement of surface waves, generated by both artificial and natural sources was recorded and the calculation of average shear wave velocity was done using a software.

In the present study, geotechnical as well as geophysical techniques have been employed to estimate the site response at different locations within Meerut City which include the city along with the undeveloped surrounding areas to be developed in due course of time. However, this was preceded by acquiring a thorough understanding of geological, geomorphological and geohydrological conditions by first gathering and compiling the existing information from all sources and then subjecting them to the field checks - in the process - correcting and supplementing it by the fresh information collected through drilling at different sites.

4.3 Geotechnical studies

The effect of earthquake ground motion depends on the properties of surface configuration of the existing material through which the waves pass. The ground motion can get increased or decreased at the surface as per the local site conditions, mainly geology. The ground motion recorded at site is dependent upon source, travel path followed by earthquake waves and the degree to which the sediments behave non-linearly. The input ground motion at any site is the result of thickness and velocities of the surface layers and the impedance of the medium (Bard, 2000). The amplification of ground motion occurs at definite frequency which depends on the thickness and velocity of surface layers. The high frequency follows

the ray-theoretical law more than the low frequency waves for a given homogeneity (Su et al., 1992). The amplification at the site is proportional to the inverse of the square root of the impedance (the resistance offered by the media to the ground particle motion). However, the low frequency waves are influenced more by resonance for which peak amplification linearly scales down with the inverse of the impedance. Therefore, the study of local subsurface geological conditions is mandatory for seismic hazard analysis.

During the present study preparation of geological, geomorphological map and study of satellite imageries were carried out. The traverses were taken around Meerut to study the geological and geomorphological elements present in the study area. For site response studies both geotechnical and geophysical studies were utilized to prepare seismic microzones of Meerut City.

4.3.1 Bore Hole Plan for Drilling

The bore hole plan on grid pattern (one grid = 11 sq km) was prepared for study area using geological, geomorphological map and master Plan of Meerut. A total 28 bore holes including 26 bore holes each of 30 m depth and 2 bore holes of 60 m depth aggregating to 900 m drilling were planned. Since the area of study exposes mainly monotonous and uniform surface geology (i.e. mostly Older Alluvium) initially bore holes were planned on a uniformly spaced rectangular grid pattern, each rectangular grid being approx of 11 sq km. However, while carrying out the drilling on the ground, various constraints, mainly non-availability of open space at demarcated sites, led to some variations in the proposed drilling site. The details of bore holes are given in the Table 4.1 and Figure 4.1. .

Table 4.1: Location details of bore holes drilled in Meerut City during FS: 2016-18

S. No.	**Name**	**Depth (m)**	**Latitude ° N**	**Longitude ° E**	**Location**
1	MER-1	30	28.92883	77.66072	D.N . Polytechnic,Rithani
2	MER-2	30	28.91961	77.71378	Jurranpur
3	MER-3	30	28.98244	77.64958	Kharauli
4	MER-4	30	29.00458	77.62286	Sandhauli
5	MER-5	60	28.91764	77.64764	Partapur
6	MER-6	30	28.97514	77.63475	Rampur Paoti
7	MER-7	30	29.0509	77.64553	Badjewra
8	MER-8	30	29.06517	77.66969	Pabli khurd
9	MER-9	30	28.96811	77.67131	Jaswant mill Sabungodam
10	MER-10	30	28.99189	77.68042	Race course,Cantt
11	MER-11	30	29.00006	77.70392	Gandhi bagh
12	MER-12	30	28.96536	77.70072	Nauchandi
13	MER-13	60	29.03506	77.65266	Sainik vihar,water tank
14	MER-14	30	28.95489	77.77044	Datauli
15	MER-15	30	28.91833	77.74347	Hajipur
16	MER-16	30	28.92181	77.77617	Jithauli,Near Power house
17	MER-17	30	28.99383	77.78586	Eslamabad chillaura
18	MER-18	30	29.02983	77.74178	Mamepur
19	MER-19	30	29.03208	77.783	Saini village
20	MER-20	30	29.07147	77.77644	Jalalpur
21	MER-21	30	29.0725	77.72947	Dulehra
22	MER-22	30	29.11542	77.69975	Daurala
23	MER-23	30	29.10175	77.73547	Water tank campus,Panwari
24	MER-24	30	29.10383	77.78681	Lawar khaas,cold storage
25	MER-25	30	28.97214	77.74356	Chaudhary Charan Singh University
26	MER-26	30	29.007	77.75453	Water tank campus,Ganganagar
27	MER-27	30	29.06728	77.70778	CPRI Modipuram
28	MER-28	30	29.02364	77.71139	Saufipur

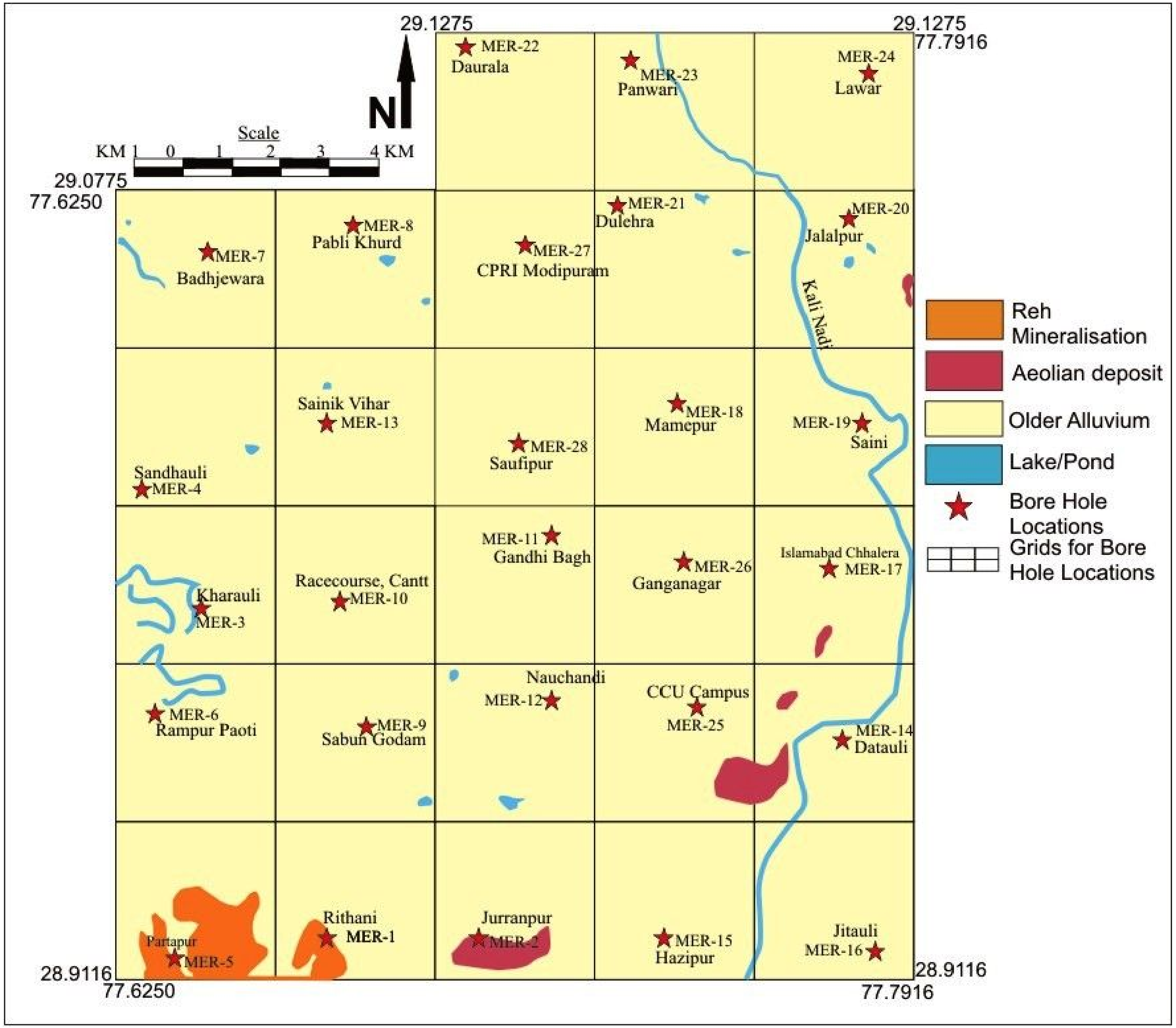

Fig. 4.1: The locations of bore holes and grids on geological map of Meerut City

4.3.2 Drilling and Standard Penetration Test (SPT)

Subsurface study to determine the site specific response of the ground for expected ground motions during an earthquake event has been carried out in Meerut City by undertaking drilling along with Standard Penetration Test (SPT) at various uniformly spread locations in the studied area (annexure-I). The SPT is a method to determine the geotechnical properties of subsurface soils. Total 20 nos. of SPT were done in each bore hole at every 1.05 m depth interval following the procedures described in IS 2131, 1981. The sampler for SPT is forcefully penetrated in a bore hole to a depth of 45 cm by hammering and counting the number of blows required for penetration of sampler by three successive intervals of 15 cm each. A hammer of 63.5 kg from a fixed height of 0.76 m is automatically dropped for penetration. The number of blows for penetration is noted down for 45 cm. The numbers of blows for first 15 cm are discarded as it may be disturbed and is ineffective for SPT. So the total numbers of blows of hammer required for penetration of last 30 cm are finally taken as the “N” value of the soil horizon at that depth. The core samples were collected taking all precautions. The scale of soil consistency for cohesive and soil compactness for non-cohesive soils in terms of SPT-N values as proposed by BS 5930:1999 is given in table 4.2.The details of SPT and samples taken are given in Annexure-I.

Table 4.2: Scale of soil consistency for cohesive and soil compactness for non-cohesive soils in terms of SPT-N valuesas proposed by BS 5930:1999

Cohesive		Non-cohesive	
Consistency	N values/30 cm	Compactness	N values/30 cm
Very soft	0-2	Very loose	0-4
Soft	3-4	Loose	4-10
Medium stiff	5-8	Medium dense	10-30
Stiff	9-16	Dense	30-50
Very stiff	17-32	Very Dense	Above 50
Hard	Above 32		

The SPT values thus obtained many times need standard corrections before these may be used for other deductions. The corrections depend on a number of factors, such as drilling method, bore hole diameter, energy transfer through length of drilling rod, weight of hammer, presence of groundwater table, etc. In the present study, while the raw ‘N’ values as measured during SPT operations have been normalized to $(N1)_{60}$ by applying the corrections for the hammer energy ratio, the overburden pressure, the borehole diameter, the rod length and the samplers with or without liners (Table 4.3) by using the following relationship (Youd *et al.,* 2001) and used for calculation of shear wave velocity and safety factor (liquefaction susceptibility):

$$(N1)_{60} = N.C_N\,.C_E\,.C_B.C_R.Cs$$

where, N is the measured standard penetration resistance, C_N is the factor to normalize N to a common reference effective overburden stress, C_E is the correction for hammer energy ratio, C_B is the correction for the borehole diameter, C_R is the correction factor for the rod length and CS is the correction for the samplers with or without liners. Nath and Thingbarijam (2011) have defined these corrections in detail as presented in Table 4.3.

The overburden pressure (C_N) is calculated as per the suggestion by Kayen et al.(1992) as follows:

$$C_N = 2.2/\,(1.2 + \sigma'_{vo}/P_a)$$

Where, CN normalizes measured N to an effective overburden pressure (σ'_{vo}) of approximately 100 kPa. The above equation limits the maximum CN value to 1.7.

Table 4.3: Correction factors applied for conversion of raw N value to the $(N_1)_{60}$ values (Nath and Thingbarijam, 2011; Skempton, 1986; Youd et al., 2001)

Factor	Size	Correction Factor
Hammer Energy Correction Factor (C_E)		
Donut Hammer	---	0.5-1.0
Safety Hammer	---	0.7-1.2
Automatic-trip Donut hammer	---	0.8-1.3
Correction Factor for Borehole Diameter (C_B)		
Borehole Diameter	65-115 mm	1
	150 mm	1.05
	200 mm	1.15
Correction for Rod Length (C_R)		
Rod Length	<3 m	0.75
	3-4 m	0.8
	4-6 m	0.85
	6-10 m	0.95
	10-30 m	1.0
Correction for Sampler based on method (C_S)		
Sampling method	Standard Sampler	1.0
	Sampler without Liner	1.1-1.3

The corrected SPT (N_160) is obtained for every site of Meerut by adopting above described procedures is used for calculation of shear wave velocity and liquefaction potential of the area. A typical datasheet for one borehole location (MER-1) showing different corrections applied on observed N value to obtain corrected N value (N1)60 is given in the Table 4.4.

Table 4.4: A typical data sheet for one borehole location (MER-1) showing different corrections applied on observed N value to obtain corrected N value (N1) 60

Typical N value correction table for BH MER-1, D. N. Polytechnic, Rithani											
SPT Depth	**SPT (N)**	**Type of strata**	**Density gm/cc**	**T. S. kN/m²**	**E. S. kN/m²**	**CN**	**CE (Hammer)**	**BH Dia. (CB)**	**Rod Length (CR)**	**Sample Method (CS)**	**(N1)60**
1.5	24	Clay	2.83	41.6290	41.62902	1.44909	1	1	0.75	1	26
3	33	Clay	2.83	83.2580	83.25803	1.13725	1	1	0.8	1	30
4.5	34	Clay	2.83	124.887	124.8871	0.93586	1	1	0.85	1	27
6	30	Clay	2.83	166.516	166.5161	0.79506	1	1	0.85	1	20
7.5	29	Sand	2.66	195.641	195.6417	0.71935	1	1	0.95	1	19
9	19	Sand	2.66	234.77	234.77	0.63775	1	1	0.95	1	11
10.5	26	Sand	2.66	273.898	273.8983	0.57278	1	1	1	1	14
12	23	Sand	2.66	313.026	313.0267	0.51982	1	1	1	1	11
13.5	17	Sand	2.66	352.155	352.155	0.47583	1	1	1	1	8
15	23	Sand	2.66	391.283	381.4733	0.43870	1	1	1	1	10
16.5	30	Sand	2.66	430.411	415.6967	0.40695	1	1	1	1	12
18	39	Sand	2.66	469.54	440.11	0.37948	1	1	1	1	14
19.5	26	Sand	2.66	508.668	464.5233	0.37637	1	1	1	1	9
21	28	Sand	2.66	547.796	488.9367	0.36128	1	1	1	1	10
22.5	30	Sand	2.66	586.925	513.35	0.34735	1	1	1	1	10
24	31	Sand	2.66	626.053	537.7633	0.33446	1	1	1	1	10
25.5	29	Sand	2.66	665.181	562.1767	0.32249	1	1	1	1	9
27	30	Sand	2.66	704.31	586.59	0.31135	1	1	1	1	9
28.5	31	Sand	2.66	743.438	611.0033	0.30095	1	1	1	1	9
30	33	Sand	2.66	782.566	635.4167	0.29123	1	1	1	1	9

4.3.3 Subsurface Geology

At the surface, the Quaternary sediments mainly of the Older Alluvium comprising clayey soil with or without *kankar* and aeolian sediments of Indo-Gangetic basin are present in the area. The purpose of drilling is to know the sub surface configuration of sediments. The drilling has helped us to get an insight into the subsurface litho-configuration of the area. The bore hole logs (annexure-I) were used for preparation of schematic model / cartoon (Figure 4.2) showing subsurface geology of the study area in 3D.

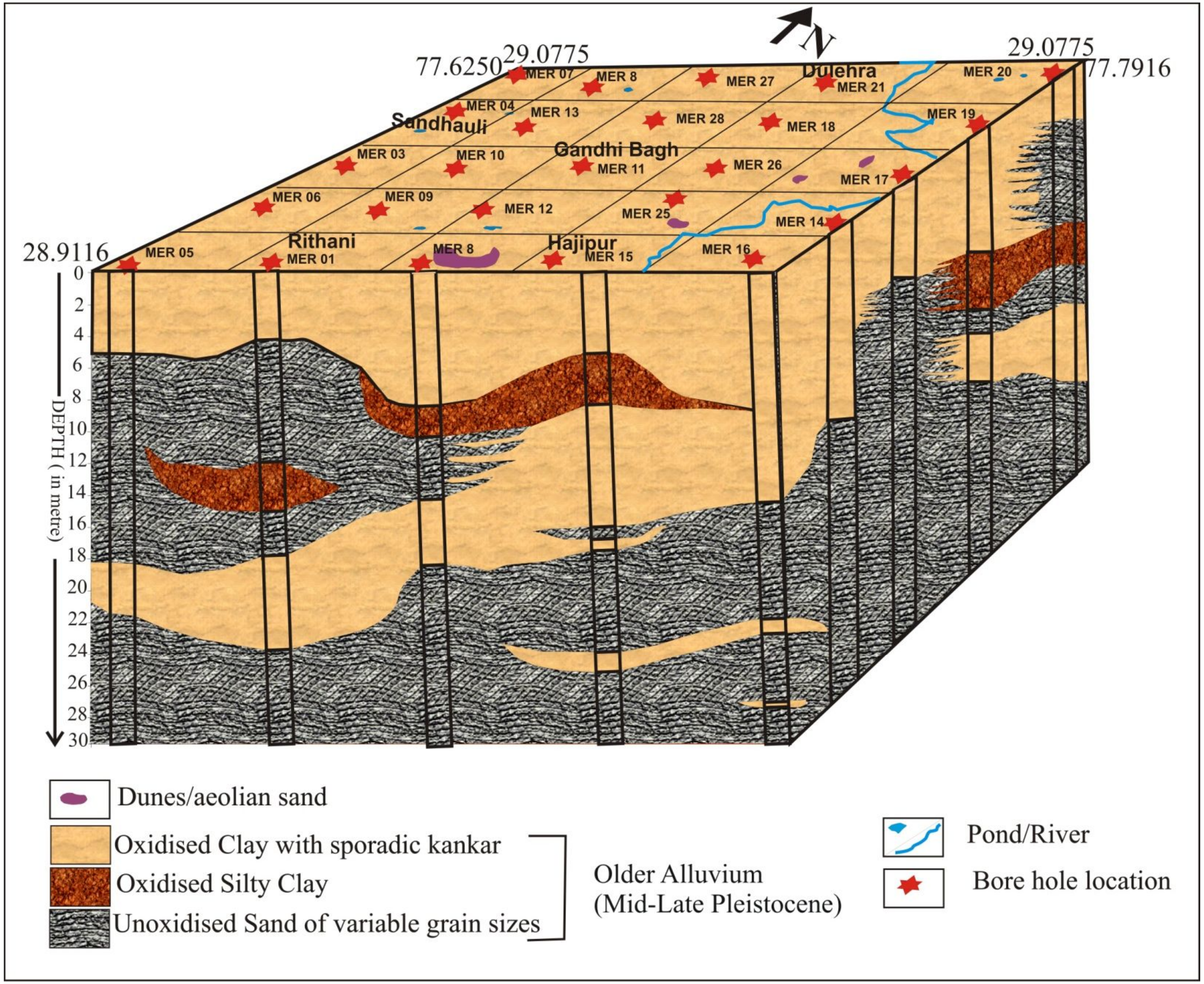

Fig. 4.2: Schematic block diagram showing subsurface geology on the basis of bore hole data at target locations in Meerut City

The 3D cartoon (Figure 4.4) depicts broadly two cycles of deposition as indicated by two levels of fluvial sand deposits with intervening clay layers. At the top, oxidised clay / silty clay with concretions are present in all bore holes representing prevalence of oxidation processes of pedogenesis for a long period without deposition on the surface of the Older Alluvium. Below this, the micaceous sand of variable grain sizes (fine to medium grained) fluvial deposition phase is present. Below this sand layer, again presence of clay/ silty layer with sporadic concretions in majority of bore holes represents a phase of lean flood plain deposition with occasional period of weathering. Further below, presence of non-oxidised sand layer of variable grain sizes up to a depth of 30 m depicts another phase of fluvial cycle of deposition. The section study and core logging data show that the top layer of oxidised clay is composed of small nodules of calcareous and ferruginous materials. At places, the concretions form *kankar* beds which probably were formed by the prolonged weathering of clay materials from these thick clay beds. The depth of groundwater table varies in the study area from 8.5 m to 29 m.

During FS 2016-17, an additional objective to understand the evolutionary history of interfluve region between Ganga and Yamuna rivers had been incorporated in the present investigation, but in the same year, the Term Review Committee, Northern Region had discontinued this objective for further study. Two bore holes of 60 m depth were drilled to know the evolutionary history of the interfluves region of Ganga and Yamuna rivers in which Meerut City is situated. The litho logs of two bore holes at Partapur (MER-5) and Sainik Vihar (MER-13) show broadly three cycles of fluvial deposition. The end of each cycle of deposition is marked by presence of calcrete and iron nodules bearing oxidised clay horizon and well oxidised sand beds. Each fluvial cycle might have initiated with high energy deposition of coarse to medium grained channel sand and ends with the low energy flood plain clay or fine sand/silt deposits having profuse oxidation / pedogenisation. The samples for OSL dating had been collected from base of each cycle and few from top horizon of the cycle. In Total, 6 OSL samples had been collected (Annexure-I) from bore hole No. MER-5 at depth of 20.2 m, 30.8 m, 40.2 m, 44.2 m, 48.2 m and 58.7 m. The OSL results of last three samples collected at the depth of 44.2 m, 48.2 m and 58.7 m (Annexure-X) show erroneous results, probably due to mixing of sediments or exposure to sunlight during sampling or analytical process causing over dispersion in De values. So, the results of three samples taken at 20.2 m, 30.8 m and 40.2 m drill depth showing quartz OSL ages as 24±1 ka, 27±2 ka and 30±ka respectively have been considered for present study. The first sample (i.e. 24±1 ka)

taken from the base of the youngest cycle of the deposition suggests initiation of the youngest major cycle of deposition before 24 ka BP. The second OSL sample was taken below top of the second older cycle (after the oldest cycle reported in this borehole) of deposition and third sample above its base. They yielded quartz OSL age 27±2 ka and 30±ka respectively. It can be interpreted from these quartz OSL age data that second deposition cycle might have initiated before 30 ka BP and ended after 27 ka BP.

4.4 Geophysical studies

Geophysical investigations comprising Ambient Noise / micro tremor survey at 321 sites, Vertical Electrical Resistivity Soundings (VES) at 100 sites and Multichannel Analysis of Surface Waves (MASW) survey at 56 sites have been carried out by the Geophysics (Seismotectonic) Division, Northern Region spreading over an area of 300 sq km of Meerut City (Figure 4.4). Geophysical surveys have been taken up with the objective to determine predominant frequency and site amplification from noise survey site response study, average shear wave velocity upto 30m depth from MASW survey and thickness of various lithological formations in the area from Vertical Electrical Resistivity Sounding (VES) studies.

Noise recordings have been carried out at sampling rate of 100 Hz through moving stations at different places for an average period of 60 minutes by deploying short period digital seismograph (ALTUS, K-2 kinemetrics Inc., USA) coupled to three numbers of short period seismometers (RANGER, SS-1, Kinemetrics Inc., USA). The three seismometers were firmly placed on the ground and one was aligned in East-West, the other in North-South and the third one in the vertical directions at every setting (Figure 4.3 and 4.4). In general, station intervals between noise observation sites varied in the range of 1.0 km to 1.5 km depending on the availability of suitable location i.e. free of influence of trees, source of monochromatic noise and strong topographic features as far as possible. Ambient noise data was processed using the Geopsy (Geophysical Signal database for noise array) software suite. The recorded ambient noise data was split in to 30 Sec time windows. The H/V is computed by ratio of geometric mean of horizontal (NS and EW) components with vertical component. A Konno and Ohmachi smoothing technique (Konno and Ohmachi, 1998) was applied to the spectral ratios with smoothing constant of 30 and 5% cosine taper for a clear predominant frequency(fo) peak. The site response parameters like predominant frequency (fo) and peak

amplification (Ao) have been estimated from ambient noise for 321 sites in the frequency band of 0.5 to 10 Hz for the present work.

Field Photographs showing data acquisition in Noise survey(1), VES survey(2) and MASW survey(3)

Fig. 4.3: Field Photographs showing data acquisition in A- Noise, B- VES and C- MASW survey, Meerut city, District Meerut, Uttar Pradesh

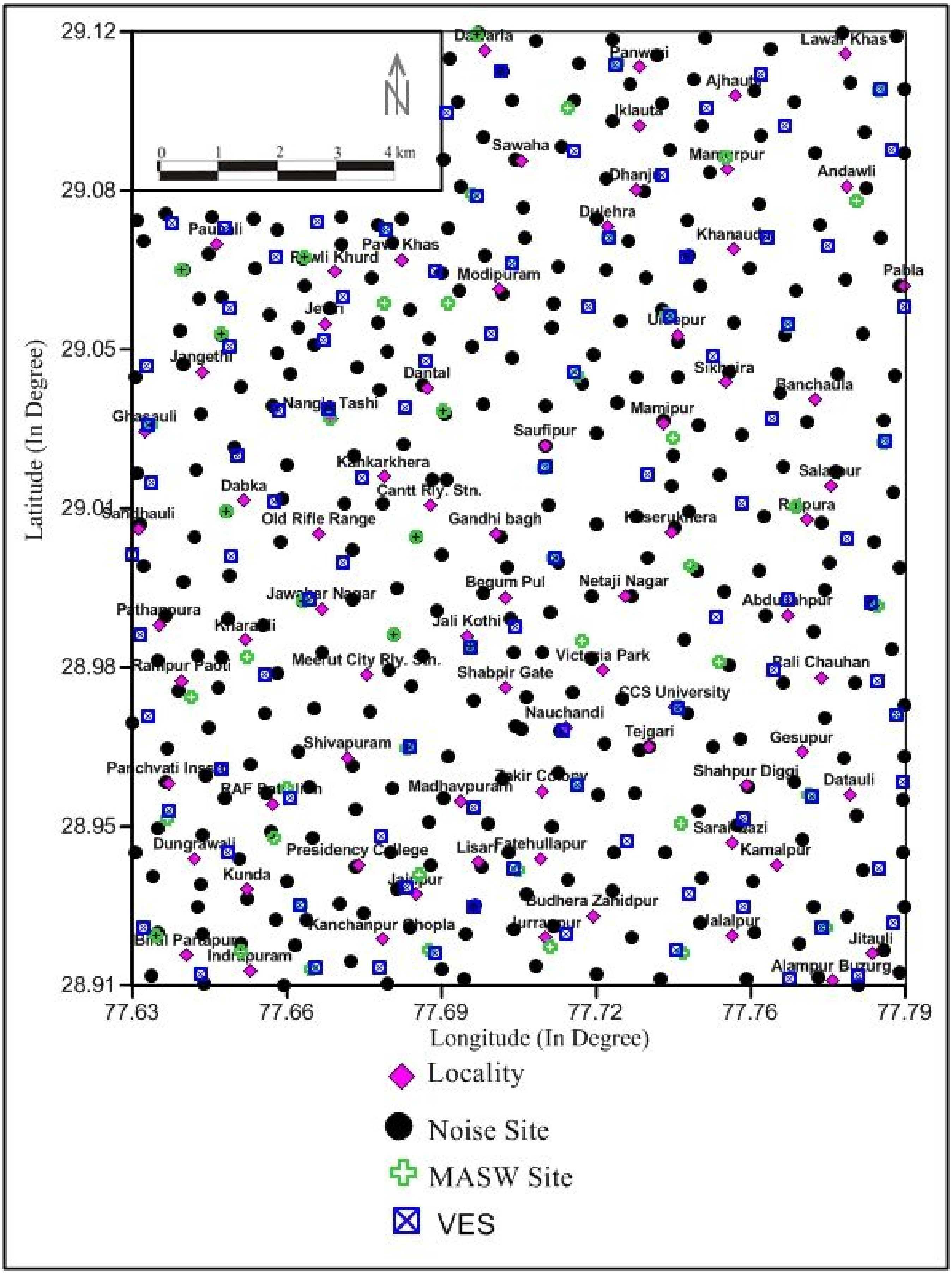

Fig.4.4: Location of Noise, VES and MASW observations in Meerut City

The Stratavisor°NZXP° signal enhancement seismograph coupled with 4.5Hz geophone is used for acquisition of the seismic data. Surface wave is generated by both artificial and natural sources. MASW uses both active and passive micro-tremor sources. The exploration depth depends on the frequency of measurement and survey array length. General specifications of surface wave survey for this study are shown in Table 4.5.

Table 4.5: General Specifications of conducted Surface Wave Survey

Survey Item	Source Type	Target frequencies (sensor)	Array length	Target Depth
MASW(Active Part)	Active (Hammering)	5~30Hz 4.5Hz Geophone	Maximum:115m Minimum:55m	~15m
MASW(Passive Part)	Passive(Micro-tremor)	2~30Hz 4.5Hz Geophone	Maximum:115m Minimum:55m	20~60m

Data acquisitions in MASW (Passive) includes recording of surface waves that are generated by ambient activities, such as cultural noise e.g. highway traffic, wind movement, construction activities etc. and in MASW (Active), seismic energy generated using sledge hammer is recorded. In this active method, a 10kg sledge hammer is used as the active source. A linear array of twelve to twenty four 4.5Hz geophones is used depending on the availability of space in an area. Based on evaluation of initial measurements, a geophone spacing of 10m, 5 m or 3m is selected for conducting MASW survey. The spread length of array ranges from 115m to 55m. Layout of locations where MASW survey has been conducted in Meerut city is shown in Figure 4.3 and 4.4. The parameter and settings used for acquiring MASW (Active/Passive) data are given in Tables 4.6 and 4.7. The software programs Surface Wave Analysis Wizard (Pickwin) and Wave Eq (Surface Wave Analysis) from the Seisimager software package were used for the processing of the MASW data. The processing includes two main steps described as follows:

1. The first step is to calculate the dispersion, or change in phase velocity with frequency using Pickwin module.
2. The next step is to calculate the shear wave velocity (Vs) profile by mathematical inversion (based on the least square method) of the dispersive phase velocity of surface waves using Wave Eq module.

Table 4.6: MASW (Passive) Acquisition Parameters

Parameter	**Setting**
Spread configuration	Linear
Spread length	Maximum 115m & Minimum 55m
Geophone Interval	10m, 5m & 3m
Total number of geophone	Maximum 24 & Minimum 12
Geophone Type	4.5Hz vertical geophone
Source	Ambient Microtremor
Trigger	Software trigger
Sample Interval	2ms
Record length	32 seconds each record, total of at least 20 records

Table 4.7: MASW (Active) Acquisition Parameters

Parameter	**Setting**
Spread configuration	Linear
Spread length	Maximum 115m & Minimum 55m
Geophone Interval	10m, 5m,& 3m
Total number of geophone	Maximum 24 & Minimum 12
Geophone Type	4.5Hz vertical geophone
Shot location	–First shot off-end at a near offset of one-half the geophone interval –Middle shots in between geophones –Last shot off the opposite end by the same near offset
Source equipment	Sledge hammer(10 kg) and striker Plate
Trigger	Hammer switch taped to hammer handle and connected to seismograph trigger port
Sample Interval	0.5ms
Record length	2s

VES surveys employing Schlumberger array have been carried with spread length (AB) varying from 100m to 1000m depending on available/favourable ground condition at 100 different locations. In VES, a known amount of electrical current is sent into the ground through a pair of current electrodes (AB) and potentials are measured in between these

current electrodes with another pair of potential electrodes (MN) on the ground. Multiplication of ratio of the measured potential difference to current input along with 'geometric factor' of electrode configuration gives 'apparent' resistivity of the 'inhomogeneous' ground. To probe the resistivity variation with depth, the separation between the current electrodes (AB) is increased successively. Apparent resistivity values obtained in the field are plotted on Log-log graph sheet against half current electrode separation (AB/2) to get the VES curve at the point of observation. These VES curves are initially interpreted using partial master curve matching technique utilizing two layer master curves and auxiliary point chart curves (Orelenna and Mooney, 1966). The interpreted results are further refined using DOS based computer program Resist and windows based software1X-1D.

4.5 Shear Wave Velocity

The site response of earthquake ground motions are solely based on the geotechnical properties of upper 30 m (Finn, 1991; Anderson et al., 1996; Boore et al., 1993).NEHRP, United States propounded that the response to shaking at most frequencies of engineering concern depends on the shear wave velocity of uppermost 30 m column. The site response of earthquake ground motions are solely based on the geotechnical properties of upper 30 m (Finn, 1991; Anderson et al., 1996; Boore et al., 1993). The shear wave velocity [V_S ($_{30}$)] of 30 m soil/ sediment column is calculated using SPT ($N_1$60 value/ corrected N values), geotechnical properties of the soils and subsurface disposition of soil units at 28 different sites of Meerut City. To get a perspective of overall seismic response at different sites on the ground, we estimated the weighted average of shear wave velocities separately calculated at 20 different levels within a depth column of 30 m in each bore hole. The obtained average shear wave velocities have been used for classification of sites based on National Earthquake Hazard Reduction Programme (NEHRP). Shear wave velocities of the subsurface soil column has been computed using the different empirical relationship as shown in Table 4.5. Average Shear Wave Velocity of each bore hole for entire column of 30 m has been computed on the basis of following relationship:

$$V_s^{30} = \frac{30}{\sum_{i=1}^{N}\left(\frac{d_i}{v_i}\right)}$$

Where *di* = *thickness of the i^{th} soil layer in metre;*

Vi = shear wave velocity for the i^{th} layer in m/s and *N = no. of layers in the top 30 m soil strata which will be considered in* evaluating *Vs 30 values.*

Table 4.8: The empirical relationships used for calculation of shear wave velocity (Vs30)

Author	Soil Type	Vs (m/s)
Hanumantha Rao(2008)	a) All Soils	$Vs = 86 (N)^{0.42}$
Uma Maheswari(2010)	a) Sands b) Clays	$Vs = 95.64\ N^{0.301}$ $Vs = 100.53\ N^{0.265}$ $Vs = 89.31\ N^{0.358}$
Uma Maheswari(2010)	All soils	$Vs = 95.64\ N^{0.301}$
Ohta and Goto (1978)	a) All Soils	a) $Vs=85.35 (N)^{0.348}$ b) $Vs = 62.14\ N^{0.219}\ H^{0.230}\ ST$ H = Depth; ST = 1 (clay); 1.09 (fine sand); 1.07 (medium sand); 1.14 (coarse sand); 1.15 (gritty sand); 1.45 (gravel)
Seed and Idriss (1982)	All soils	$VS = 61 (N)^{0.5}$

The average shear wave velocities of different sites for upper 30 m column by corrected SPT N_160 values using empirical relationships of different authors have been calculated (Annexure III). The graphical representation of Vs30 shows similar trends in every relationship (Fig. 4.5) along with slight variation in the values from 200 m/s to 307 m/s. The average shear velocities calculated by all relationships put the studied area in soil class 'D' of NEHRP classification. However, the values of average shear wave velocity at different sites in Meerut City by Hanumantharao, 2008 (as given in the standard operating procedures (SOP) of GSI) is relatively has a better correlativity with the MASW derived average shear velocity values. Therefore, for the purpose of further derivatives this method has been used in this report. The average shear wave velocity calculated as per relationship given by Hanumantharao, 2008 is in the range of 244 m/s to 307 m/s. The regression analysis between Vs30 and raw SPT values and corrected SPT values (N_160) has been attempted to show the difference of R^2 (correlation coefficient) between them (Fig. 4.6).

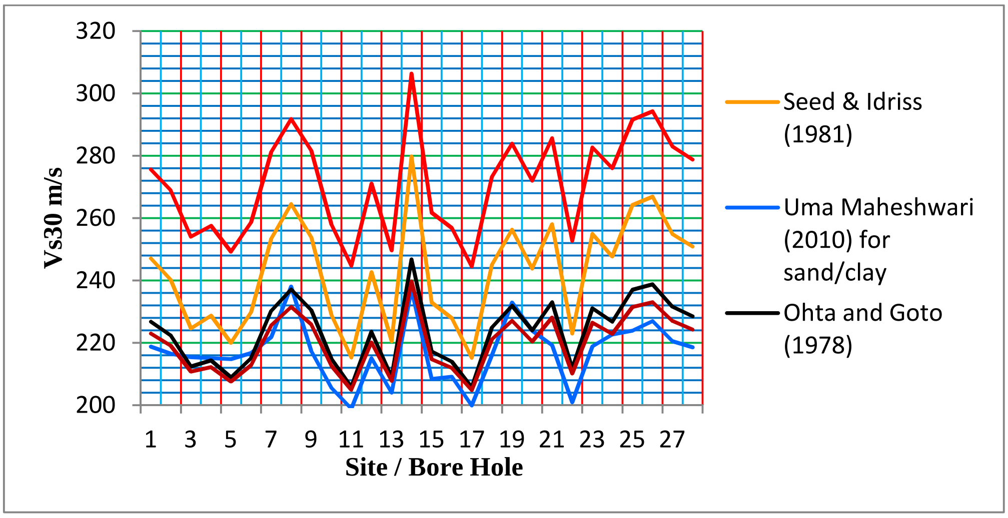

Fig. 4.5: The graphical representation of Vs30 values at different sites/ bore holes by using empirical relationships of different authors

A

B

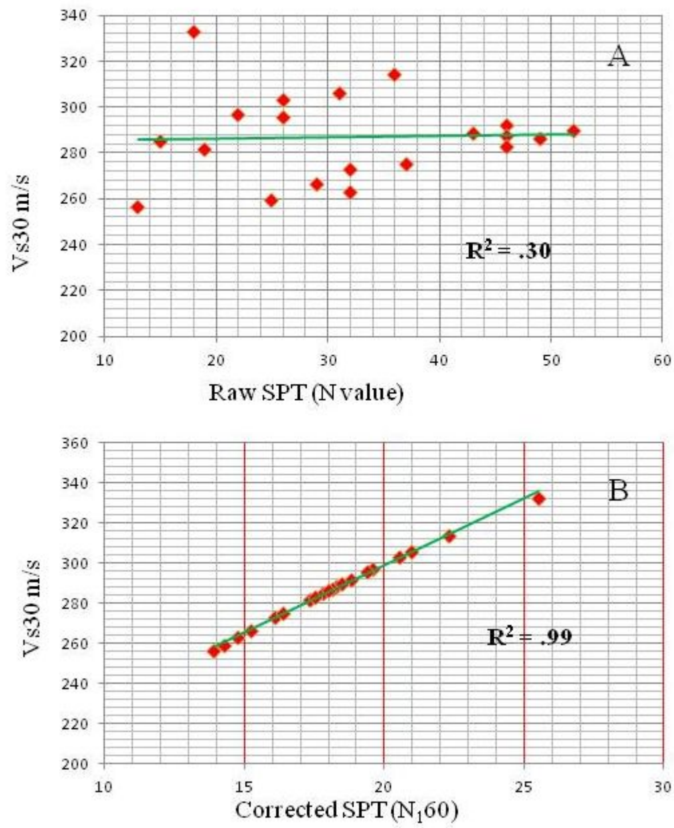

Fig. 4.6: The correlation between A) Vs30 and uncorrected SPT values and B) Vs30 and corrected SPT $N_1$60

The average shear wave velocity down to 30m depth by MASW survey has been determined using Seisimager Software. The overall variation of average shear wave velocity

down to 30m depth of sites within Meerut City ranges from 238.5m/s to 355.8m/s (Annexure IV) as obtained by geophysical method, i.e. MASW survey at 56 locations including few near bore hole sites. The 2D profiles of shear wave velocity of individual layers at different sites are shown in Annexure V. The Vs30 obtained through geotechnical method based on $N_1 60$ values (corrected N values) range from 244 m/s to 307 m/s (Annexure III) as estimated at 28 bore hole sites. Data density of shear velocity values obtained by geophysical method is more (i.e. total 56 nos., out of which 20 nos. lie near the bore hole sites) in comparison to data obtained by geotechnical method (28 nos.). The shear wave velocity obtained through geotechnical and geophysical methods at the borehole sites is almost similar in some cases. For example at Pabli khurd, the shear wave velocity obtained by geotechnical method is 291 m/s while 292 m/s by geophysical (MASW) method. However, at some sites, the value obtained from the two methods are little different, which may be due to slight variation in location of observation or other intrinsic reasons. The data collected through geotechnical studies and MASW survey is not from the same sites (except at few sites), therefore, the small variations in the Vs30 values recorded by both methods may not be indicating anything of reckoning.

In ground response analysis, shear wave velocity of individual layers up to a few meter depths below ground surface play a very important role. The Vs30 obtained by both the methods, puts studied part of the Meerut City in soil class ‘D’ of NEHRP code provisions, which ranges from 180 m/s to 360 m/s (Figure 4.7 and table 4.10). The Vs30 in the studied part of Meerut varies from 248 m/s to 310 m/s (by geotechnical method), 238.5 to 355.8 m/s (through geophysical method). This rather short range of the variation in Vs30 in the studied part indicates that there won’t be any significant changes in the ground motion response to a large earthquake at different sites. In simple words, the overall variation in site responses assessed/ estimated in the area is too small to predict any remarkable changes in the effects of the earthquake over different parts of the city and its surroundings.

Considering above facts, an average shear velocity map is prepared (Figure 4.8) using data obtained through both geotechnical and geophysical methods. The advantage is that while a better data distribution of shear wave velocity values by combining the data becomes available, it also helps in arriving at a better confidence level by selecting the data by comparing those from two sources, respectively.

The average shear wave velocity is relatively low in the western part near Sainik Vihar, Kharauli, Rampur Paoti, in northern part near Daurala, in eastern part near Eslamabad Chillaura and in south eastern part near Jithauli and Hazipur areas. The value of average

shear velocity at different sites in Meerut City corresponds to the Soil Type-D of the site classes of NEHRP (Table 4.10). Site specific elastic response spectra proposed by UBC (Uniform Building Code), 1997 for NEHRP soil classes for peak rock acceleration of $2 m/s^2$ is shown in Figure 4.7.

Table 4.9: Vs30 values at different sites based on both geotechnical and geophysical data.

No	Long	Lat	Vs30	Location
1	28.92883	77.66072	275.567	D.N . Polytechnic, Rithani
2	28.91961	77.71378	268.914	Jurranpur
3	28.98244	77.64958	254.041	Kharauli
4	29.00458	77.62286	257.544	Sandhauli
5	28.91764	77.64764	249.199	Partapur
6	28.97514	77.63475	258.601	Rampur Paoti
7	29.0509	77.64553	281.229	Badjewra
8	29.06517	77.66969	291.727	Pabli khurd
9	28.96811	77.67131	281.64	Jaswant mill Sabungodam
10	28.99189	77.68042	257.925	Race Course, Cantt
11	29.00006	77.70392	244.65	Gandhi bagh
12	28.96536	77.70072	271.059	Nauchandi
13	29.03506	77.65266	249.633	Sainik Vihar, water tank
14	28.95489	77.77044	306.325	Datauli
15	28.91833	77.74347	261.648	Hajipur
16	28.92181	77.77617	256.752	jithauli, Near Power house
17	28.99383	77.78586	244.484	Eslamabad Chillaura
18	29.02983	77.74178	273.217	Mamepur
19	29.03208	77.783	283.889	Saini village
20	29.07147	77.77644	271.976	Jalalpur
21	29.0725	77.72947	285.593	Dulehra
22	29.11542	77.69975	252.693	Daurala
23	29.10175	77.73547	282.666	Water tank campus, Panwari
24	29.10383	77.78681	275.94	Lawar khaas, cold storage
25	28.97214	77.74356	291.55	CCU, Campus
26	29.007	77.75453	294.161	Water tank campus, Ganganagar

27	29.06728	77.70778	282.952	CPRI Modipuram
28	29.02364	77.71139	278.762	Saufipur
29	28.9150	77.6635	295.9	Play ground of Adhyan School
30	28.9625	77.6840	311.1	Ramlila Maidan, Transport Nagar
31	28.9846	77.6980	336.9	Play ground of Faiz-e-amm Degree college
32	28.9869	77.6813	314.6	CMT Ground, Cantontment Area
33	28.9940	77.6618	341	Army Ground Jawahar Nagar
34	29.0135	77.6451	288	Dabka village
35	29.0515	77.6440	331.5	St. John Inter College, Jangethi
36	29.0652	77.6354	283.8	Near Mahavir international School
37	29.0079	77.6860	290.4	Grass Mandi footbaal Ground, Meerut Cant.
38	28.9354	77.6870	317.1	Nagla Sherkhan
39	28.9190	77.6890	309	West of Gogole Village
40	28.9222	77.6299	340.9	Near Saraswati Public School
41	28.9474	77.6323	321.2	Shrinathji Institute of Technical education
42	29.0581	77.6931	296.5	Vill. Dwarkapur
43	29.0034	77.7158	308.7	Kulwant Singh Stadium, Cantt
44	29.0351	77.6918	331.1	Behind Sharda Farm, Vill. Dantal
45	28.9541	77.6584	342.8	Near Vill. Sundra, RAF Battallion
46	29.0318	77.6289	319	Vill Ghasauli
47	28.9550	77.7208	308.7	Abdullah Farm, Near Hapur Chungi
48	28.9855	77.7221	306.8	Circuit House, Meerut
49	28.9364	77.7080	351.8	Lisari Bhag
50	28.9433	77.6555	273.5	Middle School,Pootha, Meerut.
51	29.0740	77.6796	256.4	North of Pabli Khas Village.
52	29.0580	77.6791	261.2	Jewri Village.
53	28.9809	77.7515	305.4	Military farm no.2 Abdullapur
54	29.1000	77.7187	314.8	BP Inter College, Bharala
55	29.0815	77.6983	316.9	SVP University
56	29.0556	77.7401	289.2	Uldepur
57	29.0533	77.7662	324.6	Mukhtyarpur Nagla
58	28.9696	77.7898	305.4	Road to Medhpur, Medhpur

59	29.0894	77.7528	305.5	Near Kali Nadi, Mamurpur
60	29.0800	77.7810	333.4	Andwali
61	29.0229	77.7137	348.2	Rajpura
62	29.0016	77.7453	316.6	Aadarsh Park, Mawana Road
63	29.0145	77.7681	299.2	Rajpura
64	28.9465	77.7433	304.8	Sector 03, Jagriti Vihar Extension

Table-4.10: NEHRP soil types based on shear wave velocity of upper 30 m column (BSSC, 1997, UBC, 1997)

Soil Types	Rock/ Soil Description	**Average shear wave velocity (Vs30) m/s**
A	Hard rock	> 1500
B	Rock	760-1500
C	Dense soil/soft rock	360-760
D	Stiff soil	180-360
E	Soft soil[1]	<180
F	Special soils requiring special evaluation[2]	---
[1]Site class E also includes any profile with more than 3 m of soft clay, defined as soil with plasticity index >20, water content >40% and undrained shear strength <25kPa. [2]Site class F includes: i- soils vulnerable to failure or collapse under seismic loading (i.e e., liquefiable soils, quick and highly sensitive clays and collapsible weakly-cemented soils); ii- Peat and/or highly organic clay layers more than 3 m thick; iii- Very high plastic clay (PI >75) layers more than 8 m thick; iv- Soft to medium clay layers more than 36 m thick.		

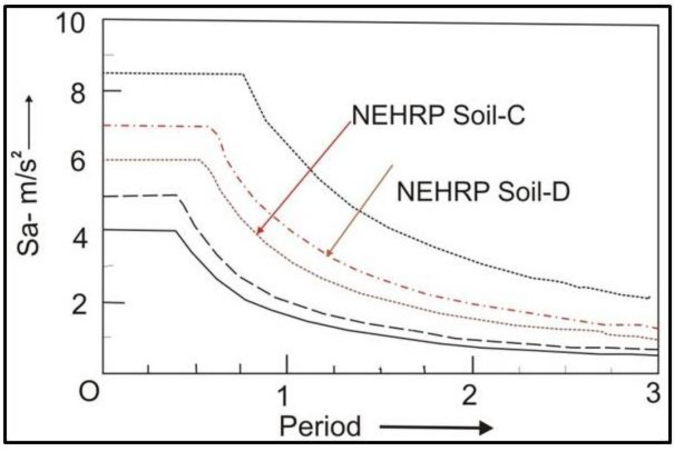

Fig. 4.7: Site specific elastic response spectra proposed by UBC, 1997 for NEHRP soil classes (at $2 m/s^2$ rock acceleration)

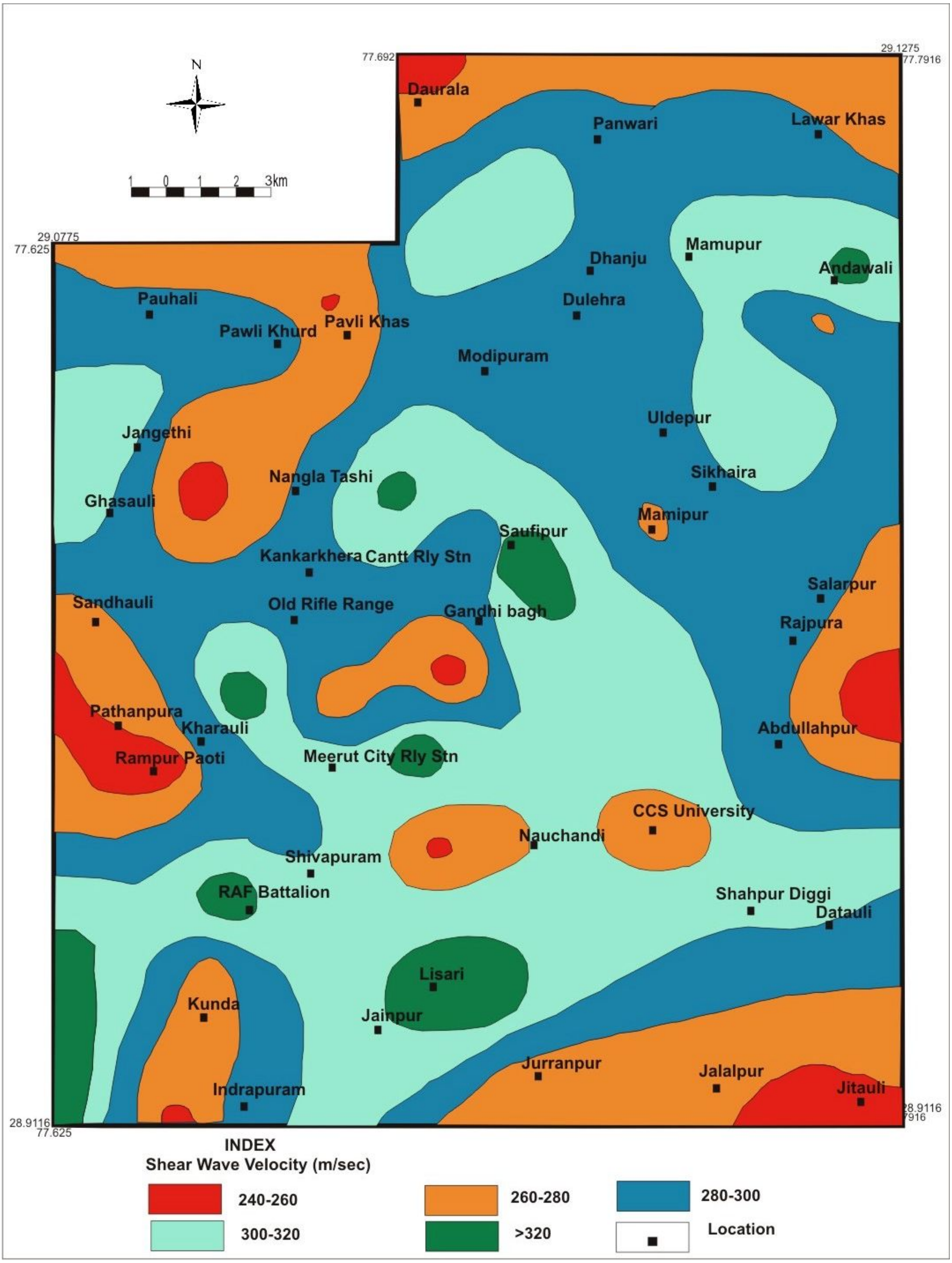

Fig. 4.8: Average shear wave velocity (Vs30) map of Meerut City (based on geotechnical and geophysical data)

4.6 Peak Amplification

The Average Horizontal Spectral Amplification for strong motion at the bore hole sites is computed on the basis of obtained Vs30, in period range of 0.4 to 2.0 seconds (0.5 to 2.5 Hz) using following empirical relationship proposed by Borcherdt et al., 1991:

ASHA = 600/ Vs for strong motion

The amplifications values thus estimated using Vs30 obtained by geotechnical (SPT) method are in the range of 1.96 to 2.37.

The peak amplifications (Annexure VI) estimated through geophysical survey from the site response HVSRV curves (Annexure VII) show variation in the range of 1.008 - 2.761. However, the two isolated point data of anomalous values more than 2.5 were discarded for preparation of peak amplification map. Finally, the peak amplification map is prepared incorporating the data of geotechnical and geophysical studies (Figure 4.9). Overall, the peak amplification in the area is on the lower side in the predominant frequency range of 2.0 Hz to 4.5 Hz (Figure 4.11). Broadly corroborating to the lower Vs30 zones, the higher amplification domains are present in western part near Sainik Vihar, Kharauli, Rampur Paoti; in northern part near Daurala, Pauhali, Modipuram; in eastern part near Eslamabad Chillaura and in south eastern part near Jithauli and Hazipur in Meerut City. At few localities isolated higher amplification are obtained which correlatable with the presence of loose overburden soil there, such situation is likely to amplify the ground motion which likely to cause moderate to high damage during a big earthquake in the neighbouring region.

The low amplification and relatively higher predominant frequencies within 2.0 Hz to 4.5 Hz in the area may be due to presence of almost uniform geological setting i.e. Older Alluvium up to 30 m depth. The uppermost surface layer of Older Alluvium horizon is consolidated along with presence of kankar beds, leading to a litho-configuration with somewhat un favourable impedance contrast. Further presence of very thick alluvial cover of Gangetic foredeep in the Meerut City is also likely to dampen the incoming seismic waves by absorbing considerable part of the mechanical energy, eventually attenuating the amplification effects depending on the thickness of the soft sediments and absence of impedance contrast for incoming seismic waves.

4.7 Predominant Frequency

The predominant frequency is estimated by ambient noise survey at 321 sites (Annexure VI) in the frequency band of 0.5 Hz to 10 Hz for the present work. The overall variation in predominant frequencies of sites within Meerut City ranges from 0.61 Hz to 9.33 Hz. However, the majority of predominant frequency in Meerut City falls in the range from 2.0 Hz to 4.5 Hz. The large variation may reflect the variation of sediment thickness above bedrock. The soil predominant frequency is an indicator of the bedrock topography (Paraloi et al., 2002).

Generally, in an environment of variable soil thickness, the frequency may be interpreted in terms of variable depth of bedrock. However, this is not always the case because the frequency of the ground motions depends not only on the thickness of the soil cover but also the shear wave velocity (or in other words the elastic response) of the media through which the wave traverses. In the present case, we have a situation where it is well known that the hard rock does not occur, say above 1000 m, which broadly should not cause a variation in frequencies such as those described above. This, in turn, would imply that the possible variations in the soil stiffness in the soil profile in the area of study might have been responsible in the variation in predominant frequencies found out during the course of investigation.

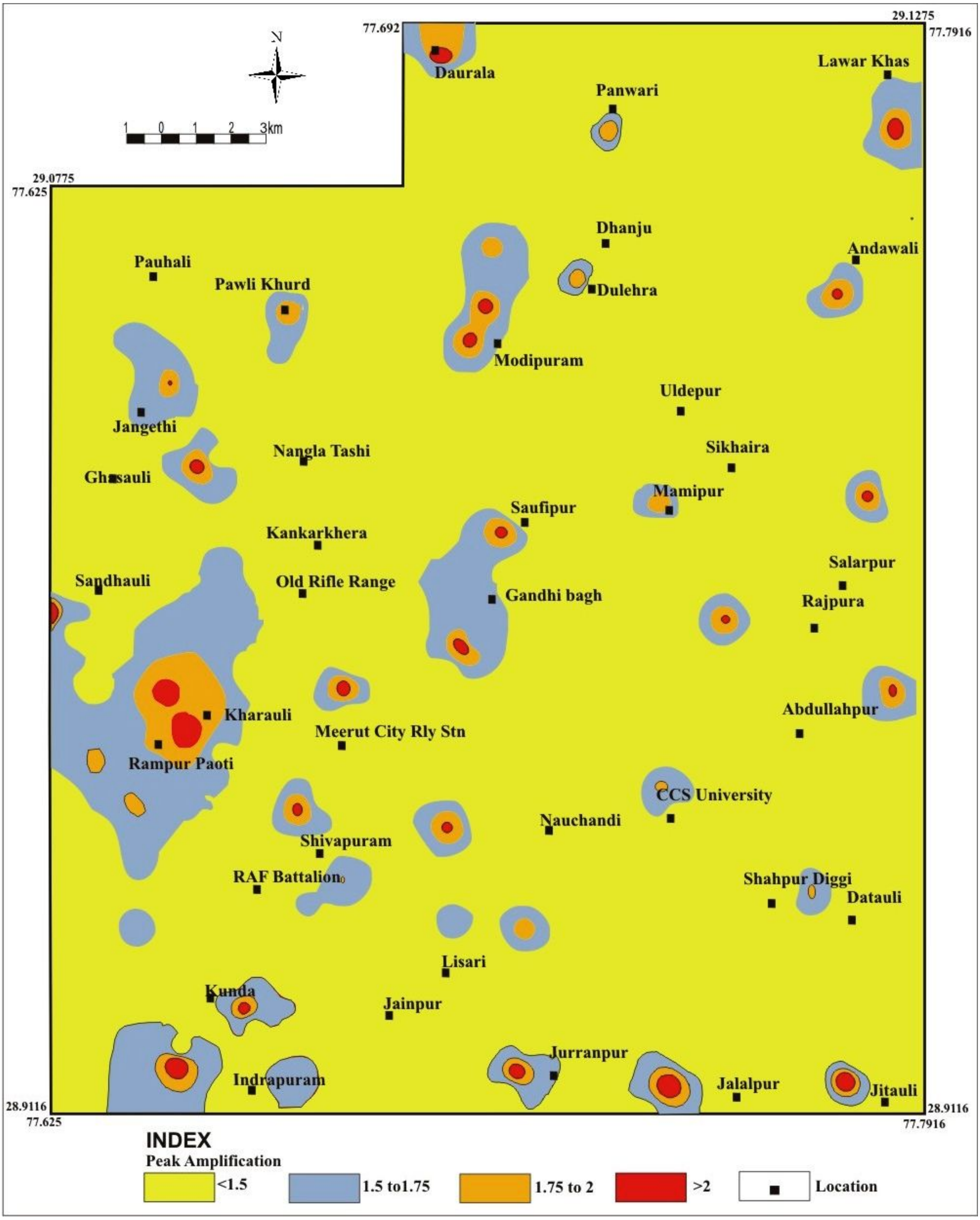

Fig. 4.9: Peak amplification map of Meerut City

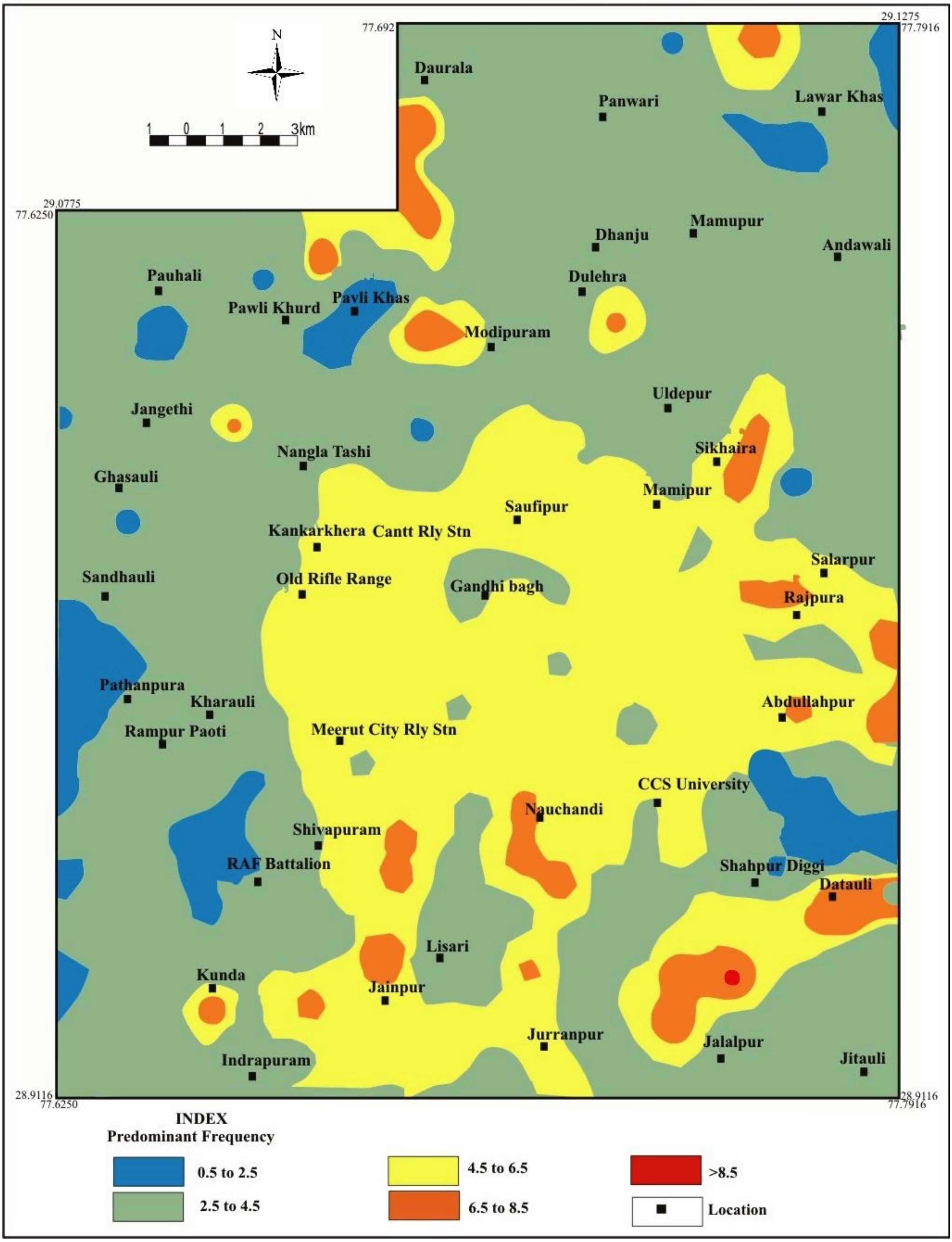

Fig. 4.10: The predominant frequency map of Meerut City.

4.8 Scatter Plot of Predominant Frequency vs Peak Amplification

The scatter plot of Meerut city has been prepared to show the relationship between predominant frequency and peak soil amplification of sites (Figure 4.11). Scatter plot shows that majority of the localities have peak soil amplification in the range of 1.0 to 1.5 in predominant frequency range of 2.0 Hz to 4.5 Hz. In the frequency range of 2.0 Hz to 4.5 Hz, there are also few sites having soil amplification more than1.5. This implies that majority of sites/structures in Meerut city having natural frequency in the range of 2.0 Hz to 4.5 Hz may be at relatively low risk of seismic hazard. However, some locations are there wherein similar structures having 2 to 5 storeys may relatively at moderate risk. Another cluster with predominant frequency in the range of 7.5 Hz -9.3 Hz and soil amplification less than 1.5 are at low risk against major earthquake.

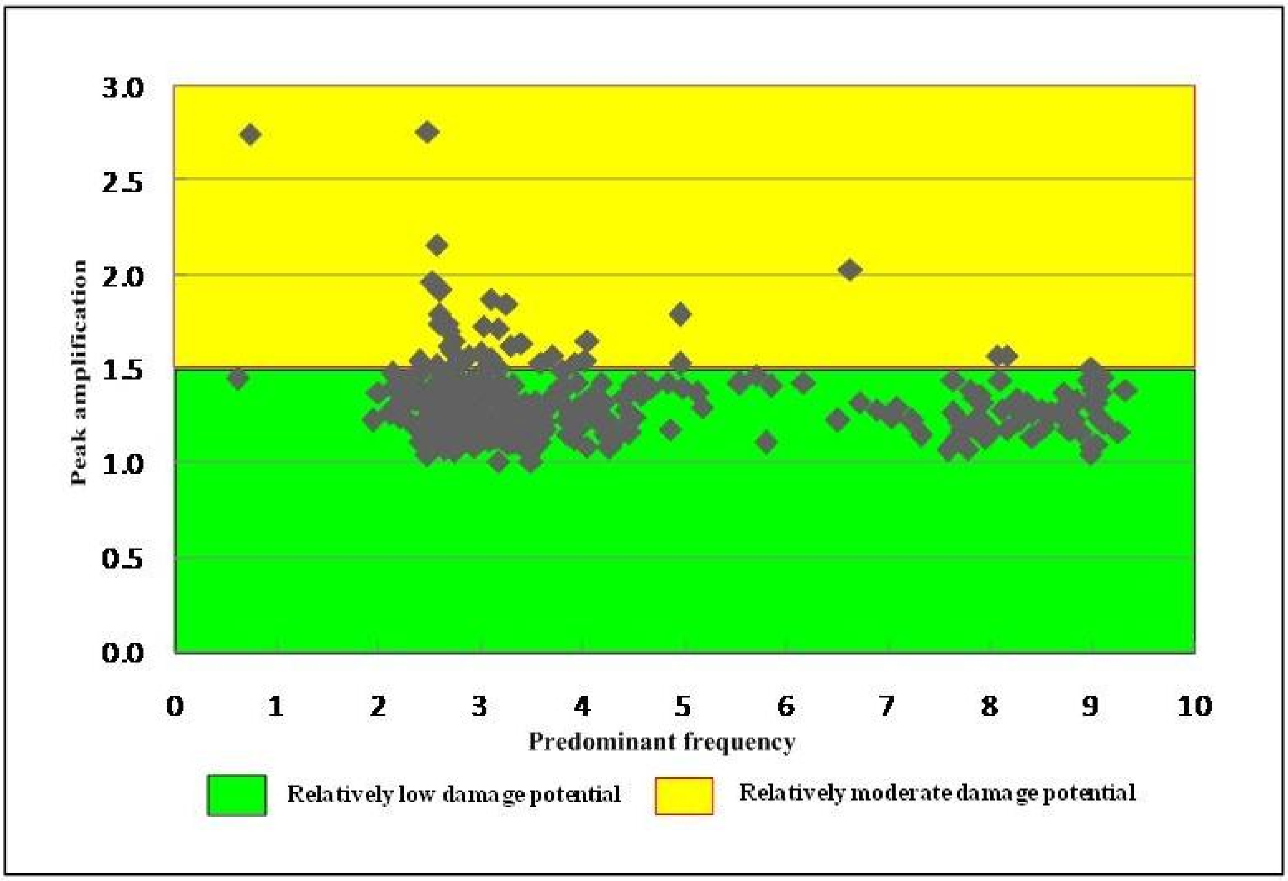

Fig. 4.11: Scatter plot (predominant frequency and peak amplification) of Meerut City

4.9 Vertical Electrical Resistivity Sounding (VES) Survey

The nature of vertical electrical resistivity sounding (VES) curves (Apparent resistivity vs half current electrode spacing) (Annexure VIII) varies from place to place due to variation in subsurface soil condition (lithological variations and composition of materials) of the overburden and presence of groundwater. The overall variation of resistivity is ranging from 3.8 Ohm-m to 2508 Ohm-m and maximum depth encountered is 47.4m. This wide range of variation in resistivity is mainly due to lithological variation, degree of consolidation, variation in grain size of clastic unit and presence of ground water. The detailed analysis of electrical resistivity sounding curves (Annexure IX) reveals mainly H, HK, HA, AKHKH, and HQ type of curves indicating 3-5 layered subsurface configuration in Meerut City. Out of these curves HK type curve is predominant in the study area.

The top layer with resistivity varying from 6.0 Ohm-m to 678.4 Ohm-m (0.5 m to 5.5 m thick), the second layer from 5.2 Ohm-m to 2508 Ohm-m (0.7 m to 33.3 m thick), the third layer from 11.9 to 1273 Ohm-m (1.2 m to 39.6 m), the fourth layer from 5.6 to 919.1 Ohm-m (8 m to 35.3 m thick), the fifth layer from 12.9 to 1436.0 Ohm-m. The resistivity value at site VES-19 is 3.8 ohm-m has been inferred due to presence of perched water table/ ponds in nearby area.

The inferred lithology / water table based on vertical electrical resistivity sounding (VES) curves at Panwari is correlated with lithology/ water table directly observed at same site from bore hole data (Figure 4.12). The lithological variation recorded in bore hole shows discrepancy from inferred lithology by VES study. The water table recorded in this bore hole is at 14.55 m depth, however, it is at 19.5 m depth by indirect method of VES survey.

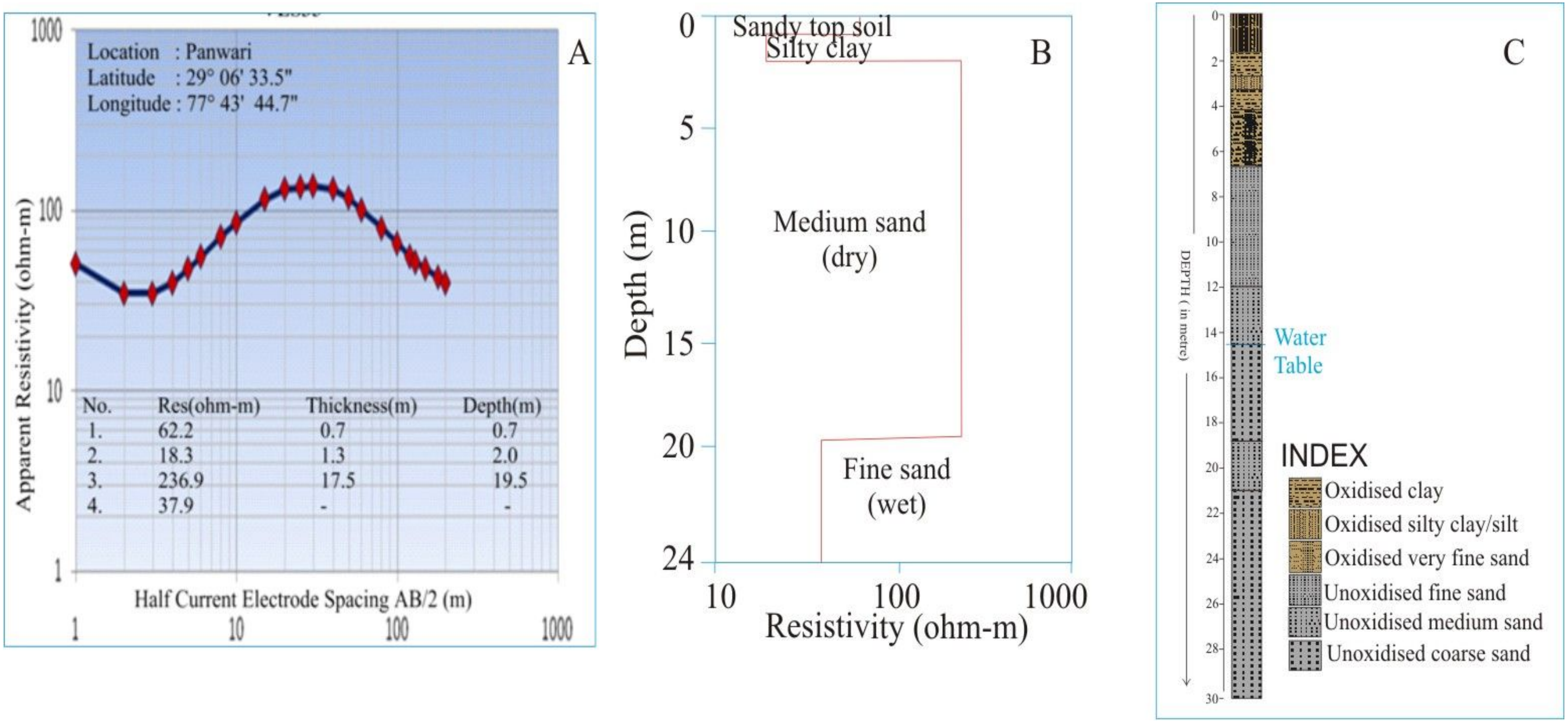

Fig. 4.12: Correlation between, A)- Interpreted vertical electrical sounding curve; B)- VES curve derivative profile section showing lithology and water table and C)- Bore hole log showing lithology and water table at Panwari, Meerut

V. LIQUEFACTION HAZARD STUDIES

Liquefaction is defined as the transformation of a granular material from a solid to a liquefied state as a consequence of increased pore-water pressure and reduced effective stress (Marcuson, 1978). Liquefaction is the phenomena connected to soil performance of site which is of great importance essentially for stabilization of foundations. Seismic hazard assessment with respect to liquefaction potential is very crucial in microzonation studies. Most important earthquake induced ground failures are attributed to liquefaction (Seed and Idriss, 1982, and Idriss, 1990). Liquefaction hazard evaluation generally deals with three issues viz. liquefaction susceptibility, initiation of liquefaction and effect of liquefaction.

Field evidence of liquefaction generally includes surficial observations of sand boils, ground fissures, or lateral spreads. During an earthquake, base rock movements along the fault generate shear waves that propagate through overlying soils. Liquefaction results when these shear waves, passing through saturated sand layers, distort the granular structure and cause loosely packed grains to collapse due to reduction of shear strength of saturated sandy sediments by increasing pore water pressure or shear forces. This densification causes an increase in pore pressure if drainage cannot occur. If the pore pressures exceed roughly sixty percent (60%) of the soil's effective stress, large settlements and translational deformations can occur (Seed and Idriss, 1982). The geologic and hydrologic factors that affect liquefaction susceptibility are the age and the type of sedimentary deposits, the looseness of cohesion-less sediments and depth of the ground water table (depths less than 12 m to 15m). Ground water levels have a great influence on the Liquefaction potential. The susceptibility of older soil deposits to liquefaction is generally lower than that of newer deposits. Soils of the Holocene age are more susceptible than soils of Pleistocene age.

Liquefaction commonly follows moderate to great earthquakes throughout the world under a particular set of geo-environmental conditions. The 1964 Alaska earthquake, the 1964 Niigata, Japan earthquake, the 1967 Caracas, Venezuela earthquake and the 1971 San Fernando, California earthquake have induced liquefaction in large areas. In India, the 1934 Bihar-Nepal earthquake caused widespread liquefaction. Recently, the 2001 Kutch (Bhuj) earthquake produced spectacular effects of liquefaction including lateral spreads, sand blows, sand craters, etc. During 8th October 2005 Kashmir earthquake too, liquefaction was witnessed in riverine sediments in Jammu area at a distance of about 250 km from the epicentre.

The data collected during the exploration for determining the site response factors have been utilised to work out liquefaction susceptibility in Meerut City. The subsurface geometry based on the lithologs of boreholes drilled, reveal that there are presence of clayey soil at the top followed by grey sand of variable grain sizes and silt. The fine sand and silt horizons are most likely susceptible for liquefaction. The grain size analysis (annexure-II) of the subsurface sediments indicates that many sand layers fall within the limits of the most liquefiable sands of Tsuchida and Hayashi (1971). The correlation of the sediments present in the boreholes with respect to the grain size distribution curves (Annexure-II) indicates that quite a number of the sand layers at shallow depth fall within the limits of the most liquefiable class. In saturated conditions, the sand layers would be susceptible to liquefaction during earthquake intensity more than VI on MSK scale. However, in Meerut City, the shallowest water table is 8.5 m near Partapur in south western part of the area. In the western and north eastern part which is away from main city, the water table is also shallow. However, in main city, the water table is generally deeper (>22m). This implies that in Meerut City where the saturated conditions and sediment horizons susceptible to liquefaction are present in the north eastern, western and south western part liquefaction may take place in case of occurrence of a strong earthquake. However, the presence of liquefiable layers and absence of saturated conditions in central and eastern part of Meerut City will have remote possibility of liquefaction in the rare event of a very strong earthquake.

In order to determine the liquefaction potential, it is necessary to find out the relative liquefaction susceptibility of the area. The susceptibility data, when combined with the liquefaction opportunity, spell the liquefaction hazard or the liquefaction potential of an area.

In the present study, an attempt has been made to calculate the safety factor as a measure of liquefaction susceptibility by utilising the analytical results of soil samples and other data collected during drilling investigation.

5.1 Liquefaction Susceptibility

Liquefaction 'susceptibility' is a measure of a soil's inherent resistance to liquefaction, and can range from not susceptible, regardless of seismic loading, to highly susceptible, which means that very little seismic energy is required to induce liquefaction. Susceptibility has been evolved by comparing the properties of top soil deposits of the region under study to the other soil deposits where liquefaction has been observed in the past (based on Seed et al., 1985). Liquefaction susceptibility is evaluated based on the primary relevant soil properties such as grain size, fine content, and density, degree of saturation, SPT-N

values and age of the soil deposit in each of the bore hole logs. Generally soil may be susceptible for liquefaction if:

(1) There is presence of sand layers at depths less than 20 m,

(2) The water table depth is less than 10 m, and

(3) SPT value 'N' blow counts are less than 20.

Liquefaction potential of a given site is generally done using ground motion characterization, intensity, shear resistance of soil and its sensitivity to ground shaking sequence, and knowledge of several soil parameters.

It's well known that liquefaction generally takes place where the groundwater is available at shallow depth. Most of the liquefaction reports are from areas where depth to groundwater is not deeper than 10 m. However, stray reports of liquefaction have also been reported from areas where depth to water table was in the range of 20 m.

5.2 Factor of Safety and Liquefaction susceptibility

The Quaternary sediments of fluvial nature are present in Meerut City. The Older Alluvium consists of sand, silt and clay. Liquefaction susceptibility has been estimated resorting to popular technique of Standard Penetration Test (SPT) at 28 sites. The N value data obtained have been suitably corrected and analysed for liquefaction susceptibility. Liquefaction susceptibility is generally evaluated by comparing measure of earthquake loading and liquefaction resistance and it is expressed in terms of factor of safety. Seed and Idriss (1971 and 1985) have elaborated the concept and provided classical method (cyclic stress approach) to ascertain the liquefaction susceptibility and associated hazard of the area. The seismic capacity of the soil horizons has been ascribed to them in terms of SPTN values.Liquefaction susceptibility of a given site is generally estimated using ground motion characterization in terms of intensity, shear resistance of soil and its sensitivity to ground shaking sequence, and knowledge of several soil parameters**.**Two variables are required for the estimation of liquefaction resistance of soils in the area which are as follows:

1. The seismic demand of a soil layer is represented by a Cyclic Stress Ratio (CSR).Cyclic Stress Ratio refers to both the Cyclic Stress Ratio generated by the earthquake and the Cyclic Stress Ratio required to generate a change of state in the soil to a liquefied condition.

2. The capacity of soil to resist liquefaction is represented by Cyclic Resistance Ratio (CRR).The stress ratio required to cause a change of state of the soil to a liquefied condition is referred to throughout in this text as the Cyclic Resistance Ratio.

The equation for factor of safety is given by the ratio of:

$$\mathbf{FS= CRR/CSR}$$

Where, CRR= Cyclic resistance ratio; CSR= Cyclic stress ratio.

The factor of safety represents criteria which are given as:

(i) FS < 1 for liquefiable soil i.e., failed state.

(ii) FS = 1 at the point of failure indicating vulnerability, and

(iii) FS > 1 for non-liquefiable soil i.e., stable state.

Seed and Idriss (1971) formulated the following equation for calculation of cyclic stress ratio:

$$\mathbf{CSR=0.65Amax/g\ \sigma_{VO}/\ \sigma'_{VO}\ r_d}$$

Where Amax - the peak ground acceleration has been taken as .17g which is the calculated PGA (based on scenario earthquake of M 8 and x 160.7 km epicentred at Mathura**)** in Meerut City; σ_{VO} and σ'_{VO} are the total and effective over burden pressure, $r_{d.}$is the depth reduction factor. The ratio of maximum horizontal to gravitational acceleration (Amax /g) quantifies the strength of ground shaking expected at a particular site during a specified earthquake. The ratio of total overburden stress to effective overburden stress (σ_{VO}/ σ'_{VO}) quantifies the inherent resistance of deformation of a particular sediment at a particular subsurface depth at a particular ground - water conditions. Average values of r_d have been calculated using following equation proposed by Liao and Whitman (1986):

$$\mathbf{r_d= 1- 0.00765z\ for\ z < 9.15m}$$

$$\mathbf{r_d= 1.174-0.0267zfor\ 9.15m <z<23m}$$

Where z = depth below ground surface in meters

Corrected $N_{1(60)}$ has been used for evaluation of liquefaction resistance described in the chapter Site Response Studies. For calculation of second variable i.e. CRR, Rauch (1997) used the following equation:

$$\mathbf{CRR = 1/34 – (N_160) + (N_160)/135 + 50/\ [10(N160) +45]^2- 1/200}$$

where N_160 is the corrected SPT value.

Seed and Idriss (1982) classified the terrain based on FS values in the following manner:

FS<1 high liquefaction susceptibility;

FS 1 - 1.5 moderate liquefaction susceptibility;

FS 1.5 - 2low liquefaction susceptibility;

FS>2 very low liquefaction susceptibility.

5.3 Liquefaction Susceptibility map

The liquefaction susceptibility in Meerut City has been assessed at different depths using the classification given by Seed and Idriss (1982). Adopting conservative approach the minimum value of safety factor in the bore holes in which the ground water depth is of 12 m is taken for preparation of liquefaction susceptibility map. The shallowest water table in Meerut is 8.5 m in Partapur and at 6 sites are less than 12 m. Therefore, these 6 bore holes in which depth of ground water is <12 m, are taken for calculation of safety factor. The lowest values of safety factor calculated are given in Table 5.1 and contour map prepared is given in Fig. 5.1. The safety factor values range from .85 to 1.17 up to the depth of 12 m. In the study area, high liquefaction domains are near Sainik Vihar, Daurala and Sandhauli in Meerut City. Analysis and comparison of liquefaction susceptibility map with shear wave velocity map (Figure 4.8) and ground water map (Figure 2.8) of study area shows that the high liquefaction domains are present in low velocity and low ground water table areas.

Table 5.1: Minimum value of safety factor in 6 bore holes in which ground water table is up to depth of 12 m in Meerut City, coloured rows show safety factor <1.

Bore Hole	Location	Latitude	Longitude	**Minimum safety factor**	**Depth of water table (m)**
MER-2	Jurranpur	28.91961	77.71378	1.13	12
MER-4	Sandhauli	29.00458	77.62286	0.85	12
MER-5	Partapur	28.91764	77.64764	1.17	8.5
MER-7	Badjewra	29.0509	77.64553	1.1	10.5
MER-13	Sainik vihar,water tank	29.03506	77.65266	0.93	10.5
MER-22	Daurala	29.11542	77.69975	0.88	10.5

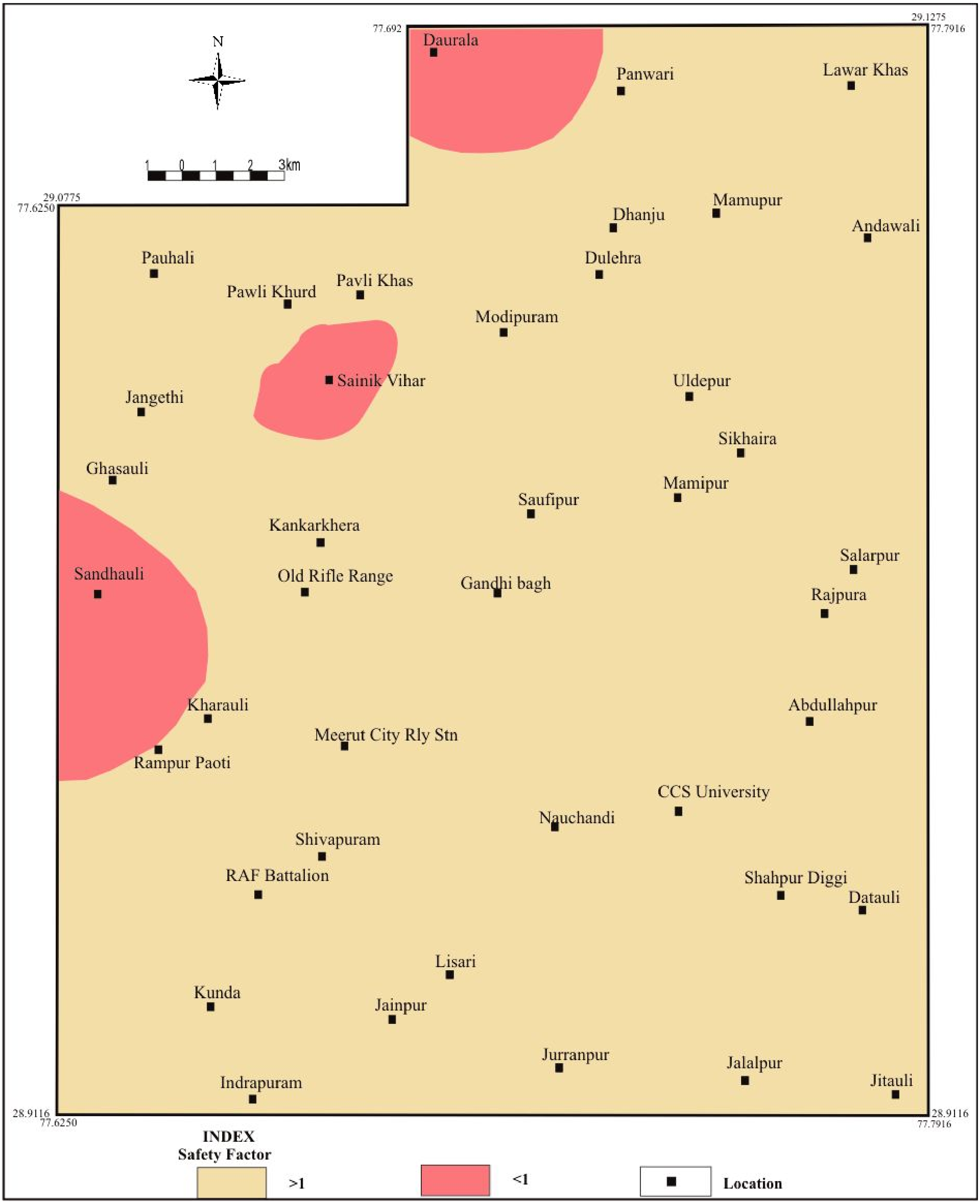

Fig. 5.1: Liquefaction susceptibility map based on safety factor up to 12 m depth

VI. INTEGRATION OF SEISMIC HAZARD MAPS

A predictive model, which conveys the temporal snapshot of the system of interest (i.e. different geo-information described in form of thematic maps) involves analysis and integration of their variables on the basis of knowledge driven method of Analytical Hierarchy Process (AHP) (Saaty and Vargas, 2001). The first step to analytical approach was to subdivide a geographic domain into smaller areas having different potential for hazardous effects of earthquake. The earthquake effects depend on 'geoscientific' attributes such as geology, geomorphology, landuse-land cover, soil coverage/thickness and 'geotechnical' attributes such as dynamic property of soil profile and water table etc. The peak ground acceleration (PGA), amplification/ site response, predominant frequency and liquefaction due to earthquake are some of the important seismological attributes.

In the present study of Seismic Microzonation of Meerut City, following thematic maps relevant to site specific seismic hazard have been considered for integration on Arc GIS platform to generate the final seismic hazard index map:

i. Geological map
ii. Geomorphic map
iii. Landuse map
iv. Average shear wave velocity map
v. Peak amplification map
vi. Liquefaction susceptibility map
vii. Predominant frequency map

Multi-criteria assessment for seismic microzonation to demarcate different seismic hazard level of an urban agglomeration has been accomplished previously in other urban regions of India, viz. Guwahati (Nath et al., 2007), Sikkim Himalaya (Pal et al., 2008), Delhi (Mohanty et al., 2007 and MOES, 2016) and Bangalore (Anbazhagan et al., 2010). The hazard mapping is achieved through multi-criteria based decision support tool formulated by Saaty (1980) referred to as Analytical Hierarchal Process (AHP) (Figure 6.1). It uses hierarchical structures to represent a problem, and thereafter, develop priorities for the alternatives based on the consensus judgement.

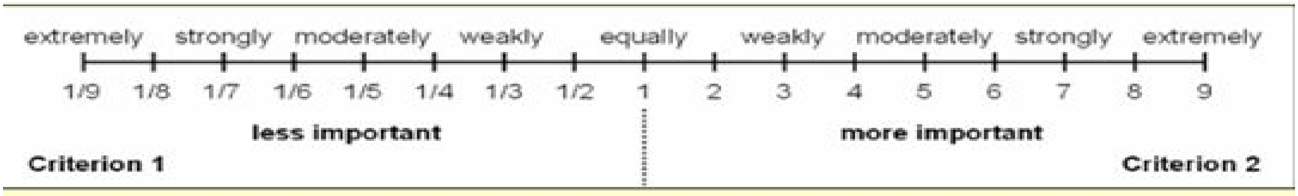

Fig. 6.1: Scale for pair wise comparison proposed by Saaty, 1980

The above mentioned comparative scale was used to obtain weights of importance of the decision criteria or thematic maps and the relative importance of each decision criterion. Pairwise comparisons were used to determine the relative importance of each alternative with respect to each other in terms of each criterion following a scale from 1 to 9 and its reciprocals. This gives a normalised weight for each criterion as shown in Table 6.1.

Table 6.1: Pair-wise comparison matrix of themes and their normalized weights.

	GEOL	**LU**	**GEOM**	**SWV**	**PA**	**LQ**	**PF**	**Normalised weights**
GEOL	7/7	7/6	7/5	7/4	7/3	7/2	7/1	0.249973
LU	6/7	6/6	6/5	6/4	6/3	6/2	6/1	0.214309
GEOM	5/7	5/6	5/5	5/4	5/3	5/2	5/1	0.178576
SWV	4/7	4/6	4/5	4/4	4/3	4/2	4/1	0.142853
PA	3/7	3/6	3/5	3/4	3/3	3/2	3/1	0.107154
LQ	2/7	2/6	2/5	2/4	2/3	2/2	2/1	0.071423
PF	1/7	1/6	1/5	1/4	1/3	1/2	1/1	0.035712

GEOL: Geology; LU: Land Use; GEOM: Geomorphology; SWV: Average Shear Wave Velocity; PA: Peak Amplification; LQ: Liquefaction susceptibility in terms of safety factor; PF: Predominant frequency.

The next step is to extract the relative importance implied by the subdivisions of each criterion/theme and to define criterion ranking which should be normalised to 1. Within each theme, the values vary significantly and are hence classified into various ranges or types collectively referred to as feature classes of a thematic layer. The associated features are ranked or scored within the weightage of theme. The initial integral ranking, *Ri*, is

normalized to ensure that no layer exerts an influence beyond its determined weight using the following relation

$$R_{norm} = (R_i - R_{min}) / (R_{max} - R_{min})$$

Where, R_{norm}, R_{min} and R_{max} are the normalized, assigned minimum and maximum ranks respectively.

Table 6.2: Normalized weights and ranks assigned to the respective themes and the features for thematic integration.

Themes	Weight	Feature/ Values	Rank	Normalized Rank
GEOL	0.249973	Aeolian	3	1
		Older Alluvium	2	0.5
LU	0.214309	Settlement	3	1
		Agriculture	2	0.5
		Forest/ Barren	1	0
GEOM	0.178576	Dunes	3	1
		Water Body	2	0.5
		Older Alluvium	1	0
SWV	0.142853	240-260	5	1
		260-280	4	0.75
		280-300	3	0.5
		300-320	2	0.25
		>320	1	0
PA	0.107154	>2	4	1
		2-1.75	3	0.66
		1.75-1.5	2	0.33
		<1.5	1	0
LQ	0.071423	<1	2	1
		>1	1	0
PF	0.035712	0.6-2.5	5	1
		2.5-4.5	4	0.75
		4.5-6.5	3	0.5
		6.5-8.5	2	0.25
		>8.5	1	0

Usually higher rank is assigned to values, which are more hazardous in nature, for example, the higher values of peak amplification will have the higher rank and lower values will have lower rank. In case of shear wave velocity, the lower values will be assigned higher rank and higher values will get lower rank depending upon their relative role in earthquake hazard or to positively or negatively influencing input seismic ground motion. The normalized ranks assigned to the features of each theme are given in Table 6.2.

6.1 GIS Integration

Geographical Information System (GIS) provide suitable platform for logical integration of inputs and their analysis and retrieval or development of a hazard index map wherein the seismic hazard parameters are integrated /weighted and coupled with ground information using Analytic Hierarchy Process (AHP).

In probabilistic approach, to mitigate the earthquake damage, the three interacting factors geological, geomorphological as well as land use pattern have significant role. However, the area shows homogeneous setup in terms of geology and geomorphology. Therefore, the rank assigned to geological theme in such a way that both Aeolian (rank=3) and Older Alluvium (rank=2) exposed in study area get significant importance during the integration. The shear wave velocity, peak amplification and liquefaction susceptibility of the area having direct bearing on site seismic hazard have also been considered. The average shear wave velocity (Vs30) map and peak amplification maps were prepared based on site specific geotechnical (SPT-N values) and geophysical studies. All these thematic layers have been integrated on ArcGIS platform to prepare the final seismic hazard microzonation map as per standard operating procedure (SOP) of GSI for the same purpose. AHP rating has been assigned to every sub-unit/polygon of the layers/thematic maps. Values of each source layer have been extracted in the centroid of mapping unit/grid. Addition of all source layer values has given the final value (AHP_{total}) of microzonation map over each mapping unit. The extraction of area has been carried out considering the assigned importance of theme and the rank.

The integrated hazard map gives the Hazard Index (HI), which is the integrated factor depending on the weights and ranks of the geoscientific, geotechnical attributes; ground motion parameters and liquefaction susceptibility. Finally, the integration of all thematic layers is achieved through following formula on GIS platform for preparation of seismic hazard microzonation map of Meerut City:

$$HI = GEO_W.GEO_R + LU_W.LU_R + GEOM_W.GEOM_R + SWV_W.SWV_R + PA_W.PA_R + LQ_W.LQ_R + PF_W.PF_R / \sum W$$

Where, HI represents the Hazard Index, and $_W$ and $_R$ represents the assigned weight and ranking respectively.

The final seismic hazard microzonation map is prepared based on addition of normalised weightage and rank values of different thematic maps. The thematic maps (Themes/ Geofactors) used for integration are geology (Figure 2.3), geomorphology (Figure 2.4), land use (Figure 2.9), shear wave velocity (Figure 4.8), peak amplification (Figure 4.9), liquefaction (Figure 5.1) and predominant frequency (Figure 4.10) discussed in detail in previous chapters. Seismic hazard microzonation map prepared by weighted overlay/integration of above mentioned thematic maps (Themes/ Geofactors) is shown in Figure 6.2.

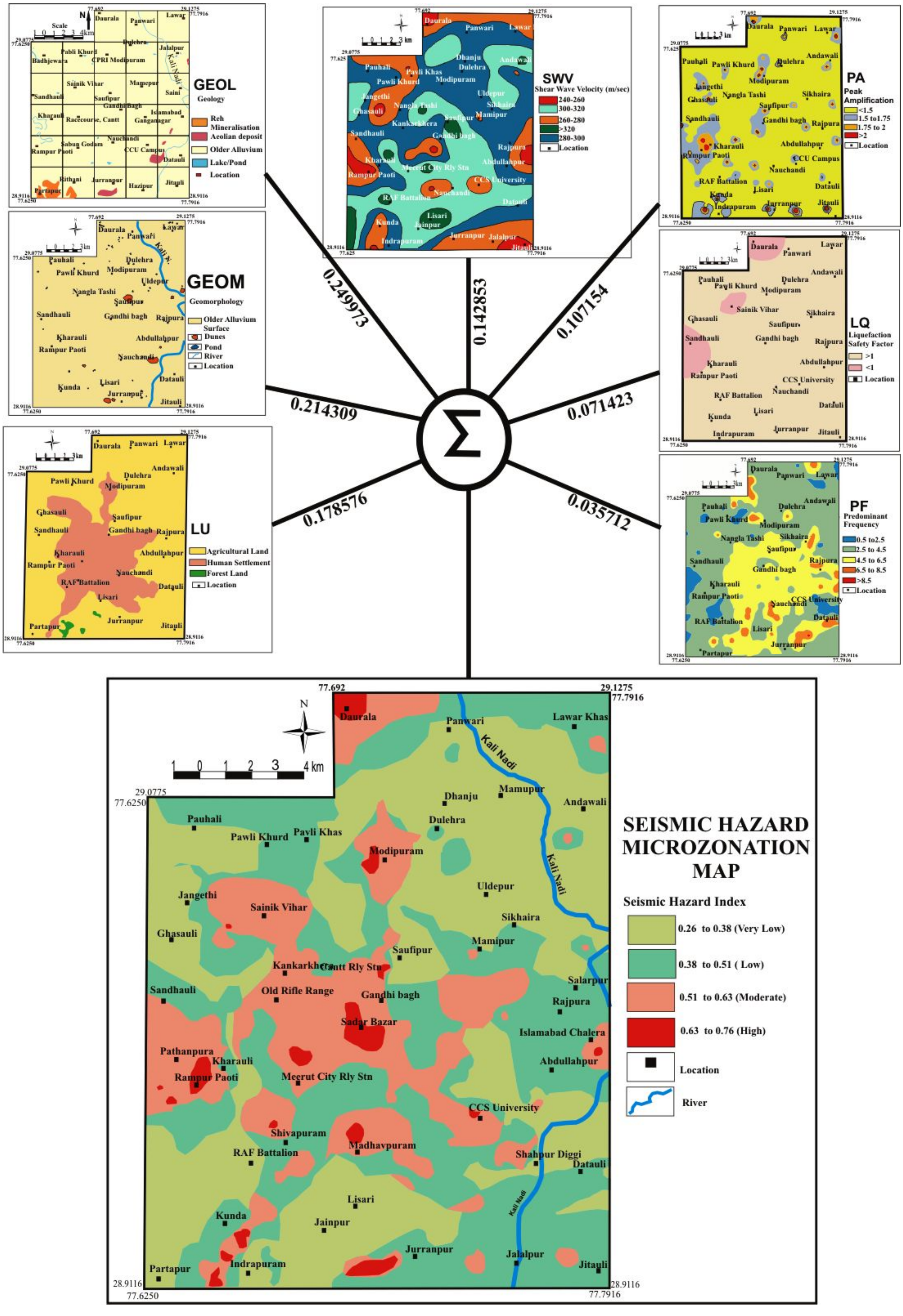

Fig. 6.2: Seismic hazard microzonation map of Meerut City (Thematic maps: GEOL-geological map, GEOM-geomorphological map, LU-land use map, SWV-shear wave velocity map, PA-peak amplification map, LQ-liquefaction susceptibility map and PF-predominant frequency map)

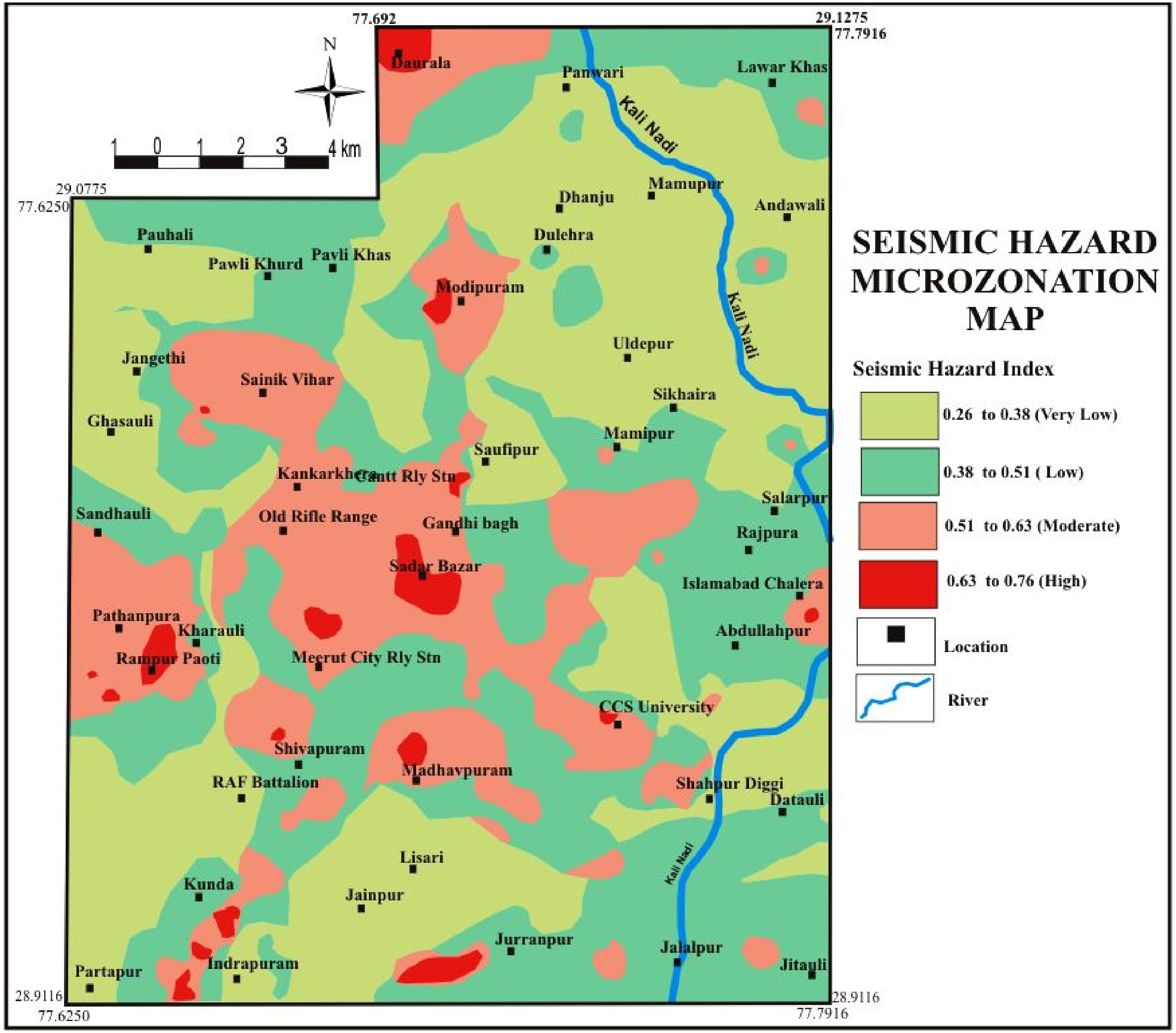

Fig. 6.3: Seismic hazard microzonation map of Meerut City

6.2 Results

The Hazard Index thus obtained (Fig. 6.2 and 6.3) varies from 0.26 to 0.76, which have been divided into four groups viz. (i) Hazard Index 0.26-0.38, (ii) Hazard Index 0.38-0.51, (iii) Hazard Index 0.51-0.63 and (iv) Hazard Index 0.63-0.76. On the basis of Hazard Index, the studied part of Meerut City and adjoining areas has been broadly classified into four zones of the seismic hazard. The Hazard Index 0.26-0.38 is attributed to very low seismic hazard; 0.38-0.51 is attributed to low hazard, 0.51 -0.63 is attributed to moderate hazard and 0.63-0.76 is attributed to high seismic hazard. As per the seismic hazard microzonation map, isolated seismic highs are present in the northern part near Daurala, in south of Gandhi bagh near Sadar Bazar, in the west near Rampur Paoti and Kharauli, in the south around Partapur, Indrapuram and Jurranpur and small patch in the east around Abdullahpur. The “high" seismic hazard zones are observed where either shear wave velocity is low or high peak amplification and possibility of liquefaction (SF= <1). However, the isolated high seismic hazard zone in the southern part near Jurranpur is observed mainly due to geological component like presence of Newer Alluvium (i.e. aeolian deposits). Out of 300 sq km studied area, 75% area falls under low and very low seismic hazard zone, 20% area falls under moderate hazard zone, and very less approximately 5% of the total area falls under high hazard zone (Figure 6.2 and 6.3).

6.3 Validation of Seismic Hazard Microzonation Model using ROC

After developing the microzonation model, it is important to evaluate their efficiency. The most relevant criterion for quality evaluation is the assessment of model accuracy by analyzing the agreement between the model results and the observed data (Frattini et al., 2010). Receiver Operating Characteristic (ROC) methodology initially evolved from radar signal-detection theory (Peterson *et al.*, 1954) which further drew attention in statistical quality control (Dodge and Romig, 1929; Shewhart, 1931) and statistical inference (Neyman and Pearson, 1933). Further, it was utilized in psychological testing and later on its wide use started in the field of medical test evaluation where it has emerged with enormous number of applications over the past four decades.

In Earth Sciences, the most important model prediction applications are applied in natural hazards which happen to be a major concern in the earth science researches. Several hazards are studied in earth sciences among which probably, the two most common are: landslides (Brenning, 2005) and earthquakes (Holliday et al., 2006).

Earthquake prediction is principally considered as a matter of spatial and temporal constraint where the area under threat is classified into different hazard levels and the objective tends to predict the qualitative/quantitative spatio-temporal prediction of effect of a future earthquake. Validation of the integrated Seismic Hazard Zonation maps is mainly based on the concept of accuracy where the classified area is devoid of any spatial overlap (Bonham-Carter 1994). While preparing Hazard zonation maps it is expected to face two types of errors: 1) hazard occurrences in those areas which are predicted to be stable (safe), and 2) no hazard occurrences in those areas that are predicted to be unstable (unsafe) (Soeters and van Westen 1996). Given the fact that the predictions are often probabilistic, it becomes necessary to validate the spatio-temporal models. Hence, use of ROC methodology for assessing the results worth of the predictive models.

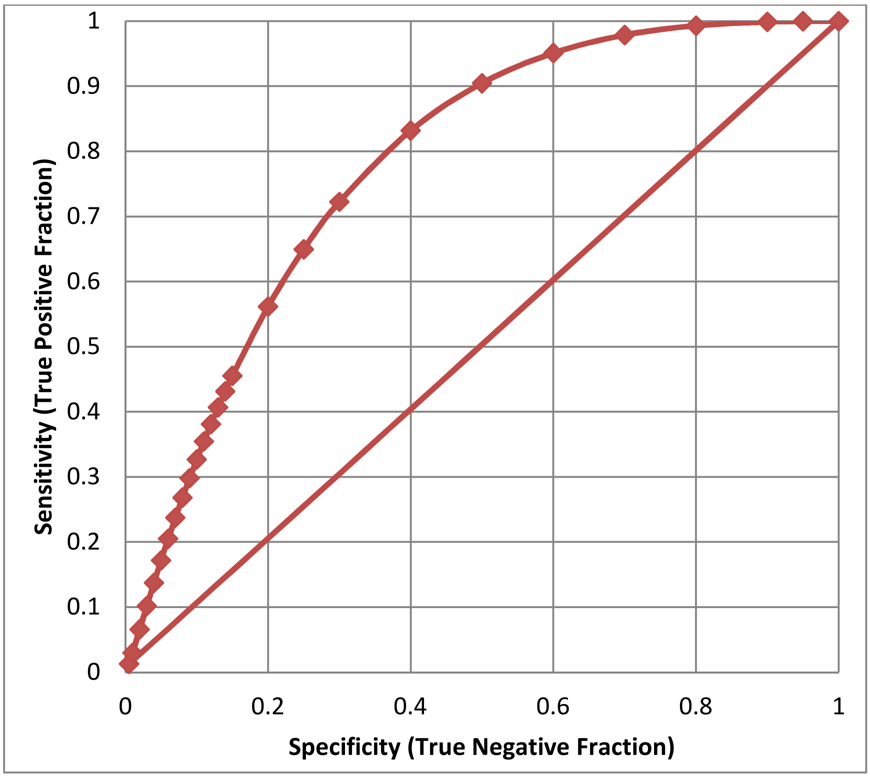

Fig. 6.4: ROC Curve of the Seismic Hazard Zonation Index map of Meerut city

ROC curve technique is based on plotting model sensitivity/ true positive fraction values calculated for threshold values versus model specificity/ true negative fraction values on a graph (Deleo 1993). Model sensitivity/true positive fraction is the grid cell correctly classified to be in high risk, while model specificity/ true negative fraction is classified grid cells with very low seismic hazard level (Pradhan and Lee 2010). Area under the ROC curve

has peak value of 1 for perfect prediction whereas value near 0.5 (straight line) suggests failure of the model. We performed ROC prediction accuracy process on our integrated seismic hazard zonation map to validate our probabilistic prediction model such that there exist no spatial overlap between the successive hazard indexes. The ROC curve is shown in figure no. 6.3.

Quantitative validation was performed by calculating the Area Under Curve (AUC) value of ROC graph. AUC is calculated as the sum of the total trapezoidal area calculated from each trapezoidal area as: $\{(X_1+X_2)/2\} / (Y_1-Y_2)\}$ where, X_1, X_2… and Y_1, Y_2,... are consecutive true positive and true negative rates, respectively. The AUC from ROC curve (Fig. XX) has been calculated to be 0.78 with estimated standard error of 0.05. This validation shows that the integrated seismic hazard zonation index map of Merrut city holds fairly good prediction accuracy of the model.

VII. SUMMARY AND CONCLUSIONS

During FS 2016-17 and 2017-18, an integrated seismic microzonation study covering 300 sq km area was carried out to unravel the seismic response in different parts of Meerut City encompassing the main city and surrounding suburbs as per Master Plan of Meerut 2021 (www.census2011.co.in) for input seismic ground motion due to nearby earthquake. The integrated study includes geological, geomorphological, geohydrological, geotechnical and geophysical investigations. It involves compilation, collection and integration of geological and geomorphological information along with 900 m drilling in 26 boreholes of 30 m each and 2 boreholes of 60 m each with core logging and SPT operations, geotechnical analysis of 110 core samples and geophysical investigations including site response studies by noise / microtremors at 321 sites, 100 vertical resistivity soundings (VES) and 56 stations MASW survey.

The Meerut City is settled on Quaternary sediments of Indo-Gangetic Plain within interfluve of Ganga in the east and Yamuna in the west. These fluvial Quaternary sediments are represented by the Older Alluvium and Newer Alluvium. The Older Alluvium comprises polycyclic sequence of oxidised, yellow to brown coloured silt-clay and micaceous sand. Disseminations of *kankar* as nodular concretions occur within clay-silt layers. The Newer Alluvium is represented by isolated patches of aeolian deposits on the older flood plain in the eastern and southern parts near Kali *Nadi* along with the active flood plain of Kali River. The thickness of the alluvial cover in the area is about >2000 m.

The Vs30 range from 238.5 m/s to 355 m/s puts the studied part in soil class 'D' of NEHRP code provisions having Vs30 range from 180 m/s to 360 m/s. This limited range of variation of Vs30 suggests that there is not likely to be major difference in the seismic response at different sites of Meerut City. The majority of peak amplification values range from 1.0 to 1.5 in the frequency range of 2.0 Hz to 4.5 Hz. The maximum peak soil amplification is 2.4 times. The overall variation of predominant frequency of the sites within Meerut City ranges from 0.6 Hz to 9.3 Hz with the most common areas being in the range from 2.0 Hz to 4.5 Hz.

Small variation in the Vs30 values resulting in more or less uniform expected amplification of incoming seismic waves is mainly due to presence of almost uniformly

distributed Older Alluvium at the surface. The older Alluvium exposed at surface is well consolidated having occasional *kankar* beds.

The liquefaction susceptibility for groundwater level <12 m depth in 6 bore holes has been estimated based on scenario earthquake of M 8, h 15 km epicentered at Mathura. The seismic capacity is ascribed in term of SPT results with corrected $N_1 60$ values. A relatively high liquefaction domain (<1 safety factor) has been identified near Sainik Vihar, Sandhauli and Daurala areas.

The integrated seismic hazard microzonation map on GIS platform prepared by integrating all seven thematic layers suggests presence of isolated seismic high zones (5% of total area) near Daurala, Gandhibagh, Rampur Paoti, Kharauli, Partapur, Indrapuram, Jurranpur and Abdullahpur. The "high" seismic hazard zone is mainly low shear wave velocity or high peak amplification and possibility of liquefaction potentiality.

The whole gamut of different studies suggests that there is not significant variation in the site response values at different locations arrived at either by the geotechnical method or through geophysical survey in Meerut City. As is evident from the study, the individual input parameters (viz. geology, geomorphology, land use, shear wave velocity, peak amplification, liquefaction and predominant frequency) are not showing significant variation in the study area. It can be inferred that there may not be significantly different response in different parts of the studied area of Meerut City for incoming ground motion due to future earthquake. However, the integration has taken the limited data variation of thematic layers to classify into different levels or zones of hazard. Nevertheless, it is suggested that the zones of isolated high seismic hazard zones should be taken care for construction of any major structure.

7.1 Conclusions

The salient points of this study along with conclusive remarks/ inferences drawn from the integrated survey covering 300 sq km area of Meerut City using the inputs from geological, geotechnical and geophysical data for the seismic microzonation study are given below:

i. The M 7.5, 1803 Mathura earthquake located at a distance of about 160 km from Meerut is the strongest seismic event within 300 km radius which has produced strongest effects in Meerut Region. Accordingly, computation based on Shebalin and Karnik relationship for maximum credible earthquake of magnitude 8.0 at a depth of 15 km occurring at the

location of 1803 Mathura earthquake lying at about 160 km distance gives maximum intensity of >VIII at Meerut. Further on the basis of the attenuation relationship for peak ground acceleration for the Himalayan Region, we get 0.17g vertical PGA at engineering bed rock.

ii. The study area/Meerut City is located within the interfluve of Ganga and Yamuna River system on the Quaternary sediments of Indo-Gangetic Plain. These sediments are represented by the Older Alluvium and the Newer Alluvium. Spatially at surface, mainly Older Alluvium of the middle to late Pleistocene is exposed with few small pockets of aeolian deposits of the Newer Alluvium. The subsurface geology interpreted on the basis of logs of 26 bore holes of 30 m depth each and section studies show presence of two generalised cycles of fluvial deposition. However, two bore holes of 60 m depth each show presence of broadly three cycles of deposition where the youngest cycle started at about 24 ka BP (quartz OSL date) and second deposition cycle (i.e. younger than the oldest one) might have initiated before 30 ka BP and ended after 27 ka BP.

iii. The groundwater level in the area varies from 8.5 m to 29 m depth below ground level (bgl). The groundwater level is deeper in the central part of Meerut City and shallower in the western part.

iv. The raw SPT (N value) of each bore hole has been corrected to N_160 and is used for computation of Vs30 and liquefaction susceptibility.

v. The values of shear wave velocity at different sites in Meerut City and the surrounding areas have been estimated through geotechnical and geophysical methods and correspond to Soil Type - D (i.e. stiff soil) of the Site classes of NEHRP Code Provisions (1997). The average shear wave velocity in central and eastern parts of the study area is higher near Nauchandi and CCU campus while lower in the western, south western and south eastern part, of the area near Sainik Vihar, Daurala and Jithauli. The lower Vs30 values show that the subsurface soil media up to 30 m depth may pose problem for structures to withstand the impact of earthquake event or horizontal seismic loading as such subsurface soil may amplify the ground motions.

vi. The peak amplification varies from 1.0 to 2.35. This amplification is mostly in the frequency range of 2.0 Hz to 4.5 Hz. The areas near Kharauli, Sainik Vihar, Partapur, Jithauli, Gandhibagh and Modipuram are of moderate to high peak amplification which suggests moderate to higher potential for damage during earthquake.

vii. The analysis of grain size and derivative curves indicates that the sediment horizons susceptible to liquefaction are present at shallower depths in the area. It therefore implies

that the areas having deeper water table are safer from liquefaction hazard. However, liquefaction susceptibility for six sites where ground water level was at <12 m depth has been calculated based on scenario earthquake of M8, h 15 km epicentered at Mathura. The seismic capacity is ascribed in term of SPT results with corrected N_160 values. The methodology enunciated by Seed & Idriss (1982) has been followed and seismic demand (CSR) and capacity (CRR) were determined eventually to identify high liquefaction domains near Sainik Vihar, Sandhauli and Daurala areas.

viii. The predominant frequency of sites and corresponding peak amplification within Meerut City varies in the range of 0.61-9.33 Hz (i.e. predominant frequency in the range of 2.0 to 4.5 Hz) and 1.0 to 2.35 respectively. The central and eastern parts of the area show higher predominant frequency than the northern and western parts. Engineering structures having natural frequency in the range of 2.5 Hz - <4.5 Hz i. e. double storied to G + 3 in the area are more prone to damage during an earthquake.

ix. The integrated seismic hazard microzonation map prepared by integrating all the thematic layers on Arc GIS platform suggests that out of 300 sq km studied area, 75% area falls under low and very low seismic hazard zone, 20% area falls under moderate hazard zone and only 5% of the total area falls under high hazard zone (Figure 6.2).

x. The seismic high zone is present in isolated patches near Daurala, Gandhibagh, Rampur Paoti, Kharauli, Partapur, Indrapuram, Jurranpur and Abdullahpur. It is suggested that while designing the construction of major engineering project/multi storied buildings in such areas, adequate aseismic inputs should be incorporated to withstand the incoming motion from a big earthquake in the surrounding region.

xi. The integrated seismic hazard microzonation map depicting ‘very low’ to ‘high hazard’ zones basically suggests relative hazard levels, not necessarily in the absolute sense of the meaning of the used adjectives as ‘high’, ‘low’ etc.

xii. The validation of seismic hazard microzonation model using ROC (receiver operating procedure) curve gives calculated value 0.78 with estimated standard error of 0.05, which shows that the integrated seismic hazard microzonation map of Merrut city holds fairly good prediction accuracy.

REFERENCES

Aki, K. and Richards, P.G. (1980): Quantitative seismology, V.I: San Francisco, W.H. Freeman, pp 557.

Anbazhagan, P., Thingbaijam, K. K. S., Nath, S. K., Narendara Kumar, J. N. and Sitharam T. G. (2010): Multi-criteria seismic hazard evaluation for Bangalore city, India, Journal of Asian Earth Sciences 38 (2010) 186–198.

Anderson. J. G., Lee, Y., Zeng, Y. and Day, S. M. (1996): Control of Strong motion by upper 30meters, Bull. Seism. Soc. Am., 86, pp 1749 - 1759.

Asiatic Annual Register (1804): View of History of Hindustan and of the politics, commerce and literature, Campbell Lawrence Dundas, London, Published in 1806.

Bard, P. Y. and Bouchon (1985): The two dimensional resonance of sediment filled valleys, Bull. Seism. Soc. Am., Vol.75, pp519 - 541.

Bard, P.Y. (2000): Local effects of strong ground motion**:** Physical basis and estimation methods in view of Microzonation Studies, Lecture note in International Training Course Seismology, Seismic Data Analysis, Hazard Assessment and Risk Mitigation. Postdam, Germany.

BIS 2002 IS: 1893-Part 1 (2002): Indian Standard Criteria for Earthquake Resistant Design of Structure Part 1-Resistant Provisions and Buildings; Bureau of Indian Standards, New Delhi.

BMPTC (2006): Vulnerability Atlas of India first revision, Building materials and technology promotion council, ministry of urban development, government of India.

Bonham-Carter, G. F. (1994): Geographic Information System for Geoscientists: Modelling with GIS, Pergamon / Elsevier Science Ltd., p 8.

Boore, D. M, Joyner, W. B. and Fumal, T. E. (1993): Estimation of response spectra and peak acceleration from western North American earthquakes, an interim report, United States Geological Survey, Open file report, pp 93-509.

Borcherdt, R.D. (1970): Effects of local geology on ground motion near San Francisco Bay, Bull. Seism. Soci. Am., 60, pp 29-61.

Borcherdt, R. D., Wentworth, C. M., Janssen, A., Fumal, T. and Gibbs, J. F. (1991): Methodology for predictive GIS mapping of special study zones for strong ground shaking in the San Francisco Bay region, Proceedings of the fourth International Conference on Seismic Zonation August 25-29, standard, California, 3, pp.545 - 552.

Brenning, A. (2005): Spatial prediction models for landslide hazards: review, comparison and evaluation. Natural Hazards and Earth System Sciences, 5, 853-862.

BS 5930 (1999): Code of practice for site investigations, British Standard Institutions, London.

BSSC (1997): NEHRP Recommended provisions for seismic regulations for new buildings, Part-1.

Dasgupta, S., Pande, P., Ganguly, D., Iqbal, Z., Sanyal, K., Venaktraman, N. V.,Dasgupta, S., Sural, B., Harendranath, L., Mazumadar, K., Sanyal, S., Roy, A., Das, L. K., Misra, P. S. and Gupta, H. (2000): Seismotectonic Atlas of India and its Environs,Geological Survey of India, Calcutta, India.

Deleo, J. M. (1993): Receiver operating characteristic laboratory (ROCLAB): software for developing decision strategies that account for uncertainty. In: Proc. 2nd Int. Sym. uncertainty modelling and analysis. Computer Society Press, College Park, pp 318-325.

Dodge, H. and Romig, H. (1929): A method of sampling inspection. Bell Systems Technical Journal, 8, pp 613-631.

Fin, W. D. Liam (1991): Assessment of liquefaction potential and post-liquefaction behaviour of earth structures, Proc. 2nd Int. Conf. of recent advances in geotech. Earthquake eng. And soil dynamics, vol. II, pp 1833 – 1851.

Frattini, P., Crosta, G. and Carrara, A. (2010): Techniques for evaluating the performance of landslide susceptibility models. Engineering Geology 111(1-4), 62-72.

Gadhole, S.K., Khullar V.K., (1991): Quaternary Geology and Geomorphology of parts of Muzaffarnagar, Bijnor and Meerut Districts, U.P. Unpublished Report, GSI.

Gupta, I. D. (2005): Probabilistic Seismic Hazard Analysis with Uncertainties, Proceedings of the Symposium on Seismic Hazard Analysis and Microzonation, Roorkee,Vol. I, pp. 97–117.

Hanumantharao, C. and Ramana, G.V. (2008): Dynamic soil properties for microzonation of Delhi, India. Journal of Earth System Science 117(2), 719-730.

Holliday, J. R., Rundle, J. B., Turcotte, D. L., Klein, W., Tiampo, K. F. and Donellan, A. (2006): Space- time clustering and correlations of major earthquakes, Physical Review Letters, 97, 238501.

http://en.wikipedia.org/wiki/Meerut

Idriss, I. M. (1990): Response of soft soil sites during earthquakes, Proc. H. Bolton Seed Memorial Symposium, pp 273 – 290.

Iyengar, R. N. and Ghosh, S. (2004): Microzonation of earthquake hazard in Greater Delhi area, Current Science, Vol. 87, No. 9, 10 November 2004.

Iyengar, R. N. (2000): Seismic Status of Delhi Megacity', Current Science, vol. 78, No.5, 568-574.

Joshi, K. C., Pande, P. and Narula, P. L. (1996): Landslide hazard zonation and its correlation with coseismic slides during Uttarkashi earthquake of 20th October 1991, Proc. Seventh Int. Symp. of Landslides, Trondheim, Norway, pp.977-982.

Joshi, K. C., Pande, P. And Narula, P. L. (2005): Landslide hazard zonation and its correlation with coseismic slides during Uttarkashi earthquake of 20th October, 1991, Proc. VII int. Sym. Landslides, Trondheim, June, 1996, pp 977-982.

Joshi, K. C., Sharda, Y. P., Singh, J., Gupta, S. K., and Pande, P. (2007): Geotechnical studies for seismic microzonaion of Delhi, Geol. Soc.Ind., Vol, 70, pp.950 - 962.

Konno, K. and Ohmachi, T. (1998): Ground motion characteristics estimated from spectral ratio between horizontal and vertical components of microtremor, Bull. Seism. Soci. Am., 88, pp. 228-24

Karnik, V. (1969): Seismicity of European area, part, I, Reidel Publishing ompany, Dordrecht.

Kayen, R. E., Mitchell, J. K., Seed, R. B., Lodge, A., Nishio, S. And Coutinho, R. (1992): Evaluation of SPT, CPT and shear wave based methods for liquefaction potential assessment

using Loma-Prieta data, Proc., 4th Japan-US workshop on earthquake resistant design of life line fac. and countermeasures for liquefaction, vol. 1, pp 177 - 204.

Lermo, J. and Chavez-Garcia, F. (1993): Site effect evaluation using spectral ratios with only one station, Bull. Seism. Soc. Am., Vol. 83, pp 1574 – 1594.

Liao, S. S. C. and Whitman, R. V. (1986): Catalogue of liquefaction and nonliquefaction occurrences during earthquakes, Res. Rep., Dept. of Civ. Eng.., Massachusetts Institute of Technology, Cambridge, Mass.

Marcuson, W. F. III (1978): Definition of terms related to liquefaction, Jour. of geotech. Eng., ASCE, 104 (9), pp 1197-1200.

Mohanty, W. K., Walling, M. Y., Nath, S. K. and Pal, I. (2007): First order seismic microzonation of Delhi, India using geographic information system (GIS), Natural Hazard 40, 245–260.

MOES (Ministry of earth sciences) 2016: A report on Seismic Hazard Microzonation of NCT Delhi on 1:10,000 scale, National Center for Seismology, Ministry of Earth Sciences, Government of India.

Molnar, P. (1987): The distribution of intensity associated with the 1905 Kangra earthquake and bounds on the extent of rupture zone, Journ. Geol. Soc. India, vol 29, pp 221-229.

Muktinath, K. N. and Srivastava, J. P. (1968): The Delhi earthquake of 27th August, 1960, Rec., GSI, vol. 65 (2), pp367-382.

Nakamura, Y. (1989): A method for dynamic characteristics estimation of subsurface using microtremor on the ground, Q.R. Railway Tech. Res. Inst., 30.

Nath S.K. and K.K.S. Thingbarijam (2011): Probabilistic Seismic Hazard Assessment of India, Seismic Hazard Microzonation Manual, Ministry of Earth Sciences.

Nath, S.K., Thingbaijam, K.K.S., Raj, A., Shukla, K., Pal, I., Nandy, D.R., Yadav, M.K,Bansal, B.K., Dasgupta, S., Majumdar, K., Kayal, J.R., Shukla, A.K., Deb, S.K.,Pathak, J., Hazarika, P.J. and Paul, D.K. (2007): Seismic scenario of Guwahati City. In:Proceedings of the International Workshop on Earthquake Hazard andMitigations, 7-8 December, pp. 210-218.

NDMA (2011): Development of probabilistic seismic hazard map of India, Technical report of WCE, National Disaster Management Authority, Govt. of India, New Delhi.

Narula, P. L., Absar, A., Pande, P. and Shankar, R. (1996): Changes in chemistry of thermal waters consequent to the Uttarkashi earthquake in Northwest Himalaya, Geothermal energy in India (eds. U. L. Pitale and R. N. padhi), GSI sp. Pub., 45, pp 209-222.

Neyman, J. and Pearson, E. S. (1933): On the problem of the most efficient tests of statistical hypotheses, Philosophical Transactions of the Royal Society, London, A231, 289-337.

Ohta, Y. and Goto, N. (1978): Emperical shear wave velocity equation in terms of characteristics soil indexes, J. Earthquake Engineering and Structural Dynamics, vol.6, pp 167 - 187.

Oldham, T. (1883): A catalogue of Indian Earthquakes from earliest times to the end of A.D. 186, Mem. GSI, No. X, 129, 1883.

Orellana, E. and Mooney, H.M. (1966): Master tables and curves for vertical electrical soundings for layered media, Intercieneia Madrid.

Pal, I., Nath, S.K., Shukla, K., Pal, D.K., Raj, A., Thingbaijam, K.K.S. and Bansal, B.K. (2008): Earthquake hazard zonation of Sikkim Himalaya using a GIS platform. NaturalHazards 45, 333–377.

Parolai, S., Bormann, P. and Milkereit, C. (2002): Short Note "New Relationships between Vs, Thickness of Sediments, and Resonance Frequency Calculated by the H/V Ratio of Seismic Noise for the Cologne Area (Germany), Bulletin of the Seismological Society of America, Vol. 92, No. 6, pp. 2521–2527, August 2002.

Peterson, W. W., Birdsall, T. G. and Fox, W. C. (1954): The theory of signal detectability. Transactions of the IRE Professional Group on Information Theory, PGIT, 2-4, 171-212.

Rauch, A. F. (1997): An empirical method for predicting surface displacement due to liquefaction induced lateral spreading in earthquakes, Ph. D. dissertation, Virginia Polytechnic Institute and state university, VA.

Saaty, T.L., 1980. The Analytic Hierarchy Process. McGraw-Hill, New York, NY.

Saaty, T. L. and Vargas, L. G. (2001): Models, methods, concepts and application of the AHP, Int. Ser. In operation research & management science, Springer, Newyork, pp, 333.

Seed, H. B. and Idriss, I. M. (1971): Simplified procedure for evaluating soil liquefaction potential," Journal of the Soil Mechanics and Foundation Division, ASCE,Vol. 97, No.9, pp 1249 - 1274.

Seed, H.B., and Idriss, I.M. (1982): Ground motions and liquefaction during earthquakes, Monograph No.5. Earthquake Engineering Research Institute Berkeley California, 134P.

Seed, H. B., Tokimatsu, K., Harder,Jr., L. F. and Chung, R. (1985): Influence of SPT Procedures in soil liquefaction resistance evaluation, Jour. Geotech. Eng., ASCE, 111 (12), pp 1425 – 1445.

Seismotectonic Atlas of India and Its Environs (2000): Special Publication, Geological Survey of India.

SeisImager/SW^L Manual (2006): Windows software for analysis of surface waves. Pickwin^{L}v.3.2, WaveEq^{L}v. 2.2 and GeoPlot^{L}v.8.2.5. Manual v. 2.2. Including explanation of surface wave data acquisition using Geometrics Seismodule Controller Software (v. 9.14) for ES-3000, Geode, and StrataVisor NZ seismographs. Geometrics, Inc.

Sharma, M. L. (1998): Attenuation relationship for estimation of peak ground horizontal acceleration using data from strong-motion arrays in India, Bull. Seism. Soc. Am., 88(4), pp 1063-1069.

Shebalin, N. (1958): Correlation between earthquake magnitude and intensity, Studia geophysiac et geodaetica, 2, pp 86-87.

Shewhart, W. (1931): Economic Control of Quality of Manufactured Products van Norstand, New York.

Skempton, A. W. (1986): Standard Penetration Test Procedures, Geotechnique, vol. 36, No. 3, pp 425 - 447.

Soeters R., Van Westen, C. J. (1996): Slope stability: recognition, analysis and zonation, In: Turner A, Shuster R (eds) Landslides: investigation and mitigation, National Academy Press, Washington D C, pp 129-177.

Srivastava, L.S. and Somayajulu, J.G.(1966). The seismicity of the area around Delhi,Proceedings of the third Symposium on Earthquake Engineering, Roorkee, November 1966, pp.417-422.

Steppe, J. C. (1972): Analysis of Completeness of the Earthquake Sample in the Puget Sound Area and Its Effect on Statistical Estimates of Earthquake Hazard, Proceedings of the International Conference on Microzonation, Seattle, U.S.A., Vol. 2, pp 897 - 910.

Su. F., Aki, K., Teng, T., Zeng, Y., Koyangi, S. and Mayeda, K. (1992), The relation between site amplification factor and surficial geology in Central California, Bull. Seism. Soc. Am., Vol. 82, pp.580-602.

Thussu, J. L., Chopra, S. And Kumar, B. (1991): Quaternary geology and geomorphology of parts of Ganga Basin in Meerut, Ghaziabad and Bulandshahar Districts, U. P., GSI unpublished report.

Tsuchida, H. and Hayashi, S. (1971): Estimation of liquefaction potential of sandy soils. Proceedings of the Third Joint Meeting, US-Japan Panel on Wind and Seismic Effects, UJNR, Tokyo, 1971, pp 91-101.

UBC (1997): Uniform building code, International conference of building officials, whittier, California.G

Uma Maheswari, R., Boominathan, A. and Dodagoudar, G.R., (2010). Use of Surface Waves in Statistical Correlations of Shear Wave Velocity and Penetration Resistance of Chennai Soils. Geotechnical and Geological Engineering 28(2), 119-137.

TC4-ISSMGE (1999): Manual for zonation on seismic geotechnical hazards, Technical committee for earthquake geotechnical engineering, e-edition, www.dica.unict.it/personale/docenti/assets/TC4 manual.pdf.

www.cgwb.gov.in/district_profile/Punjab/Meerut.pdf

www.census2011.co.in /Uttar Pradesh / Meerut District / MeerutUA.

www.mdameerut.co.in

www.earthquakes.usgs.gov/earthquakes

www.imd.gov.in

Youd, T. L., Idriss, I. M., Andrus, R. D., Arango, I., Castro, G., Christian, J. T., Dobry, R., Finn, W. D.L., Hardes, L. F., Hynes, M. E., Ishihara, K., Koester, J. P., Liao, S. S. C, Marcuson, W. F., Martin, G. R., Mitchell, J. K., Moriwati, Y., Power, M. S., Roberson, P. K., Seed, R. B. and Stokoe, K. H. (2001): Liquefaction resistance of Soils: Summery report from the 1996 NCEER and 1998 NCEER/NSF workshops on evaluation of liquefaction resistance of soils. J. Geotech. Geoenv. Eng. Vol. 127, pp 817 - 833.

LOCALITY INDEX

S.NO.	LOCATION NAME	LAT ° N	LONG ° E
1	Begum Pul	77.7056	28.9950
2	Biral Partapur	77.6365	28.9180
3	Budhera Zahidpur	77.7242	28.9265
4	Cantt Rly. Stn.	77.6892	29.0147
5	Dabka	77.6491	29.0157
6	Dantal	77.6886	29.0400
7	Dulehra	77.7276	29.0746
8	Dungrawali	77.6385	28.9388
9	Fatehullapur	77.7131	28.9388
10	Gandhi bagh	77.7033	29.0086
11	Ghasauli	77.6278	29.0306
12	Indrapuram	77.6504	28.9147
13	Jainpur	77.6861	28.9311
14	Jali Kothi	77.6972	28.9867
15	Jangethi	77.6400	29.0435
16	Jawahar Nagar	77.6658	28.9925
17	Jewri	77.6665	29.0538
18	Jurranpur	77.7141	28.9218
19	Kanchanpur Ghopla	77.6788	28.9214
20	Kankarkhera	77.6792	29.0208
21	Kharauli	77.6494	28.9857
22	Kunda	77.6498	28.9321
23	Lisari	77.6994	28.9380
24	Madhavpuram	77.6958	28.9511
25	Meerut City Rly. Stn.	77.6756	28.9783
26	Nangla Tashi	77.6679	29.0335

27	Nauchandi	77.7183	28.9669
28	Old Rifle Range	77.6653	29.0086
29	Panchvati Insstt.	77.6328	28.9550
30	Pathanpura	77.6307	28.9891
31	Pauhali	77.6431	29.0708
32	Pavli Khas	77.6830	29.0676
33	Pawli Khurd	77.6686	29.0648
34	Presidency College	77.6736	28.9375
35	RAF Battalion	77.6551	28.9506
36	Rampur Paoti	77.6357	28.9771
37	Sandhauli	77.6264	29.0097
38	Shabpir Gate	77.7056	28.9756
39	Shivapuram	77.6715	28.9604
40	Victoria Park	77.7265	28.9792
41	Zakir Colony	77.7133	28.9533
42	Dawarla	77.7008	29.1125
43	Panwari	77.7344	29.1089
44	Iklauta	77.7343	29.0964
45	Sawaha	77.7089	29.0889
46	Dhanju	77.7336	29.0825
47	Modipuram	77.7042	29.0611
48	Uldepur	77.7425	29.0514
49	Mamipur	77.7395	29.0324
50	Saufipur	77.7141	29.0276
51	Kaserukhera	77.7411	29.0089
52	Lawar Khas	77.7786	29.1117
53	Ajhauta	77.7549	29.1028
54	Mamurpur	77.7533	29.0869

55	Andawli	77.7792	29.0833
56	Khanauda	77.7547	29.0697
57	Sikhaira	77.7528	29.0411
58	Rajpura	77.7706	29.0117
59	Pabla	77.7917	29.0617
60	Jitauli	77.7844	28.9183
61	Alampur Buzurg	77.7758	28.9125
62	Abdullahpur	77.7664	28.9911
63	Datauli	77.7797	28.9525
64	Jalalpur	77.7542	28.9222
65	Kamalpur	77.7639	28.9375
66	Rali Chauhan	77.7736	28.9778
67	Gesupur	77.7694	28.9617
68	Netaji Nagar	77.7311	28.9953
69	CCS University	77.7419	28.9714
70	Sarai Qazi	77.7542	28.9422
71	Shahpur Diggi	77.7575	28.9544
72	Tejgari	77.7366	28.9629
73	Pabla	77.7914	29.0619
74	Banchaula	77.7722	29.0375
75	Salarpur	77.7756	29.0189
For more localities please refer annexures.			